The Proceedings of the International Conference on Creationism

Volume 8 Article 5

2018

The Dinosauria: Baraminological and multivariate patterns

DOI: https://doi.org/10.15385/jpicc.2018.8.1.35

Neal A. Doran
Bryan College

Matthew McLain
The Master's College

Natalie Young
Bryan College

Adam Sanderson
Bryan College

Doran, N., M.A. McLain, N. Young, and A. Sanderson. 2018. The Dinosauria: Baraminological and multivariate patterns. 2018. In *Proceedings of the Eighth International Conference on Creationism*, ed. J.H. Whitmore, pp. 404-457. Pittsburgh, Pennsylvania: Creation Science Fellowship.

THE DINOSAURIA: BARAMINOLOGICAL AND MULTIVARIATE PATTERNS

Neal A. Doran, Bryan College, Department of Biology 7795, 721 Bryan Drive, Dayton, TN 37321 USA, neal.doran@bryan.edu
Matthew A. McLain, The Master's University, Department of Biological and Physical Sciences, 21726 Placerita Canyon Road, Santa Clarita, CA 91321 USA
N. Young, Bryan College, Department of Biology 7795, 721 Bryan Drive, Dayton, TN 37321 USA
A. Sanderson, Bryan College, Department of Biology 7795, 721 Bryan Drive, Dayton, TN 37321 USA

ABSTRACT

The Dinosauria pose both interesting and challenging questions for creationist systematists. One question is whether new dinosaur discoveries are closing morphospatial gaps between dinosaurian groups, revealing continuous morphological fossil series, such as between coelurosaurians and avialans. Questions such as these underscore the importance of systematics for resolving correct group memberships, including tools for visualizing morphospatial relationships. Baraminic distance correlation (BDC), three-dimensional multidimensional scaling (MDS), and a new method to baraminic studies – principal component analysis (PCA) – were applied to 18 character matrices from 2004. The data included saurischian and ornithischian dinosaur groups including (1) "basal" Saurischia, (2) Ceratosauria (including Coelophysidae), (3) "basal" Tetanurae, (4) Tyrannosauroidea, (5) "Prosauropoda", (6) Sauropoda, (7) Maniraptoriformes, (8) Therizinosauroidea, and (9) Oviraptorosauria. The ornithischians included (10) "basal" Thyreophora, (11) Stegosauria, (12) Ankylosauria, (13) "basal" Ornithopoda, (14) "basal" Iguanodontia, (15) Hadrosauridae, (16) Pachycephalosauria, (17) "basal" Ceratopsia, and (18) Ceratopsidae. BDC and MDS revealed several potential holobaramins and apobaramins, and PCA identified some divisions not recognized by the traditional methods, but since the datasets are 14 years old, many important taxa are missing.

As a result, we performed PCA on 19 newer datasets (from 2009 to 2018) and compared the results, which revealed a substantially clearer picture since only 2004. Dinosaur group ordinations commonly occur within morphospatial clusters or linear series. Holobaramins were revealed mainly as closely-spaced morphospatial series of taxa. Some series were additionally stratomorphic. Assuming holobaramins are discontinuity-bounded morphospatial series of taxa, we estimate 27 potential holobaramins within the newer data. PCA revealed that bird-dinosaur morphospatial relationships vary by dataset. Paravians likely contain two branching morphoseries, connected at the base by dromaeosaurs and avialans. The two morphoseries are functional/ecological, rather than evolutionary. Multivariate analysis offers the potential to improve our understanding of baramins and discontinuity, and provide a new perspective on questions in creation systematics such as bird-dinosaur relationships.

KEY WORDS

Dinosauria, baraminology, multidimensional scaling, baraminic distance correlation, principal component analysis, discontinuity

INTRODUCTION

Two important claims concerning dinosaurs and baraminology are that (1) the morphological space between dinosaurs is being progressively filled over time, removing discontinuities between groups, and (2) there is already "morphological continuity" within the Dinosauria (Senter 2010, 2011). These claims show the need for a creationist approach to biological character morphospace.

Plant and animal baramins have been examined across an impressive taxonomic range and provide evidence of discontinuity. Animal examples include members as diverse as mammals, insects, and flatworms. Plants groups include the magnolias, monocots, conifers and bryophytes (Wood 2008a, 2016*a*). Included in these surveys are a growing number of examples from the fossil record. These include equids (Cavanaugh et al.. 2003), archaeocete whales (Mace and Wood 2005), caseids (Aaron 2014*a*), Mesozoic avians (Garner et al. 2013), tyrannosauroids (Aaron 2014*b*), and a growing literature on fossil hominid baraminology generating debate (*e.g.,* Wise 2005; Wood 2010; Wood 2011a; Wood 2013; Wood 2016b).

Starting in 2010 a brief debate raised interesting questions, premised in part on a misunderstanding of the role of multidimensional scaling (MDS) in statistical baraminology. The claim was that common ancestry between coelurosaurians and birds was supported even by creationist usage of MDS and baraminic distance correlation (BDC). It was argued, further, that these methods demonstrated continuity of morphological form between a wide range of dinosaur groups (*e.g.,* basal Saurischia, Theropoda, Sauropodomorpha, etc.) (Senter 2010; Senter 2011; and Wood's response in Wood 2011*b*). Cavanaugh used ANOPA to find overlapping clusters of coelurosaurian theropods, including V-shaped morphospatial relationships (Cavanaugh 2011). A BDC study on Weishampel (2004) identified discontinuity in 13 of 19

character sets studied (Wood, *et. al*, 2011). A more targeted study demonstrated discontinuity between Avialae and Deinonychosauria for most datasets, though some BDC and MDS results indicated continuity (Garner et al. 2013).

Beyond dinosaurs, statistical baraminology has also been questioned within creationist circles for other reasons. One concern was that baraminic distance methods group dissimilar morphospecies, such as *Australopithecus sediba* and *Homo sapiens*, into the same holobaramin (DeWitt 2010; Habermaehl 2010; Menton 2010). A more careful critique acknowledged value in the methodology but called for more attention to genetics and genetic programs including hybridization and synapomorphies (Wilson 2010). Though Wilson's argument has validity, genetic and hybridization criteria cannot be applied to the fossil record.

Here, we survey the baraminic status of the Dinosauria using the approaches of statistical baraminology while particularly exploring Senter's questions about morphospace. One valid question raised by the previous work is whether holobaramins identified by statistical baraminology include hidden discontinuities (*e.g.,* how much more division are apobaraminic groupings, such as dinosaurs, capable of?). To address these questions, we offer an additional approach to visualize morphological space: Principal Component Analysis (PCA). Examination of character morphospace allows the visualization of holobaramins, morphological continuity and discontinuity, and even potential identification of stratomorphic series of taxa.

As a survey of the Dinosauria this work re-contextualizes previous creationist questions. Previous work on tyrannosauroids and bird-dinosaur relationships (e.g., Aaron 2014b; Garner et al. 2013) is addressed in the context of dinosaurs, as a whole. In other words, in addition to the multivariate analyses on tyrannosauroids and maniraptorans we can address whether our patterns were typical – or unique – in the broadest context. The Dinosauria also provide an opportunity to examine broad questions regarding issues of the systematics of a large, terrestrial pre-Flood fauna, and post-Creation intrabaraminic diversification.

MATERIALS AND METHODS

Analyses included traditional approaches to baraminology, including baraminic distance correlation (BDC) and multidimensional scaling (MDS). Principal components analysis (PCA) was employed to further visualize morphological continuity and discontinuity. The most recent datasets, those compiled after 2004, were mostly analyzed by PCA alone.

1. Baraminic Distance

BDISTMDS version 2.0 was used to carry out BDC calculations on datasets (Wood 2005; 2008b). Baraminic distance is a measure of correlation any two organisms share in their character states (Robinson and Cavanaugh 1998; Wood 2001). BDC obtains a distance based on linear regression as a measure of similarity. The goal is to identify groups united by significant, positive correlation (interpreted as continuity between groups) and those separated by significant, negative correlation (interpreted as discontinuity between groups). Characters that do not have a minimum standard of relevance (i.e., percentage of taxa for which the character state is known) are removed from analyses. Since a purpose of this study involved an interest in minimizing missing data, groups that retained the highest relevance were chosen. Cutoffs ranged from 95% relevance to 75%. A hypothetical outgroup was added to each data matrix to provide a consistent and easily visualized reference location. The position labeled OUTGROUP included character states of "0" and was added for visual reference to all datasets, but particularly for PCA. This outgroup assignment provided a common visual reference point for all analyses (*i.e.,* BDIST, MDS, and PCA).

2. Multidimensional Scaling

As commonly employed in baraminic distance studies, three-dimensional classical MDS was used for comparison (Wood 2005). MDS converts a matrix of Euclidean distances between objects into *k*-dimensional coordinates of the objects. In this study, *k* represents three dimensions. Unlike previous baraminic studies, this study introduces a small difference in the MDS analyses. Data points were colored and plotted in the software environment R using a three-dimensional grid rotated to highlight maximum point separations. The rotational grid is a different way to visualize data but has identical spatial interpretation as other studies in baraminology.

Secondly, the classical MDS function utilized here employed scree plots – rather than stress plots – to visualize the influence of dimensionality reduction. Scree plots employed graphs showing the eigenvalues of each component as a ratio of the eigenvalue sum over all eigenvalues. The relative eigenvalue of each component then represents the proportion of data variance explained by the component. The scree plot shows the decrease in eigenvalue with each component, with the components prior to the "break" in the plot showing the optimal number of components needed to explain the data. Explanation of the data is greatest prior to where the "scree" line levels off (i.e., axes with highest values explain the most).

An eigenvalue equation describes an eigenvector, v, of a linearly transformed matrix (T) that does not change the direction of T. T applied to the eigenvector scales the eigenvector by a scalar multiple, λ, with the following relationship:

$$T(v) = \lambda v$$

A linear transformation of a spatial grid is a type of shear mapping. Eigenvectors provide direction of shear distortions while eigenvalues are the measure of distortion generated by a transformation

Eigenvalues show variances. The scree plot depicts the eigenvalues plotted in the order they are factored, by component axes, with the first largest values explaining the majority of the variance and others showing progressively less. Scree plots display the most important components as those lying above a scree, or gradually tapering, line. Plots often depict a sharp drop followed by gradual decline.

3. Principal component analysis

In addition to BDC and 3D MDS, this study employed PCA as a second means of visualizing discontinuity. One advantage of PCA is that each component axis is biologically meaningful. Since each component axis is a multivariate combination of

discrete morphological character data, the component axes provide interpretable information. Regardless of the complexity of information reflected in some axes, one thing is clear: taxa with a high degree of morphological similarity ordinate closely while morphologically disparate taxa ordinate at greater spatial distances. As a result, the manner in which taxa cluster reveals important information for baraminology (e.g., large quadrupedal dinosaurs will cluster in one region while smaller, bipedal dinosaurs cluster separately at a spatial distance). Differences between dinosaur groups are revealed by distances in *n*-dimensional space. PCA is frequently used in biology to visualize morphological relationships and developmental patterns (e.g., for use with landmark data see Zelditch et al.. 2004, p. 15; for phylogenetic applications see Polly et al., 2013).

Principal component axes (PCs) represent shape variables with the first principal component axis representing the feature(s) that are the most responsible for variation within the class of subjects – here they are character states. Each additional PC is orthogonal to the previous PC and accounts for the next most important source of variation in the data. Thus, the second axis accounts for the second highest source of variation, and so on, until all variation is explained. Since the axes are orthogonal, it can be assumed that the data accounting for the variation along each axis is uncorrelated with the others. The sum of variation accounted for in each axis is cumulative, with most variation typically occurring within the first several components; higher component axes, representing a very small percentage of variation, often amount to little more than "noise" in the data. The advantage of PCA for baraminic studies is that it allows an additional visualization of the relationship between baraminic groups. A simple application of PCA, standard in R, uses a mean-centered ordination of traits and a covariance matrix of variables. Correlation between the principal components, and the original variables, generate component loadings. Loadings are analogous to correlation coefficients and show to what degree each variable is explained by the component.

As is true for all statistical analyses, PCA encounters a formidable problem with even the best dinosaur character matrices: missing data. Every dinosaur matrix used in this study had missing data. For example, missing data percentages for the matrices in this study dated after 2004 ranged from 24.1% up to 62.4% (average of 48%). To account for this high proportion of missing data we employed a probabilistic substitution method to replace missing data in every matrix (Stacklies et al. 2007; Stacklies et al. 2017). Missing value substitution allowed entire matrices to be analyzed that would have otherwise been incomplete and provided the most complete analysis of every matrix. In addition to probabilistic replacement, a second step to insure more accurate analyses was to remove species with an unreasonably high proportion of missing data. Unless otherwise stated, data from the 2004 matrices only included taxa with 75% or more complete character data. The most recent matrices included only taxa with 50% or more complete data.

PCA results were plotted listing taxon names for easy identification of spatial relationships. When possible, ordinations were presented as biplots containing both taxon names and variable vectors. Variable vectors indicate correlation between morphological features; common vector directions show strong correlation between morphological variables while opposed vectors indicate negative correlation. Ordination of taxa are a function of the total contribution of all positive (and negative) contributions for each variable. As a result, two or more taxa closely grouped within component space share similar morphology, and are interpreted as being biologically continuous. In contrast, spatially-separated taxa lack similarity, and distantly spaced members are interpreted as biologically discontinuous.

4. Data

Data from 37 different character matrices were employed for this study. Data sets from 2004 (Weishampel et al. 2004) were analyzed with BDC, MDS, and PCA. The 19 more recent matrices were analyzed by PCA, and two with BDC. Matrices varied in the number of taxa, variables, and proportions of missing data. For example, Weishampel's matrices ranged from six dinosaurs to 70 while character sets ranged from 20 to more than 600 characters. The highest character relevance cutoffs were used for each BDC analysis (e.g., 0.9 was preferred to 0.8). Though probabilistic replacement routines were employed for all PCA analyses, taxa with greater than 50% missing character data were generally removed. However, all taxa were analyzed in small datasets. For the 18 BDC analyses, data from Weishampel included the following:

The matrix for "basal" Saurischia consisted of 10 taxa and 107 characters. After filtering at the 0.9 character relevance cutoff we used 39 characters to calculate baraminic distances.

The matrix for Ceratosauria consisted of 18 taxa and 70 characters. After filtering at the 0.75 character relevance cutoff we used 39 characters to calculate baraminic distances.

The matrix for "basal" Tetanurae consisted of 59 taxa and 638 characters. After filtering at the 0.75 character relevance cutoff we used 199 characters to calculate baraminic distances.

The matrix for Tyrannosauroidea consisted of 24 taxa and 638 characters. After filtering at the 0.75 character relevance cutoff we used 181 characters to calculate baraminic distances.

The matrix for Maniraptoriformes consisted of 12 taxa and 220 characters. After filtering at the 0.95 character relevance cutoff we used 72 characters to calculate baraminic distances.

The matrix for Therizinosauroidea consisted of 13 taxa and 40 characters. After filtering at the 0.75 character relevance cutoff we used 18 characters to calculate baraminic distances.

The matrix for Oviraptorosauria consisted of 13 taxa and 161 characters. After filtering at the 0.8 character relevance cutoff we used 61 characters to calculate baraminic distances.

The matrix for Prosauropoda consisted of 23 taxa and 137 characters. After filtering at the 0.8 character relevance cutoff we used 31 characters to calculate baraminic distances.

The matrix for Sauropoda consisted of 12 taxa and 309 characters. After filtering at the 0.8 character relevance cutoff we used 182 characters to calculate baraminic distances.

The matrix for "basal" Thyreophora consisted of 7 taxa and 32 characters. After filtering at 0.85 character relevance cutoff we used 24 characters to calculate baraminic distances.

The matrix for Stegosauria consisted of 10 taxa and 55 characters. After filtering at 0.80 character relevance cutoff we used 22 characters to calculate baraminic distances.

The matrix for Ankylosauria consisted of 24 taxa and 63 characters. After filtering at 0.95 character relevance cutoff we used 13 characters to calculate baraminic distances.

The matrix for "basal" Ornithopoda consisted of 12 taxa and 54 characters. After filtering at 0.80 character relevance cutoff we used 22 characters to calculate baraminic distances.

The matrix for "basal" Iguanodontia consisted of 17 taxa and 67 characters. After filtering at 0.95 character relevance cutoff we used 14 characters to calculate baraminic distances.

The matrix for Hadrosauridae consisted of 21 taxa and 105 characters. After filtering at 0.75 character relevance cutoff we used 58 characters to calculate baraminic distances.

The matrix for Pachycephalosauridae consisted of 10 taxa and 35 characters. After filtering at 0.8 character relevance cutoff we used 28 characters to calculate baraminic distances.

The matrix for "basal" Ceratopsia consisted of 12 taxa and 148 characters. After filtering at 0.95 character relevance cutoff we used 26 characters to calculate baraminic distances.

The matrix for Ceratopsidae consisted of 16 taxa and 73 characters. After filtering at 0.75 character relevance cutoff we used 59 characters to calculate baraminic distances.

Matrices published since 2004 had greater numbers of taxa and character variables. These matrices were almost exclusively analyzed with PCA. Two groups were also analyzed with BDC (Ceratosauria and Sauropodomorpha) in order to compare with PCA results. Unless otherwise stated, matrices include culled datasets where taxa with less than 50% of their characters were removed; all taxa were analyzed in several small matrices. As with PCA analyses of the 2004 matrices, missing data was replaced with a probabilistic replacement routine. Dinosaur groups, and matrices, included the following:

The Dinosauria matrix consisted of 452 characters for 126 taxa (Baron 2018). We examined both the complete data set in addition to only the 36 taxa with at least 50% of their character states known.

The matrix for "basal" Saurischia consisted of 315 characters for 40 taxa (Nesbitt et al. 2009). We examined the 30 taxa with at least 50% of their character states known.

The matrix for Abelisauroidea consisted of 206 characters for 24 taxa (Brissón Egli, F. et al. 2016). We examined all 24 taxa with PCA. BDC was filtered at the 0.75 character relevance cutoff.

The matrix for basal Tetanurae consisted of 351 characters for 58 taxa (Carrano et al. 2012). We examined the 27 taxa with at least 50% of their character states known.

The matrix for Tyrannosauroidea consisted of 249 characters for 33 taxa (Brusatte and Carr 2016). We examined the 21 taxa with at least 50% of their character states known.

The matrix for Ornithomimosauria consisted of 568 characters for 98 taxa (Chinzorig et al. 2018). We examined the 37 taxa with at least 50% of their character states known.

The matrix for Therizinosauria consisted of 348 characters for 76 taxa (Zanno 2010). We examined both the full dataset and the 26 taxa with at least 50% of their character states known.

We analyzed a Maniraptoran matrix in place of Weishampel's Oviraptorosauria. The matrix consisted of 560 characters for 132 taxa (Foth and Rauhut 2017). We examined both the complete dataset and the 46 taxa with at least 50% of their character states known.

The matrix for "basal" Sauropodomorpha consisted of 375 characters for 58 taxa (Bronzati 2017). We examined the 28 taxa with at least 50% of their character states known.

Another matrix for "basal" Sauropodomorpha consisted of 370 characters for 55 taxa (Otero et al., 2015). We examined the 32 taxa with at least 50% of their character states known for PCA. BDC was filtered at the 0.75 character relevance cutoff.

The matrix for basal Thyreophora consisted of 227 characters for 49 taxa (Breeden 2016). We examined the 27 taxa with at least 50% of their character states known.

The matrix for Stegosauria consisted of 91 characters for 22 taxa (Raven and Maidment 2017). We examined all 22 taxa.

The matrix for Ankylosauria consisted of 178 characters for 55 taxa (Zheng 2018). We examined the 21 taxa with at least 50% of their character states known.

The matrix for "basal" Ornithopoda consisted of 135 characters for 69 taxa (Madzia 2017). We examined the 26 taxa with at least 50% of their character states known.

The matrix for "basal" Iguanodontia consisted of 134 characters for 67 taxa (McDonald 2012). We examined the 26 taxa with at least 50% of their character states known.

The matrix for Hadrosauridae consisted of 346 characters for 58 taxa (Cruzado-Caballero 2017). We examined all 58 taxa.

The matrix for Pachycephalosauridae consisted of 48 characters for 17 taxa (Schott 2011). We examined all 17 taxa.

The matrix for "basal" Ceratopsia consisted of 381 characters for 71 taxa (Han 2017). We examined the 40 taxa with at least 50% of their character states known.

The matrix for Ceratopsidae 152 characters for 29 taxa (Fry 2015). We examined all 29 taxa.

RESULTS

Results are described by taxonomic group, first for the saurischians and then ornithischians. Analyses included BDC, MDS, and PCA for each group. PCA for the Dinosauria was performed to better understand the overall relationships of the new Ornithoscelida (Ornithischia and Theropoda) to Saurischia (Sauropodomorpha and Herrerasauridae) (Baron et al. 2017) within a creation systematics. When all data were analyzed, three spatially-identifiable groups emerged on PC 1 and PC 2: 1) non-dinosaurs with some dinosaurs, 2) Sauropodomorpha, and 3) a combined (though distinct) Ornithischia/Theropoda association (Fig. 1). For PC 3 nearly all groups were indistinguishable except Ornithischia (Fig. 2).

The inclusive Dinosauria plots serve as a contrast to the second culled ordination plot. The second Dinosauria ordinations included

only taxa with 50% or greater complete character data; taxa with larger amounts of missing data were removed. Group ordinations visible within the inclusive dataset became more distinct when taxa with high percentages of missing data were removed (Figs. 3-4). We present possible explanations for this phenomenon in the Discussion.

The remainder of the analyses in this study employ a 50% data cutoff, unless otherwise indicated. Dinosaurs are grouped within Ornithischia and Saurischia following Weishampel et al. (2004).

1. Saurischia

A. Basal Saurischia

The baraminic distance correlation results for the Langer (2004) data matrix, in Weishampel et al. (2004), are shown in Fig. 5. Results suggest separation between the saurischians and ornithischians plus *Pisanosaurus*. Positive BDC is present between *Saturnalia*, Sauropodomorpha, and *Guaibasaurus* and between *Staurikosaurus*, *Herrerasaurus* and the outgroup. Limited negative correlation exists between the ornithischians and some saurischians. Classical MDS results show little separation between the saurischians *Saturnalia*, Sauropodomorpha, *Guaibasaurus* and other groups. The outgroup, *Eoraptor*, *Pisanosaurus* and remaining ornithischians reflect no obvious clustering (Fig. 6). PCA results suggest separation but show no clustering between the few groups represented (Fig. 7).

PCA results for Nesbitt et al. (2009) provide a more complete picture but retain the group separations. PC 1 separates dinosaurs from the non-dinosaurian outgroup taxa (Fig. 8). PC 2 separates theropods from herrerasaurids, sauropodomorphs, and ornithsichians. PC 3 reveals little distinction between dinosaur taxa, which are all clustered together, but it does separate out the non-dinosaurian taxa (Fig. 9). Pseudosuchians cluster at the bottom, whereas the only pterosaur (*Dimorphodon*) is at the top, closer to *Euparkeria*, *Erythrosuchus*, and the hypothetical outgroup.

B. Ceratosauria

The BDC results for Tykoski and Rowe's (2004) data matrix, in Weishampel et al. (2004), show three blocks of positive correlation (Fig. 10). There is shared positive correlation among coelophysoid taxa and Spinosauridae in the upper right block. There are a few instances of shared positive correlation between the coelophysoid + spinosaurid block and the middle block. The abelisauroid taxa (lower left) all share positive correlation and share negative correlation or no correlation with any other taxa. Classical MDS results show separation between Abelisauroidea and all other taxa (Fig. 11). PCA results show separation between Coelophysidae and the other taxa, but there is little clustering (Fig. 12) Abelisaurid taxa are separated out from the others through PC 1.

The BDC results for Brissón Egli et al's (2016) abelisauroid data matrix are shown in Fig. 13. BDC separates Abelisauridae from the non-abelisaurid taxa (including non-abelisaurid abelisauroids, non-abelisauroid ceratosaurs, and other non-ceratosaur taxa). The only exception is that the Jurassic, "basal" abelisaurid *Eoabelisaurus* is included in the non-abelisaurid block of taxa, correlating positively with *Ceratosaurus*, *Limusaurus*, and *Masiakasaurus*.

The Abelisauroidea matrix had a high proportion of missing data. In order to preserve enough taxa for comparison, all taxa were included regardless of their proportions of missing data. PC 1 separated abelisaurids from the other taxa (Fig. 14). Noasauridae members (*e.g., Limusaurus* and *Masiakasaurus*) are widely spaced from members of Abelisauridae, although they are not clustered closely together, nor are they readily distinguished from the outgroup taxa. *Eoabelisaurus*, as with the BDC results, does not cluster with the abelisaurids, but is instead closest to *Ceratosaurus* and *Genyodectes*, a position that matches a recent ceratosaurian phylogeny (Wang et al., 2017). The Abelisauroidea form a series along PC 3 with the noasaurids clustered toward the bottom (Fig. 15). *Eoabelisaurus* is separated from the abelisauroids, once again closest to *Ceratosaurus* and *Genyodectes*.

C. Basal Tetanurae

The BDC results for Holtz et al.'s (2004) data matrix, in Weishampel et al. (2004), for "basal" Tetanurae and Tyrannosauroidea are shown in Fig. 16. Because the matrix included several groups above the family-level, including Tyrannosauridae, the BDC chart is ambiguous, only really distinguishing between Maniraptoriformes and other theropods. The BDC is displayed as a contrast to PCA results (Fig. 17), illustrating a limit in baraminic analysis for some datasets. BDC failed to distinguish groups with high disparity: Tyrannosauroidea, Maniraptoriformes, and other Theropoda. PCA reveals complex ordination patterns in the presence of large morphospatial disparities. Non-coelurosaur theropods and Tyrannosauroidea show a discontinuous morphoseries with a common trajectory. Maniraptoriforms cluster separately.

PCA results for Carrano et al. (2012) showed a similar morphospatial series among the tetanurans (Fig. 18). Both PC 1 and PC 2 display distance between tetanurans and non-tetanuran theropods (Fig. 18). Additionally, tetanurans contain a series of spatially-connected taxa, linked gradationally from *Sinosaurus* (formerly *"D. sinensis"*) to Megalosauridae to Coelurosauria, to Allosauroidea. The spinosaurids (*Suchomimus* and *Baryonyx*) are clustered together and are slightly removed from the tetanuran series. For PC 1 and PC 2 the Megalosauridae series may be stratomorphic, with fossil record first appearance order tracking the morphoseries (Wise 1995), but recent phylogenies suggest *Monolophosaurus* is more basal than Megalosauridae (Carrano et al. 2012). Additionally, *Compsognathus* and *Ornitholestes*, coelurosaurs, are clustered among the megalosaurids. PC 3 clusters *Sinosaurus* ("*D. sinensis*") with the coelophysoids, and it separates out carcharodontosaurids from other tetanurans (Fig. 19).

D. Tyrannosauroidea

The BDC results for Holtz's (2004) data matrix, in Weishampel et al. (2004), are shown in Fig. 20. This analysis was a tyrannosauroid-focused subset of the Holtz et al. (2004) dataset. There is clear positive BDC between the Tyrannosauroidea and negative BDC compared to several theropod outgroups. Classical MDS results confirm separation between Tyrannosauroidea and all other neotheropods (Fig. 21). Due to the small dataset, PCA was employed on groups with as little as 30% complete character data. PCA results likewise support the separation between Tyrannosauroidea and other groups seen in MDS, although *Eotyrannus* was distant from the other tyrannosauroids (Fig. 22).

Tyrannosauridae from Brusatte and Carr (2016) display a similar

morphospatial series that is separated from outgroup taxa. Tyrannosaurines form one diagonal series along PC 1 and PC 2 (Fig. 23). A second series, perpendicular to the tyrannosaurine series, contains albertosaurines, *Bistahieversor*, and two non-tyrannosaurid tyrannosauroids (*Raptorex* and *Xiongguanlong*). *Eotyrannus* is not on either trajectory and is equally spaced between *Xiongguanlong* and the non-tyrannosauroid *Allosaurus*. Other "basal" tyrannosauroids (e.g., *Dilong* and *Guanlong*) cluster together at a great distance from tyrannosaurids, *Raptorex*, *Xiongguanlong*, and *Eotyrannus*. *Yutyrannus* is far from all other taxa. The plot comparing PC 3 and PC 1 shows tyrannosaurids spread out along the left side of the plot from top to bottom (Fig. 24). By contrast, non-tyrannosaurid tyrannosauroids form a series with *Raptorex* on the left and proceratosaurids on the right. This series includes all of the non-tyrannosaurid tyrannosauroids, even *Yutyrannus*. The outgroup taxa are all clustered in the lower right corner, far from any tyrannosauroids.

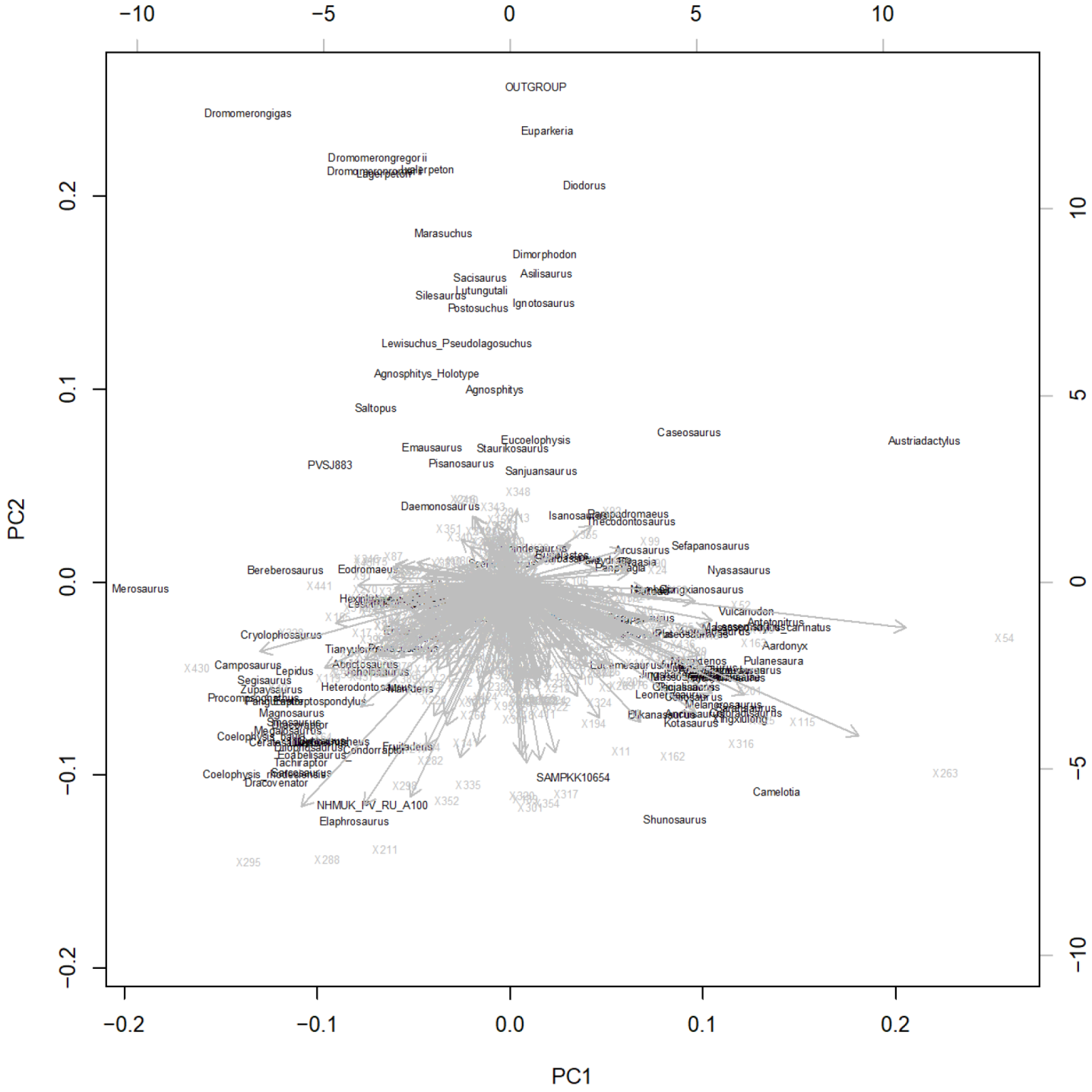

Figure 1. Biplot of PCA scores (black) and vectors (gray) for Baron et al's (2018) complete data matrix for the Dinosauria. PC 1 accounts for 32.5% of the variance and PC 2 accounts for 20.0% of the variance. Sauropodomorpha group toward bottom right while the newly revised Ornithoscelida, including ornithischians and theropods, group toward the bottom left.

E. Maniraptoriformes

The BDC results for Makovicky et al.'s (2004) data matrix, in Weishampel et al. (2004), shows three blocks of positive correlation and two taxa that are not correlated with any other taxa (the alvarezsaurid *Shuvuuia* and the oviraptorid *Citipati*, Fig. 25). One block of positive correlation contains the outgroup taxa, one contains ornithomimids, and the final one contains paravians (two dromaeosaurids, a troodontid, and *Archaeopteryx*). The paravian block is separated from the ornithomimid block by negative correlation, but no other taxa share any kind of correlation with the outgroup block. Due to the amount of missing data (*i.e.,* the majority were missing greater than 70% of the character data) only 12 taxa were analyzed. Classical MDS results also show separation between three clusters of taxa, although *Citipati* appears to be closest to the paravian cluster (Fig. 26). *Shuvuuia* is positioned far from all other taxa.

PCA reflected these observations but revealed additional complexity. The high proportion of missing data required the inclusion of any

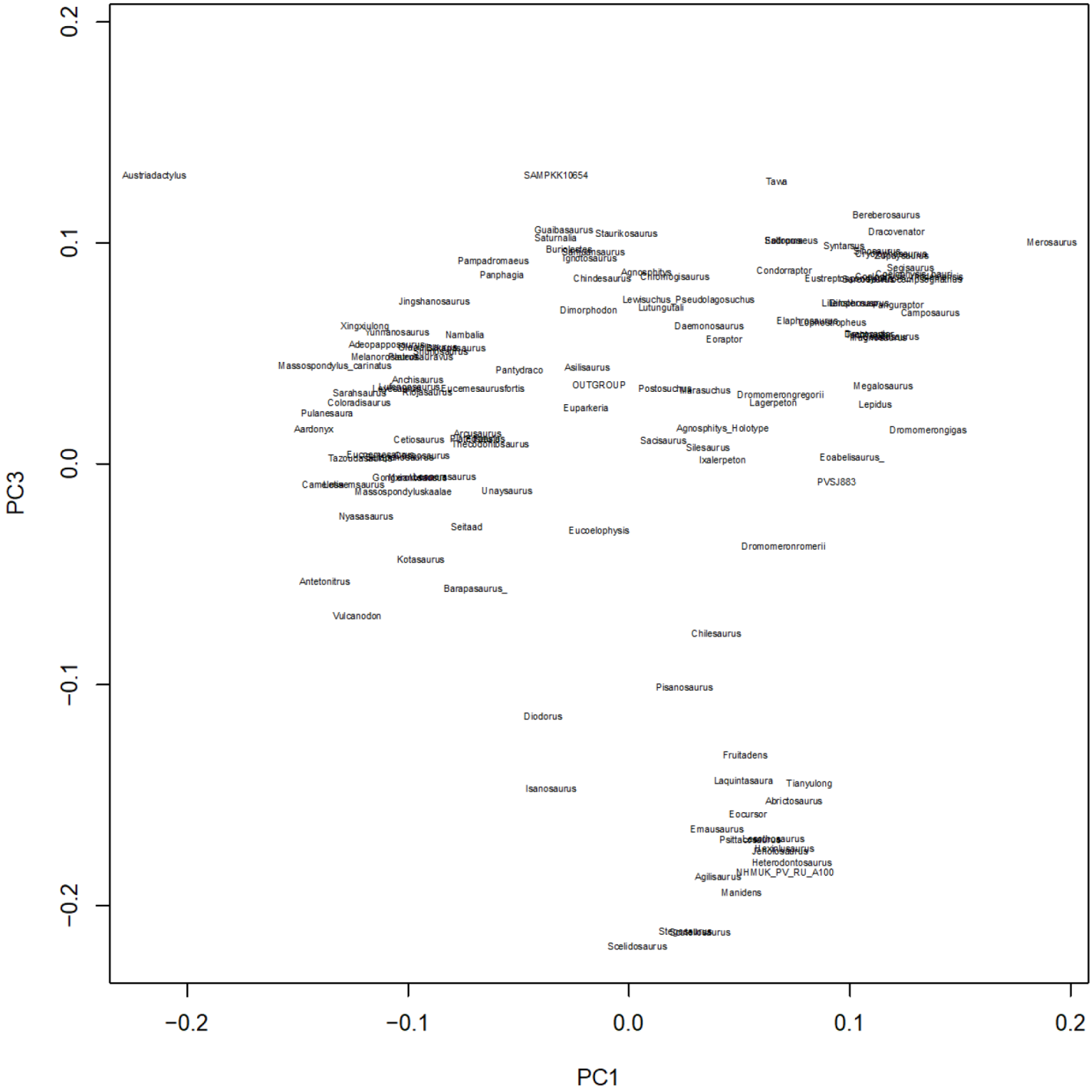

Figure 2. PCA scores for Baron's (2018) complete data matrix for the Dinosauria. PC 1 accounts for 32.5% of the variance and PC 3 accounts for 14.6% of the variance. Sauropodomorpha group toward left and Theropods to right. PC 3 separates only ornithischians (bottom cluster).

genus having 20% or more complete data. Four main clusters (Fig. 27) are obvious: Ornithomimosauria, Dromaeosauridae, Troodontidae, and Oviraptorosauria, although there is not much separation between Dromaeosauridae and Troodontidae. Two alvarezsaurids grouped together (*Patagonykus* and *Alvarezsaurus*), but they did not cluster with the other alvarezsaurids (*Mononykus* and *Shuvuuia*). Oddly, *Utahraptor* did not group with the other dromaeosaurids (it is instead close to tyrannosaurids). Avialans, especially *Archaeopteryx*, were closest to the dromaeosaurid cluster.

Ornithomimosauria for Chinzorig et al. (2018) likewise showed spatial separation from all other taxa for PC 2 (Fig. 28). A division within Ornithomimosauria is also visible between Ornithomimidae (*Gallimimus*, *Struthiomimus*, and *Ornithomimus*) and Deinocheridae (*Garudimimus* and *Deinocherius*), with *Harpymimus* grouping with the latter. PC 3 shows similar separation within the group although

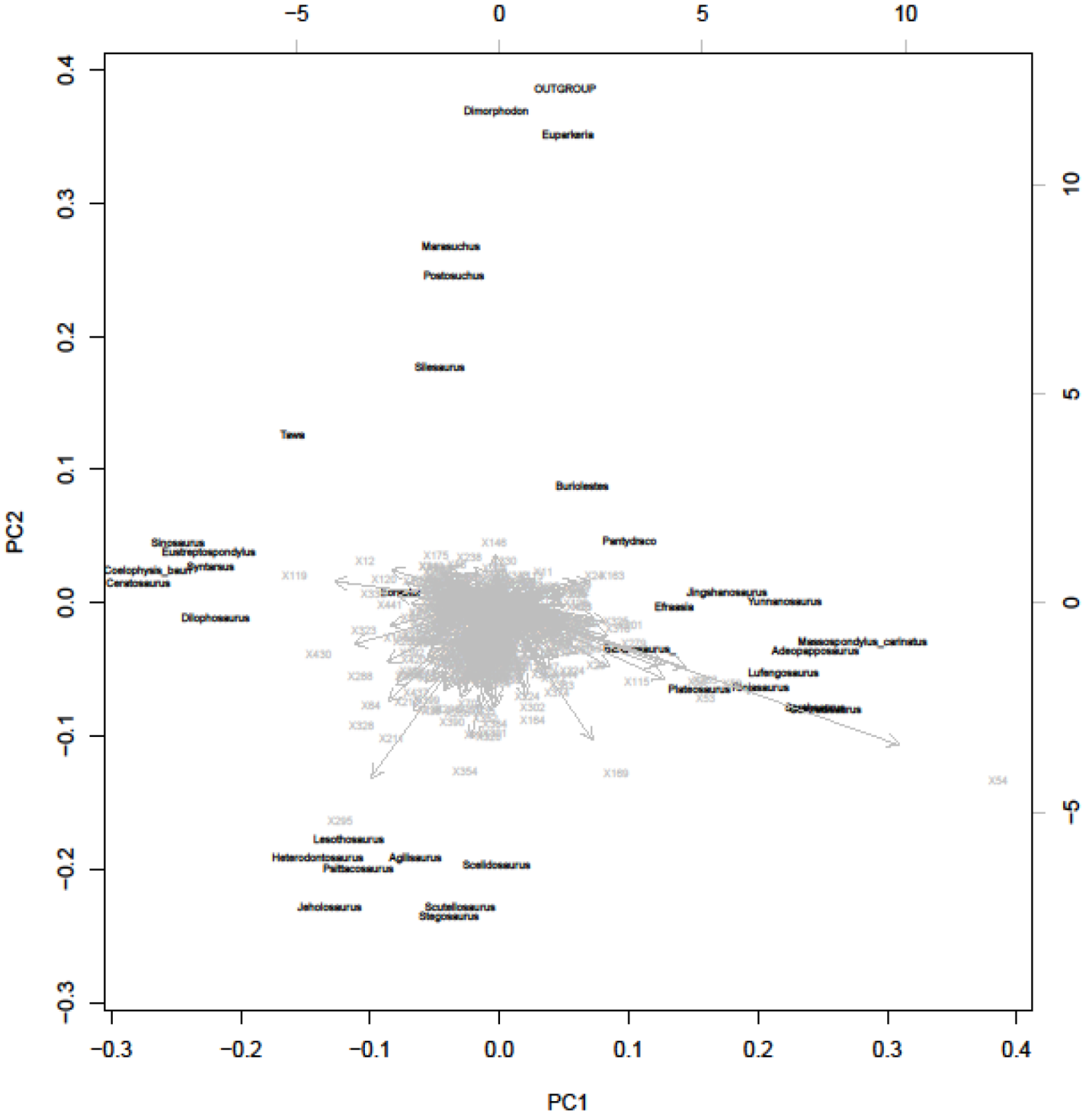

Figure 3. Biplot of PCA scores (black) and vectors (gray) for Baron's (2018) data matrix for the Dinosauria taxa with the most complete data. PC 1 accounts for 26.5% of the variance and PC 2 accounts for 17.5% of the variance. Theropods (left) show discontinuity with ornithischians (bottom) and sauropodomorphs (right).

there is not so pronounced a separation between ornithomimosaurs and other taxa and the "basal" alvarezsauroid *Haplocheirus* is within the ornithomimosaur cluster (Fig. 29).

F. Therizinosauria

The BDC results for Clark's (2004) data matrix, in Weishampel et al. (2004), for the Therizinosauroidea reveals three blocks of positive correlation: two therizinosauroid blocks and a block containing the outgroup (Fig. 30). One therizinosauroid block consists of only therizinosaurids, while the other contains non-therizinosaurid therizinosauroids and the therizinosaurid *Nothronychus*. There is no shared positive correlation between the two therizinosauroid blocks, and neither block shares any positive correlation with the outgroup taxa. The block containing only therizinosaurids shows extensive negative correlation with the outgroup taxa. Classical MDS results reflect the same separation between Therizinosauroidea and the outgroup taxa, with *Nothronychus*, *Beipiaosaurus*, and *Alxasaurus* midway between the groups (Fig. 31). For PCA, only taxa with about 50% of character data were analyzed. PCA results likewise show a great distance between Therizinosauroidea (*Beipiaosaurus*, *Alxasaurus*, *Erlikosaurus*, and *Segnosaurus*) and the outgroup taxa

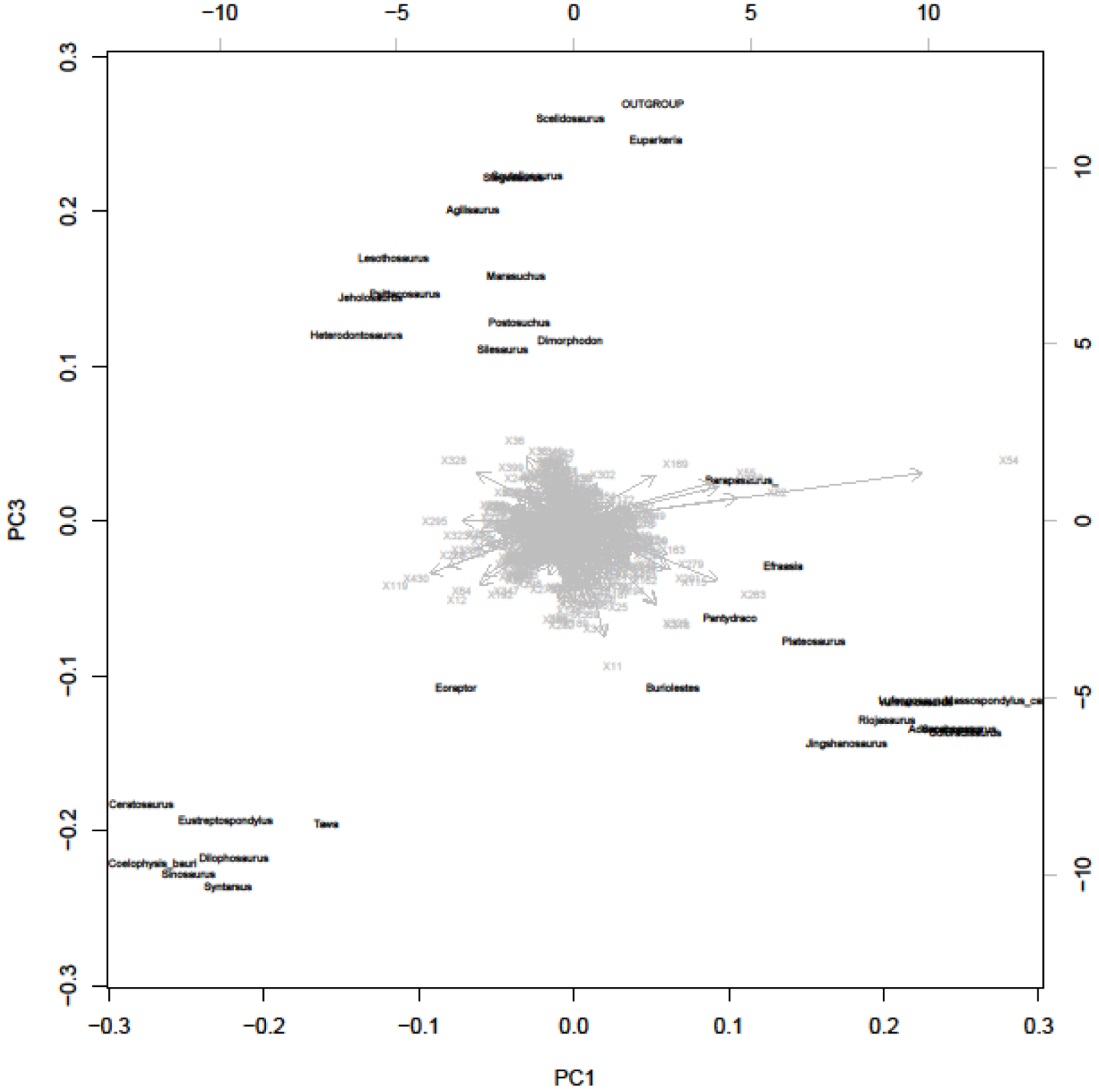

Figure 4. Biplot of PCA scores (black) and vectors (gray) for Baron's (2018) data matrix for the Dinosauria. PC 1 accounts for 26.5% of the variance and PC 3 accounts for 15.0% of the variance. Theropods and ornithischians are separated (left, top respectively) with sauropods grouped to the right.

(Fig. 32).

Zanno (2010) included a larger dataset though few Therizinosauria members included more than 50% of their characters. Because of this, all taxa were analyzed in order to retain a large enough number of therizinosaurs for analysis. Both PC 1 and PC 2 separated Therizinosauridae from the outgroups while locating them most closely to Oviraptorosauria. The non-therizinosaurid therizinosaurs (*Falcarius*, *Beipiaosaurus*, and *Alxasaurus)* are placed in between the therizinosaurids and the alvarezsaurids. In contrast, dromaeosaurids and troodontids ordinate more distantly, and ornithomimosaurs form a series that is even farther away along PC 2 (Fig. 33). PC 3 separated therizinosaurs from the non-maniraptoran theropods and troodontids (Fig. 34). At the same time PC 3 does not distinguish dromaeosaurids, oviraptorosaurs, and therizinosaurs; all exhibit a broad range of spatial overlap. Maniraptoran groups show spatial intergradation though morphospatial distinctions are present.

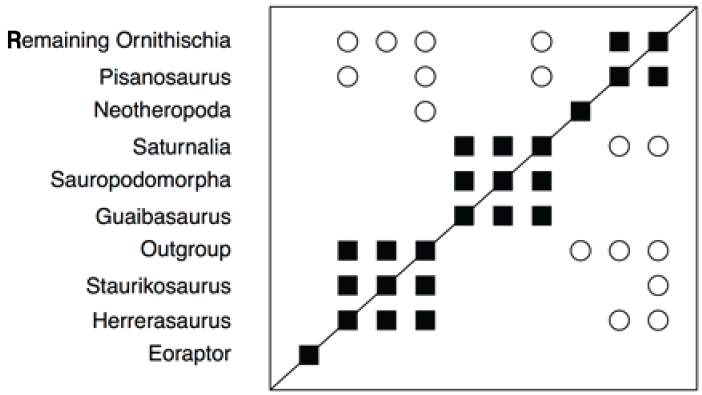

Figure 5. BDC results for Langer's (2004) data matrix of basal Saurischia, as calculated by BDISTMDS (relevance cutoff 0.9). Closed squares indicate significant, positive BDC; open circles indicate significant, negative BDC.

G. Maniraptora

The BDC results for the Osmolska et al. (2004), Makovicky and Norell (2004), Norell and Makovicky (2004), and Padian (2004) combined data, found in Weishampel et al. (2004) for Oviraptorosauria, show two main blocks of positively correlated taxa separated by negative correlation: Oviraptorosauria and the outgroup taxa (*Archaeopteryx*, *Velociraptor*, *Herrerasaurus*, and the hypothetical outgroup, Fig. 35). The oviraptorosaur *Avimimus*, however, does not correlate positively or negatively with any of the other taxa in the analysis. Classical MDS results show separation between Oviraptorosauria and the outgroup taxa (Fig. 36). For PCA, only taxa with at least 55% of character data were analyzed. PCA results likewise show space between Oviraptorosauria and the outgroup taxa. The only difference is that *Caudipteryx* is distant from all other groups (Fig. 37).

The maniraptoran matrix of Foth and Rauhut (2017) contained both more taxa and more characters than the earlier oviraptorosaur dataset. The first analysis (Fig. 38) includes all maniraptorans, without respect to missing data, and again shows spatial distinction with overlapping group ranges reminiscent of the Zanno (2010) therizinosaurian analysis (Fig. 34). Four groups of taxa can be identified: 1) Dromaeosauridae, "basal" Avialae, and

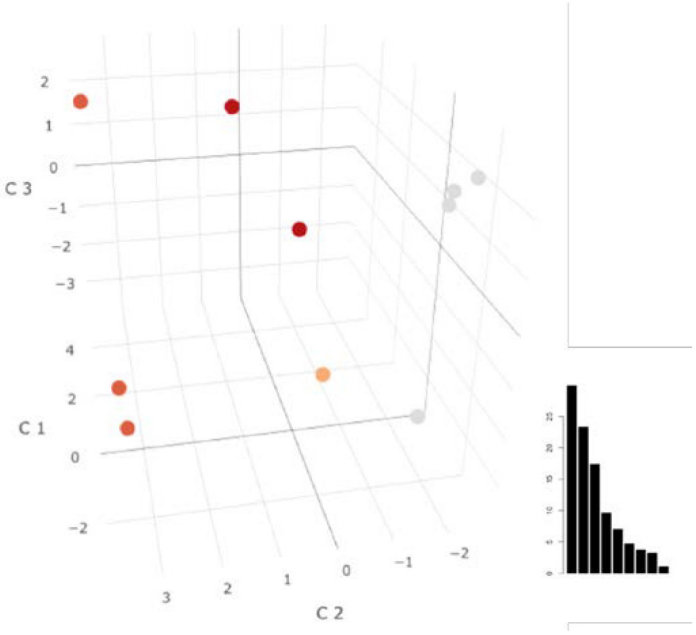

Figure 6. Three-dimensional classical MDS applied to Langer's (2004) data matrix for "basal" Saurischia. Members of Sauropodomorpha are shown in gray, *Eoraptor* in orange, *Herrerasaurus*, *Staurikosaurus*, and the outgroup are dark orange, and *Pisanosaurus* and remaining Ornithischia are red. Scree plot suggests the first three dimensions represent most of the variance.

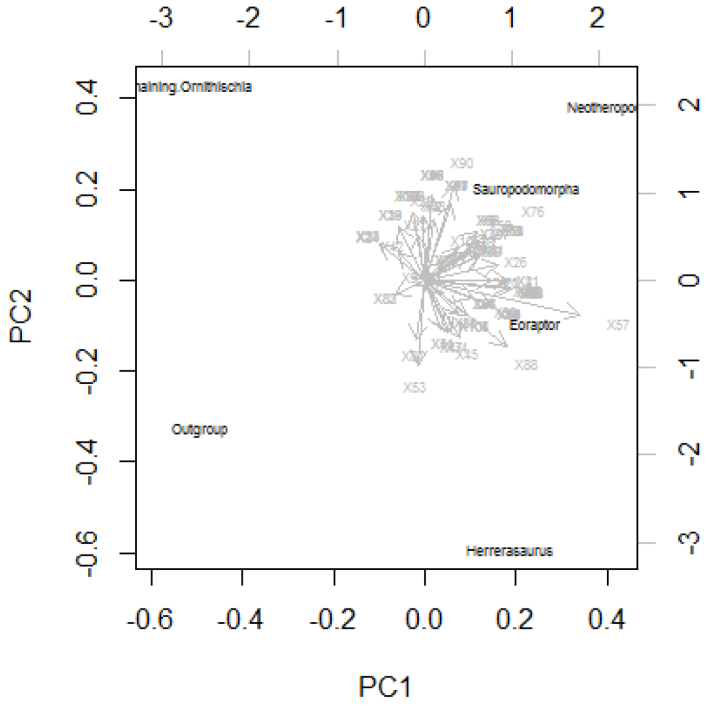

Figure 7. Biplot of PCA scores (black) and vectors (gray) for Langer's (2004) data matrix for basal Saurischia. PC 1 accounts for 37.9% of the variance and PC 2 accounts for 24.7% of the variance. Saurischians align toward the positive side of PC 1 but no other clustering is evident.

Troodontidae; 2) non-coelurosaur theropods, Tyrannosauroidea, "basal" Coelurosauria, Alvarezsauroidea, Ornithomimosauria, Oviraptorosauria, Therizinosauria, and a scansoriopterygid (*Epidexipteryx*); 3) non-avian Pygostylia; and 4) Aves + *Limenavis* + *Iaceornis*. Dromaeosaurid and "basal" avialan ranges ordinate closely, although they are still mainly distinct, for PC 1 (2a and 2b, respectively, in Fig. 38). Troodontids (2c, Fig. 38) mainly ordinate closely between dromaeosaurids and "basal" avialans, but some troodontids (*Byronosaurus* and *Zanabazar*) overlap with the "basal" avialan cluster, and anchiornithids (*Pedopenna* and *Yixianosaurus*), which are probably "basal" avialans, are indistinguishable from dromaeosaurids for PC 1. These paravian taxa are spatially separated from alvarezsauroideans (2d), oviraptorosaurs (4), ornithomimosaurs (3), and "basal" coelurosaurs (1) by PC 2. Non-avian Pygostylia (5) and Aves + *Limenavis* + *Iaceornis* (6) are separate from non-avialan dinosaurs and "basal" avialans for PC 1, and they are separated from each other by PC 2. PC 3 distinguishes ornithomimosaurs (bottom) from

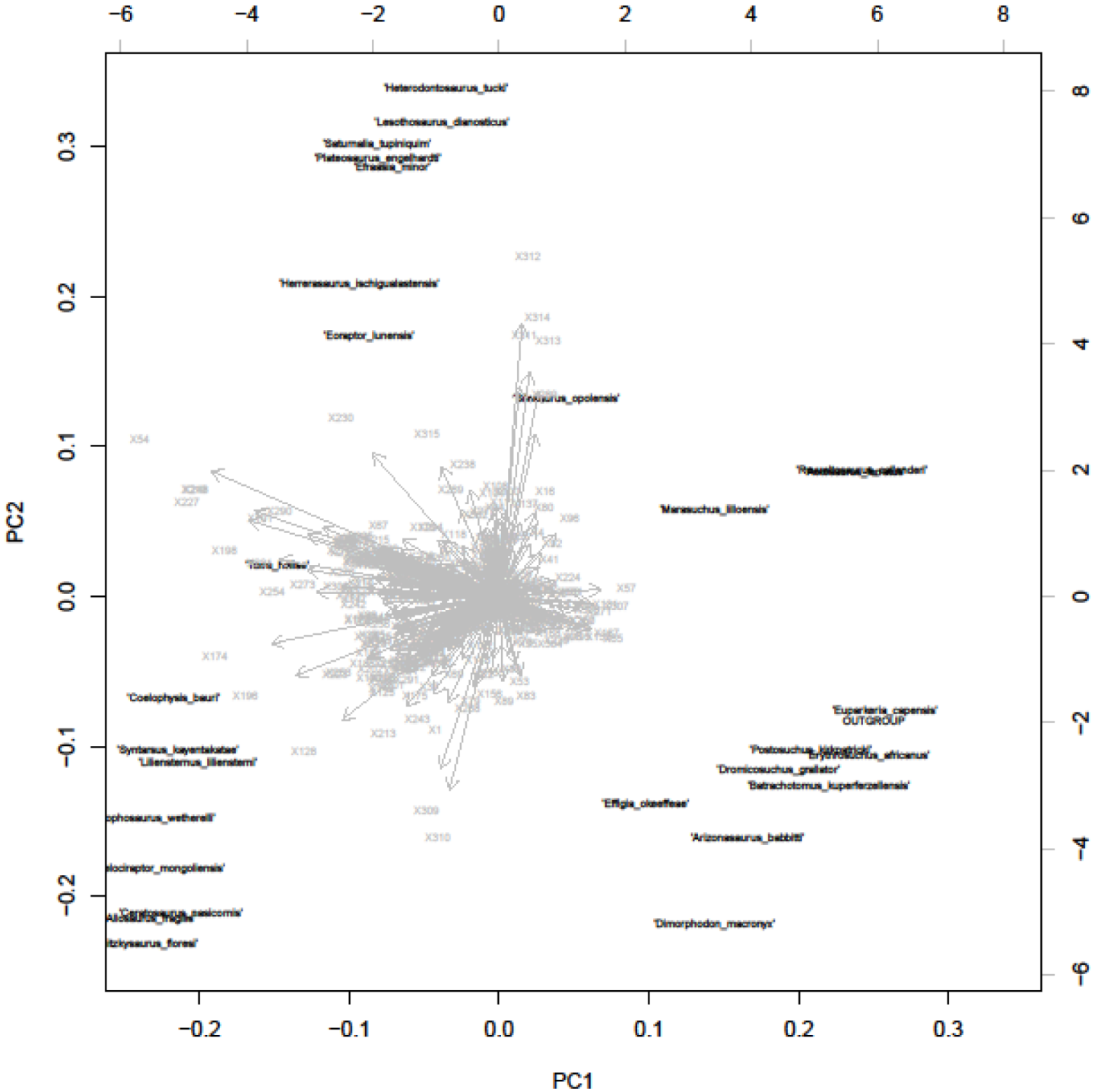

Figure 8. Biplot of PCA scores (black) and vectors (gray) for Nesbitt's (2009) data matrix for basal Saurischia. PC 1 accounts for 37.4% of the variance and PC 2 accounts for 17.1% of the variance. Discontinuity exists between theropods (left), sauropodomorphs, *Herrerasaurus*, and ornithischians (top) and outgroup taxa (right).

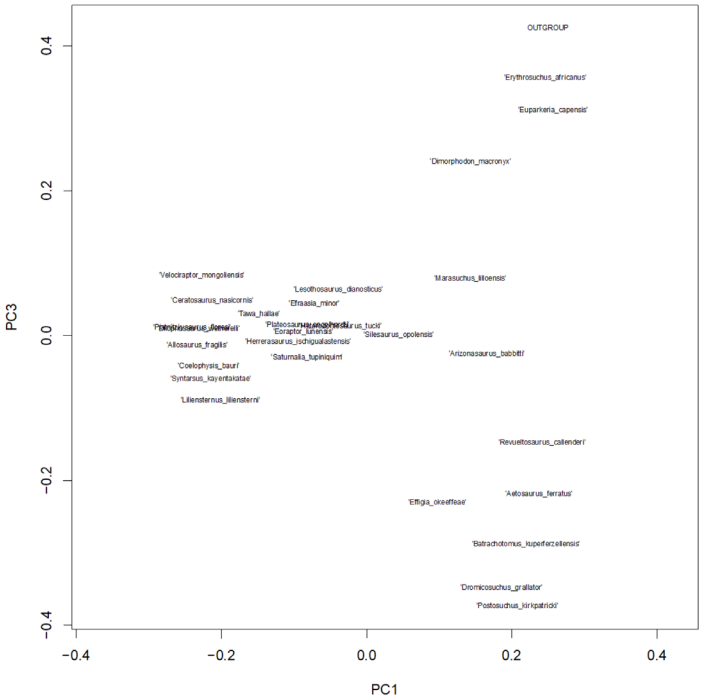

Figure 9. PCA scores for Nesbitt's (2009) data matrix for basal Saurischia. PC 1 accounts for 37.4% of the variance and PC 3 accounts for 9.1% of the variance. PC 3 does not distinguish theropods, sauropodomorphs, and ornithischians; only ingroups and outgroups are separated.

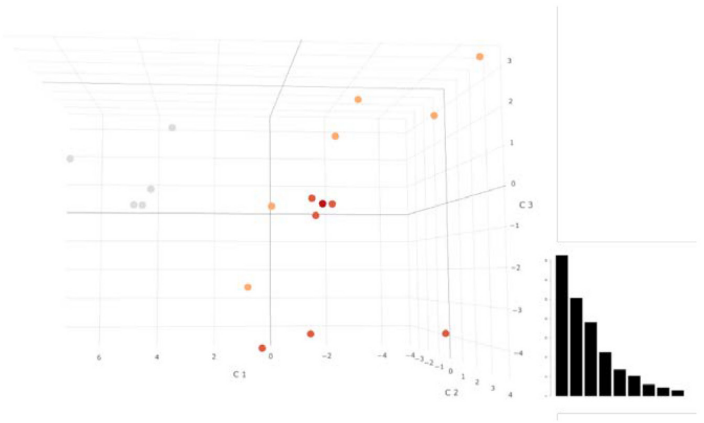

Figure 11. Three-dimensional classical MDS applied to Tykowski and Rowe's (2004) data matrix for Ceratosauria. Members of Abelisauroidea are shown in gray, outgroups (*e.g.,* tetanurans) are in light red, distant outgroup is dark red, and all other taxa are orange (*e.g.,* Coelophysoidea). The outgroup clusters near *Herrerasaurus*, Prosauropoda, and Ornithischia. Scree plot suggests variance is distributed across many axes.

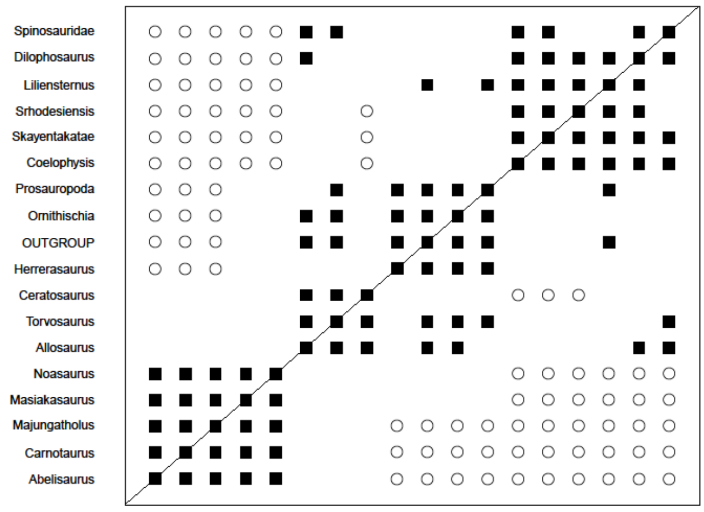

Figure 10. BDC results for Tykoski and Rowe's (2004) data matrix of Ceratosauria, as calculated by BDISTMDS (relevance cutoff 0.75). Closed squares indicate significant, positive BDC; open circles indicate significant, negative BDC.

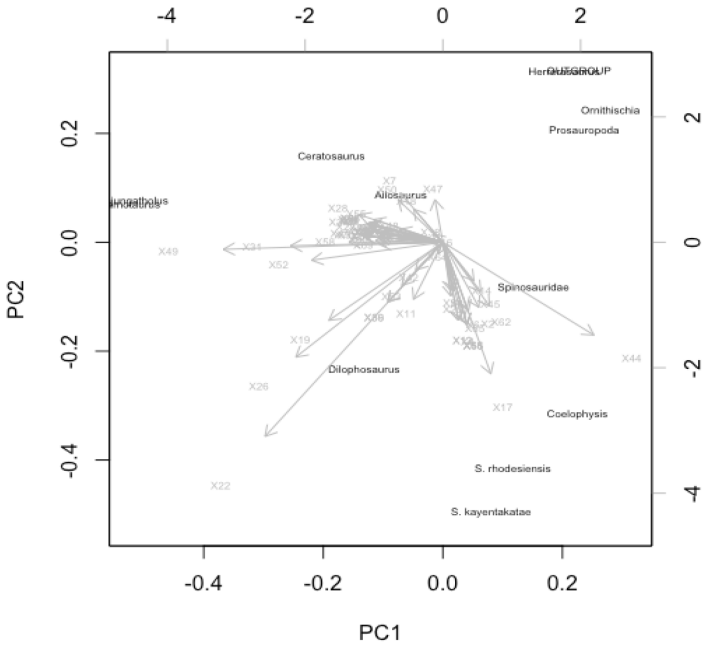

Figure 12. Biplot of PCA scores (black) and vectors (gray) for Tykowski and Rowe's (2004) data matrix for Ceratosauria. PC 1 accounts for 38.4% of the variance and PC 2 accounts for 23.3% of the variance. Coelophysidae members are in bottom right.

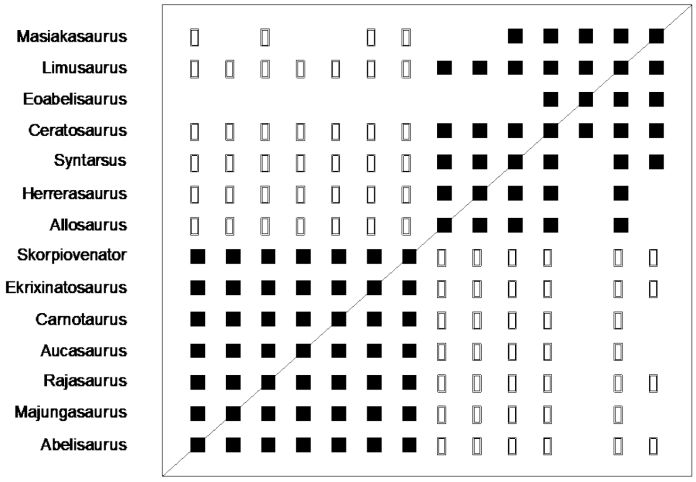

Figure 13. BDC results for Brissón Egli et al.'s (2016) data matrix for Abelisauroidea, as calculated by BDISTMDS (relevance cutoff 0.75). Closed squares indicate significant, positive BDC; open circles indicate significant, negative BDC.

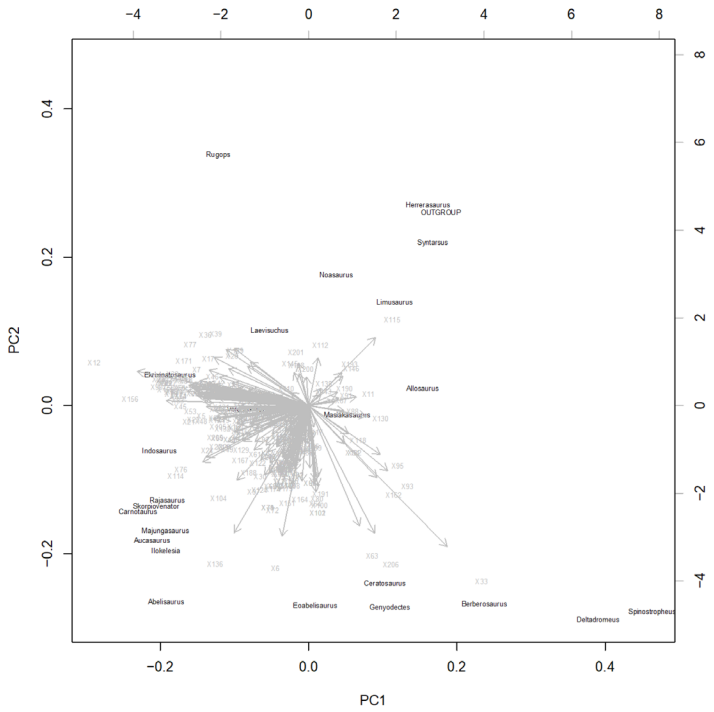

Figure 14. Biplot of PCA scores (black) and vectors (gray) for Brissón Egli et al.'s (2016) complete data matrix for Abelisauroidea. PC 1 accounts for 49.7% of the variance and PC 2 accounts for 24.7% of the variance. Abelisauridae ordinate along the left side of the plot, Ceratosauridae bottom central, and Noasauridae toward the center.

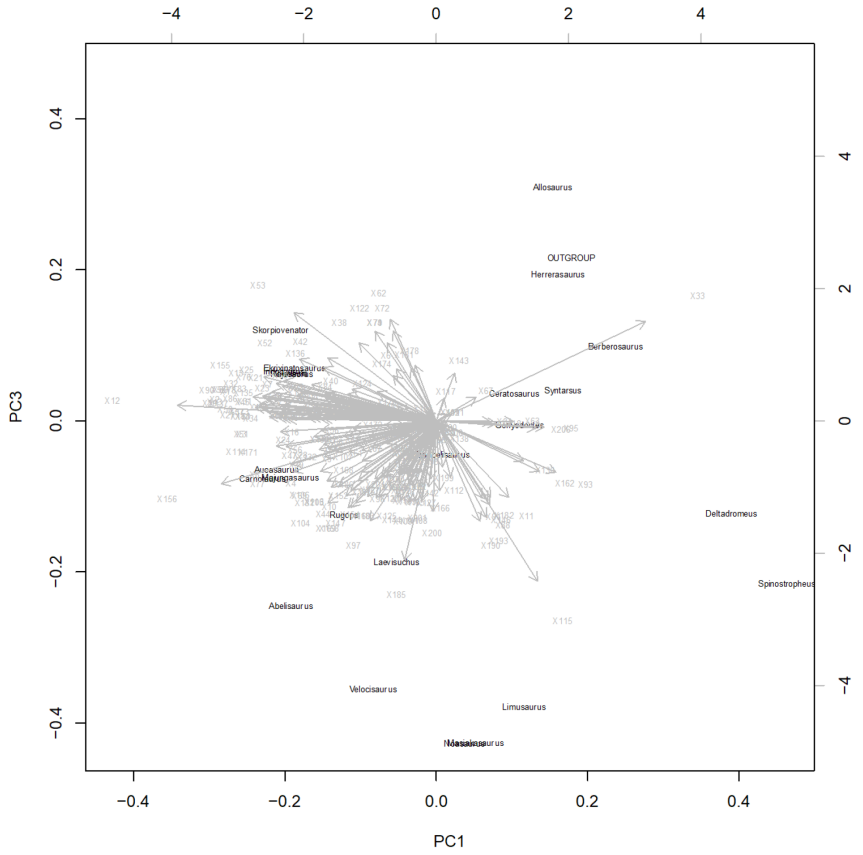

Figure 15. Biplot of PCA scores (black) and vectors (gray) for Brissón Egli et al.'s (2016) complete data matrix for Abelisauroidea. PC 1 accounts for 49.7% of the variance and PC 3 accounts for 13.8% of the variance. Abelisauridae ordinate toward the left, "basal" Ceratosauria near the center and right, and Noasauridae toward bottom.

alvarezsauroids, which are distinguished from "basal coelurosaurs" + tyrannosauroids + outgroup taxa (Fig. 39). Similarly, PC 3 draws out oviraptorosaurs and therizinosaurs (top) from the rest of the taxa, but PC 3 does not seem to distinguish between non-avialan paravians, non-avian avialans, and avians.

Analysis of the same dataset using only the taxa with more complete data yields a different spatial geometry. PCA on taxa with 50% or more complete character data resulted in a Y-shaped ordination, with two distinct morphospatial series (Fig. 40). "Basal" avialans, dromaeosaurids, and troodontids are located at the root of the bifurcation and share some spatial overlap on PC 1 and PC 3 (Fig. 41). Dromaeosaurids are distinct from "basal" avialans and troodontids on PC 2, but "basal" avialans and troodontids are not. One series above the junction included a sequential series from oviraptorosaurs, "basal" coelurosaurs + tyrannosauroids + outgroup taxa, alvarezsauroideans, and ending with ornithomimosaurs. The other series includes non-avian ornithuromophs and culminates with avians. Time of first appearance of members in each group show that the morphoseries sequence is not a chronological first-appearance order. PC 3 reveals a similar branching pattern though provides less distinction between "basal" avialans, alvarezsauroideans, dromaeosaurids, oviraptorosaurs, and ornithomimosaurs (Fig. 41).

H. "Prosauropoda"

The BDC results for Galton and Upchurch's (2004a) data matrix, in Weishampel et al. (2004), reveal two main blocks of positive correlation separated by negative correlation: a large "prosauropod" block and a small sauropod block (Fig. 42). However, the sauropod *Kotasaurus* does not share any positive or negative correlation with any other taxon in the analysis. Similarly, both classical MDS and PCA results separate the prosauropods from all outgroups (Figs. 43 and 44). Removal of the four sauropod taxa from the BDC analysis shows evidence for discontinuity within "prosauropoda" (see Fig. 98 in the Appendix).

PCA for Bronzati (2017) likewise shows separation, but in terms of three clustered groups: 1) traditional "prosauropods" + "basal" sauropods + *Dicraeosaurus*, 2) Sauropoda, 3) *Thecodontosaurus* + *Pantydraco* + Guaibasauridae + outgroup taxa. Although some sauropods seem to group with "prosauropods" in Figs. 45 and 46, "prosauropods" and these sauropods are distinct by PC 1 (Fig. 45).

Figure 16. BDC results for Holtz et al.'s (2004) data matrix of basal Tetanurae, as calculated by BDISTMDS (relevance cutoff 0.75). Closed squares indicate significant, positive BDC; open circles indicate significant, negative BDC.

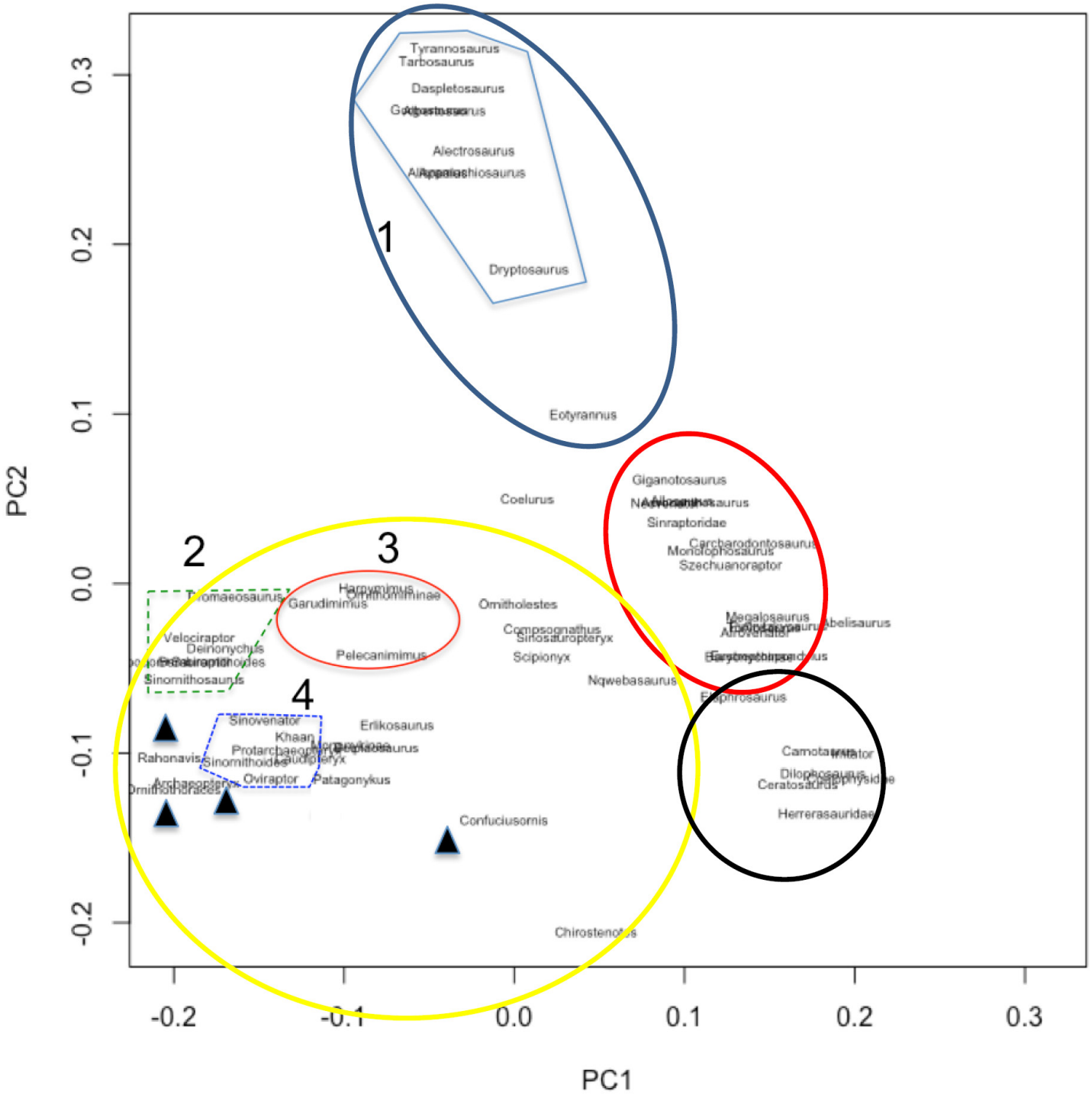

Figure 17. Biplot of PCA scores for Holtz et al.'s (2004) data matrix for basal Tetanurae. PC 1 accounts for 25.2% of the variance and PC 2 accounts for 18.8% of the variance. Four main clusters are evident: Tyrannosauroidea (blue circle), non-tyrannosauroid Coelurosauria (yellow), non-coelurosaur Tetanurae (red), and non-tetanurans (black). PCA revealed several large morphological divisions, not visible to BDIST, including: (1) a Tyrannosauroidea series; Maniraptoriformes grouped together with smaller clusters of Dromaeosauridae (2), Ornithomimosauria (3), a combined Troodontidae and Oviraptorosauria group (4), and scattered Avialae (black triangles). Non-coelurosaur tetanurans ordinate as a morphoseries toward the right.

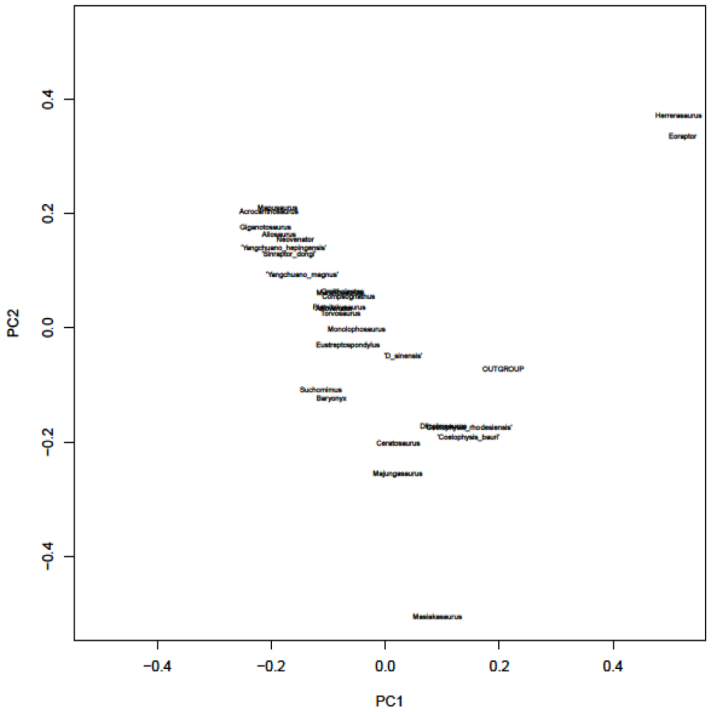

Figure 18. PCA scores for Carrano et al.'s (2012) data matrix for Tetanurae. PC 1 accounts for 29.5% of the variance and PC 2 accounts for 19.3% of the variance. Tetanurans include an almost continuous morphoseries consisting of Allosauroidea members (top), Coelurosauria (middle), and Megalosauroidea (last). Tetanurans are separate from non-tetanurans (including Ceratosauria and Coelophysoidea). Two spinosaurids (*Baryonyx* and *Suchomimus*) are distant from the other tetanurans.

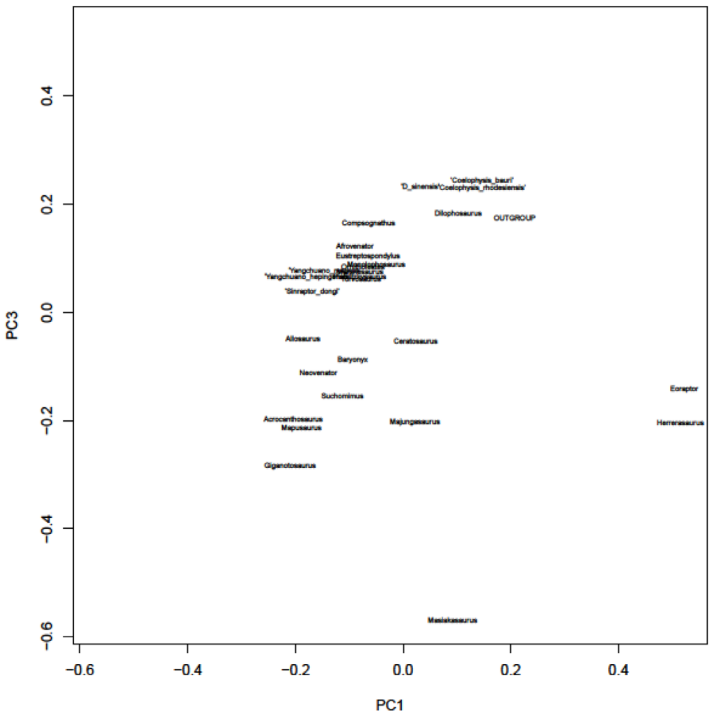

Figure 19. PCA scores for Carrano et al.'s (2012) data matrix for Tetanurae. PC 1 accounts for 29.5% of the variance and PC 3 accounts for 15.6% of the variance. PC 3 separates Allosauroidea members (left) while also distinguishing Megalosauroidea and Coelurosauria clusters.

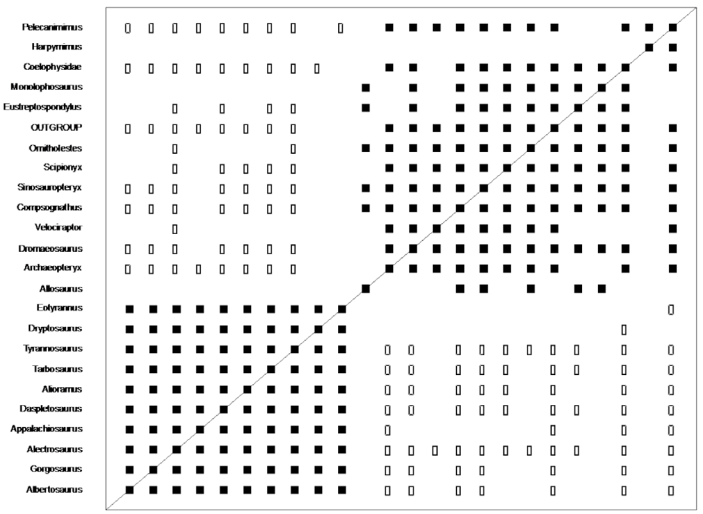

Figure 20. BDC results for Holtz's (2004) data matrix of the Tyrannosauroidea subset of basal Tetanurae, as calculated by BDISTMDS (relevance cutoff 0.75). Closed squares indicate significant, positive BDC; open circles indicate significant, negative BDC.

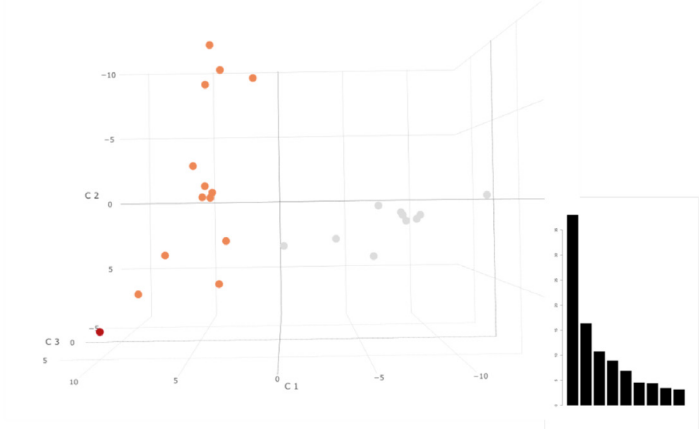

Figure 21. Three-dimensional classical MDS applied to Holtz's (2004) data matrix for Tyrannosauroidea within basal Tetanurae. Members of Tyrannosauroidea are shown in gray, other tetanurans in orange, and outgroup dark red. Tetanuran outgroups and Tyrannosauroidea form nearly orthogonal ordinations. Scree plot indicates the first axis represents most of the variance.

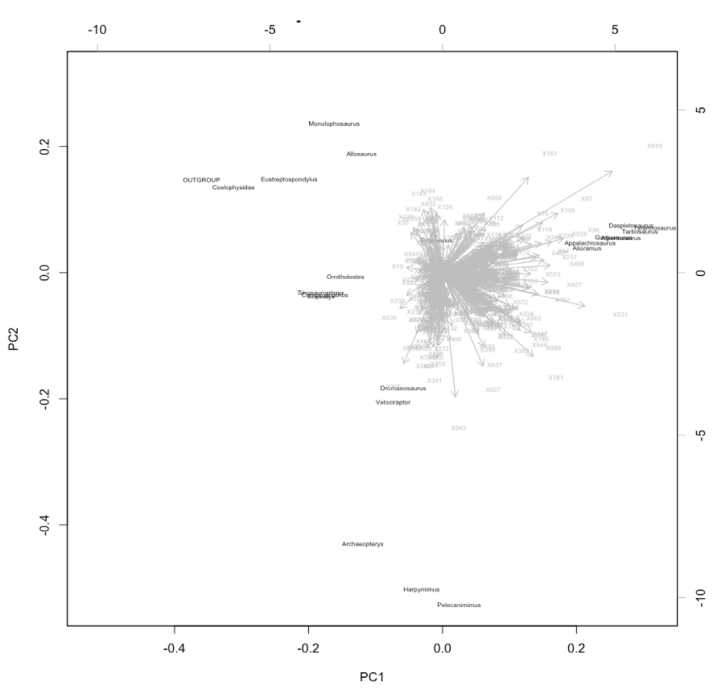

Figure 22. Biplot of PCA scores (black) and vectors (gray) for Holtz's (2004) data matrix for Tyrannosauroidea within basal Tetanurae. PC 1 accounts for 33.2% of the variance and PC 2 accounts for 23.9% of the variance. Tyrannosauroidea are tightly clustered, toward right, except for *Eotyrannus*, which is closer to the center. Outlying groups ordinate distantly from Tyrannosauroidea at nearly right angles.

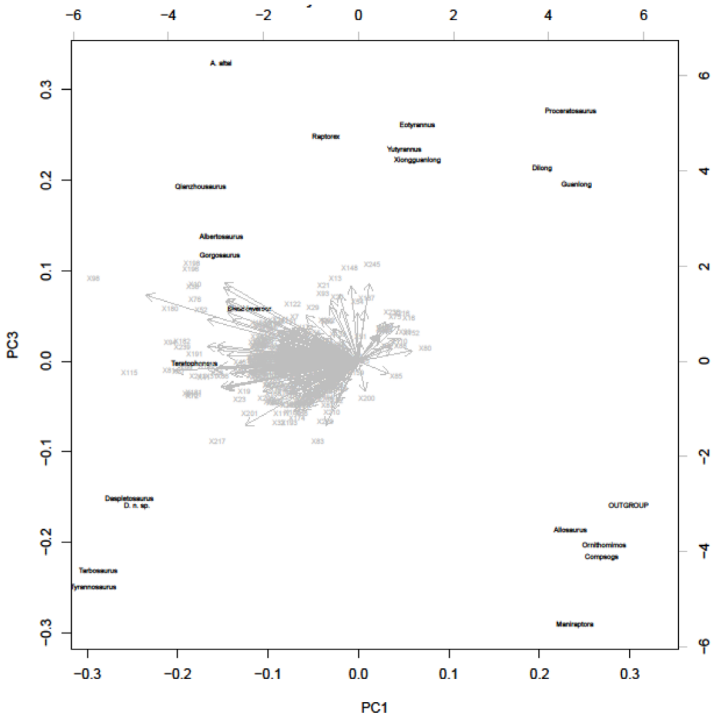

Figure 24. PCA scores for Brussate and Carr's (2016) data matrix for Tyrannosauroidea. PC 1 accounts for 58.1% of the variance and PC 3 accounts for 8.1% of the variance. PC 3 includes Albertosaurinae within the Tyrannosaurinae series. All non-tyrannosaurid tyrannosauroid taxa are distributed along the top, grouped together by PC 3. Tyrannosauroids are very distant from the outgroup taxa (bottom right).

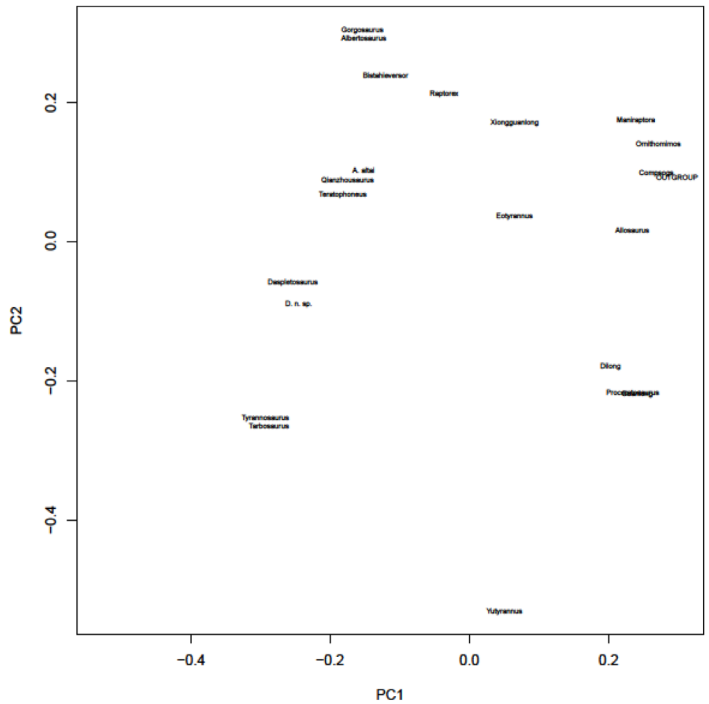

Figure 23. PCA scores for Brusatte and Carr's (2016) data matrix for Tyrannosauroidea. PC 1 accounts for 58.1% of the variance and PC 2 accounts for 12.5% of the variance. Tyrannosauridae forms a morphoseries on the left. PC 2 reveals distance between Tyrannosaurinae members including separation from Albertosaurinae (top).

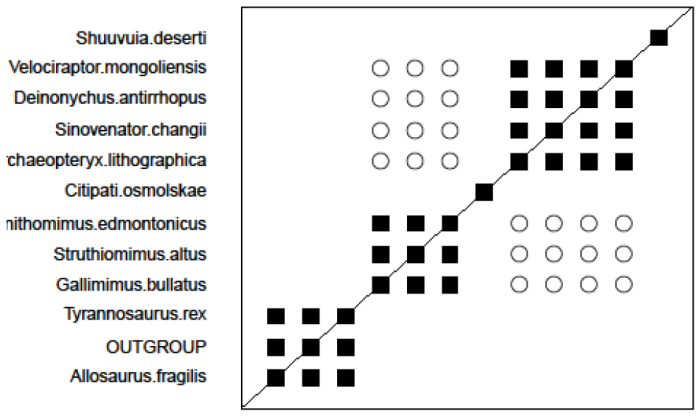

Figure 25. BDC results for Makovicky et al.'s (2004) data matrix of Maniraptoriformes, as calculated by BDISTMDS (relevance cutoff 0.95). Closed squares indicate significant, positive BDC; open circles indicate significant, negative BDC.

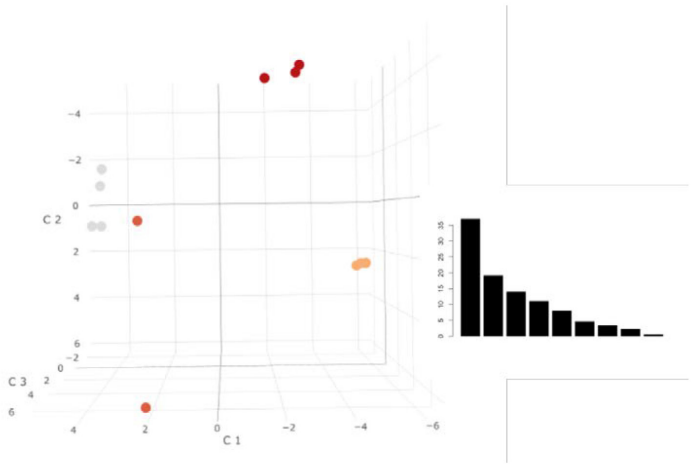

Figure 26. Three-dimensional classical MDS applied to Makovicky et al.'s (2004) data matrix for Maniraptoriformes. Members of Paraves (*Velociraptor*, *Deinonychus*, *Sinovenator*, and *Archaeopteryx*) are shown in gray, Ornithomimidae in orange, and outgroups in dark red. *Citipati* (light red) ordinates close to the dromaeosaurs with *Shuuvuia* (also light red) distantly separated from all. Scree plot indicates more variance within the first axis.

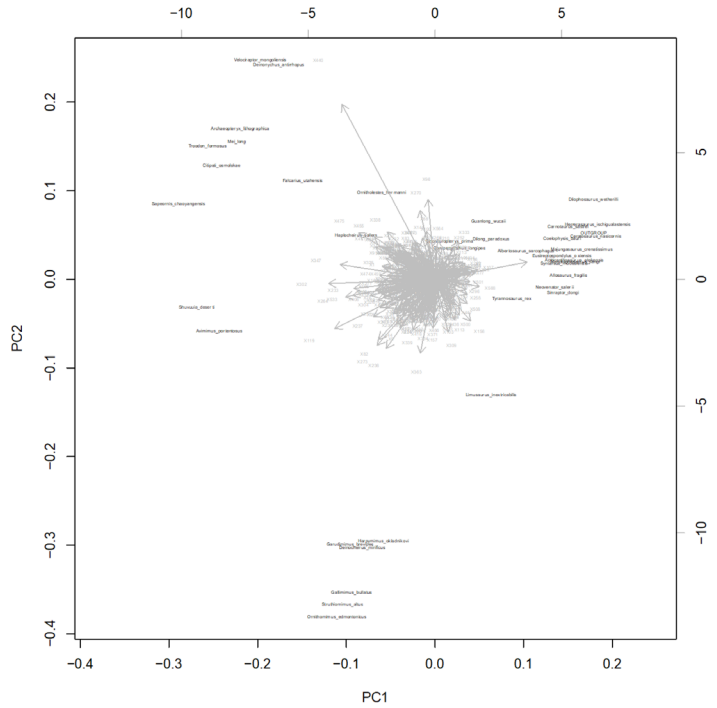

Figure 28. Biplot of PCA scores (black) and vectors (gray) for Chinzorig et al.'s (2018) data matrix for Ornithomimosauria. PC 1 accounts for 24.8% of the variance and PC 2 accounts for 16.2% of the variance. PC 2 reveals a large separation between ornithomimosaurians, maniraptorans, and outgroups. Ornithomimosaurs are divided between Deinocheiridae + *Harpymimus* and Ornithomimidae.

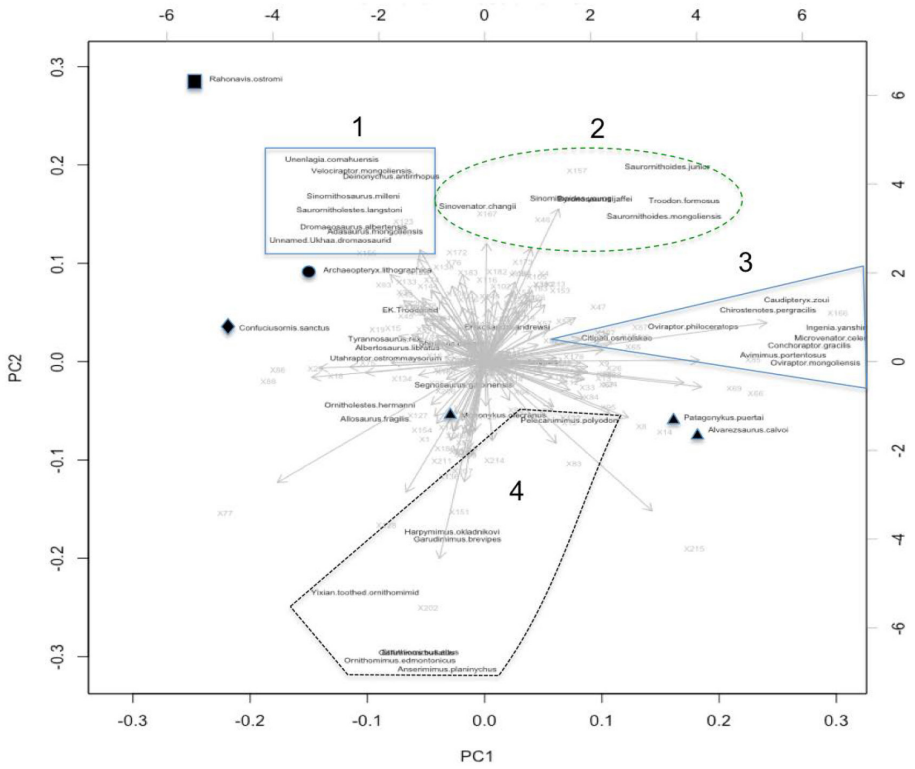

Figure 27. Biplot of PCA scores (black) and vectors (gray) for Makovicky et al.'s (2004) data matrix for Maniraptoriformes. PC 1 accounts for 29.3% of the variance and PC 2 accounts for 23.9% of the variance. Ordination distinguishes Dromaeosauridae (1), Troodontidae (2), Oviraptorosauria (3), and Ornithomimosauria (4). Alvarezsauridae is noted with black triangles, *Archaeopteryx* with a black circle, *Confuciusornis* with a black diamond, and *Rahonavis* with a black square.

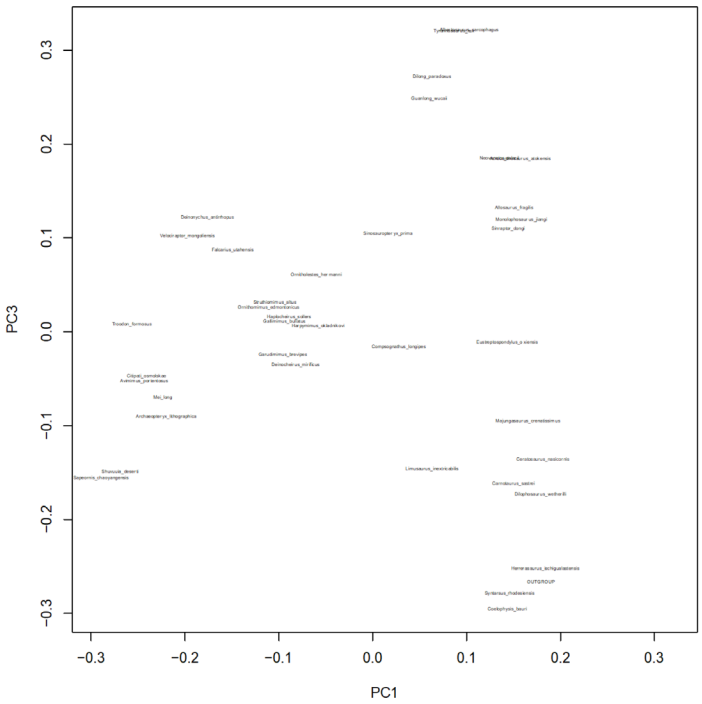

Figure 29. PCA scores for Chinzorig et al.'s (2018) data matrix for Ornithomimosauria. PC 1 accounts for 24.8% of the variance and PC 3 accounts for 11.7% of the variance. PC 3 suggests overlap between ornithomimosaurs and maniraptorans.

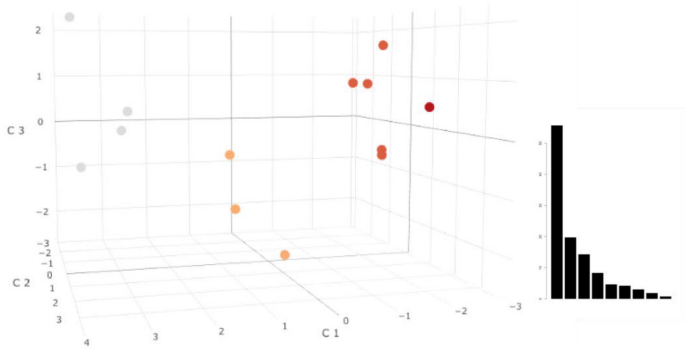

Figure 31. Three-dimensional classical MDS applied to Clark's (2004) data matrix for Therizinosauroidea. Therizinosauridae members are gray (*Therizinosaurus*, *Segnosaurus*, *Neimongosaurus*, *Erlikosaurus*), non-therizinosaurid Therizinosauroidea and *Nothronychus* in orange, non-therizinosauroid maniraptoriforms are light red, and outgroup red. Scree plot shows the first axis represents a majority of the variance.

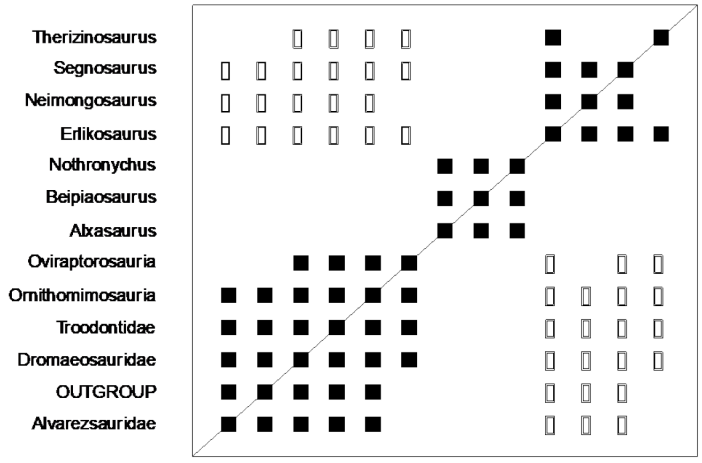

Figure 30. BDC results for Clark's (2004) data matrix of Therizinosauroidea, as calculated by BDISTMDS (relevance cutoff 0.75). Closed squares indicate significant, positive BDC; open circles indicate significant, negative BDC.

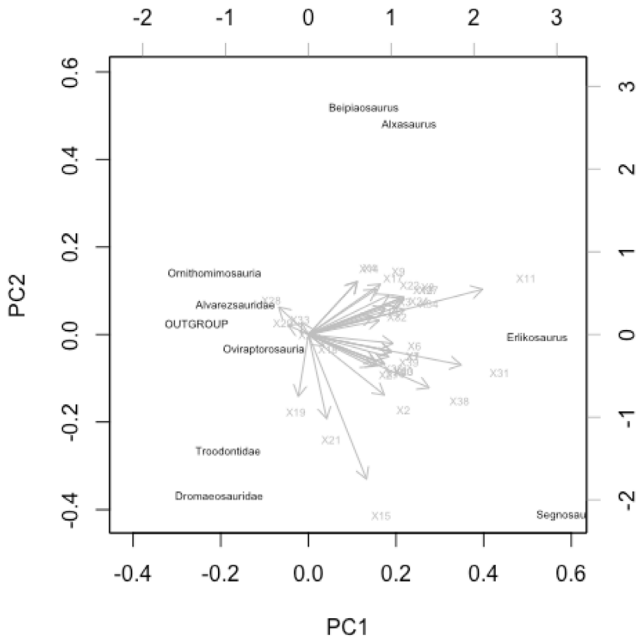

Figure 32. Biplot of PCA scores (black) and vectors (gray) for Clark's (2004) data matrix for Therizinosauroidea. PC 1 accounts for 57.8% of the variance and PC 2 accounts for 17.8% of the variance. Two members of Therizinosauroidea (*Beipiaosaurus* and *Alxasaurus*, top) are separated along PC 2 from two Therizinosauridae (*Erlikosaurus* and *Segnosaurus*, toward right).

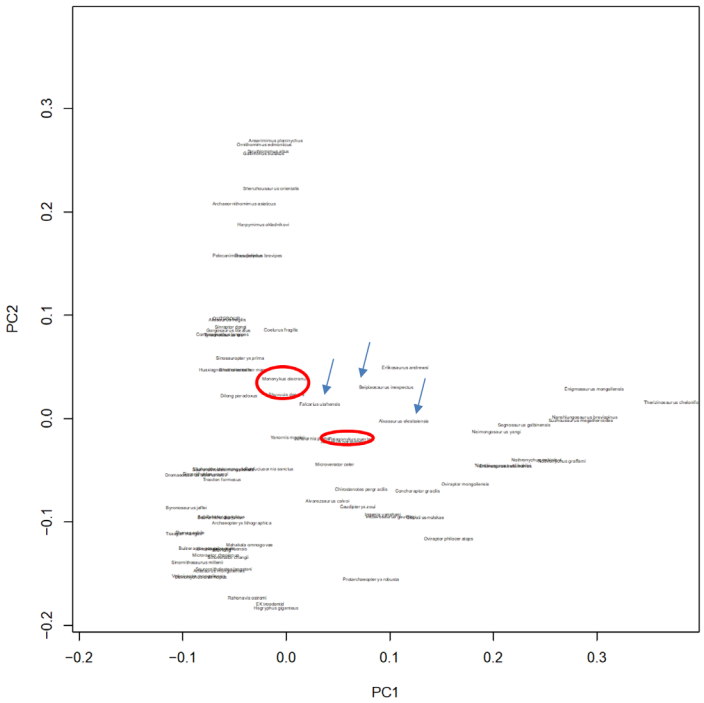

Figure 33. PCA scores for Zanno's (2010) complete data matrix for Therizinosauria. PC 1 accounts for 39.6% of the variance and PC 2 accounts for 19.4% of the variance. Therizinosaurids are separated from other maniraptorans along PC 1, towards the right, although the non-therizinosaurid therizinosaurs (blue arrows) and *Erlikosaurus* overlap with non-therizinosaur taxa. There is overlap between therizinosaurs and other taxa along PC 2.

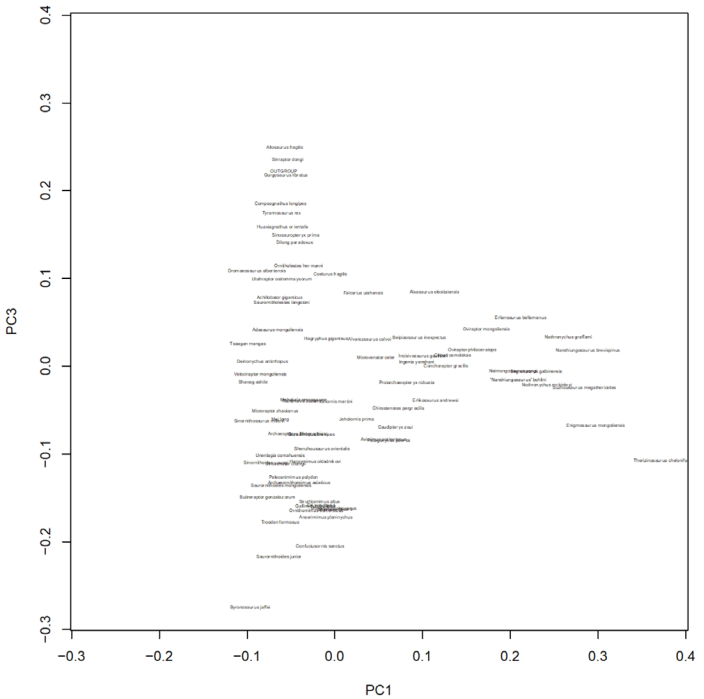

Figure 34. PCA scores for Zanno's (2010) complete data matrix for Therizinosauria. PC 1 accounts for 39.6% of the variance and PC 3 accounts for 12.9% of the variance. Most therizinosaurs are separated from other maniraptorans along PC 1, towards the right, though with little distinction along PC 3.

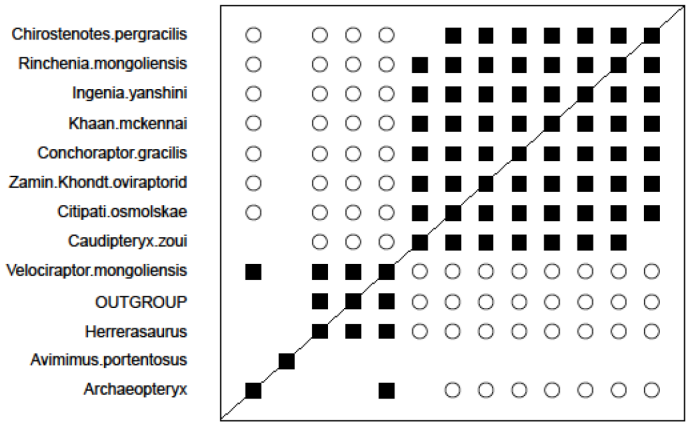

Figure 35. BDC results for Weishampel et al.'s (2004) data matrix of Oviraptorosauria, as calculated by BDISTMDS (relevance cutoff 0.8). Closed squares indicate significant, positive BDC; open circles indicate significant, negative BDC.

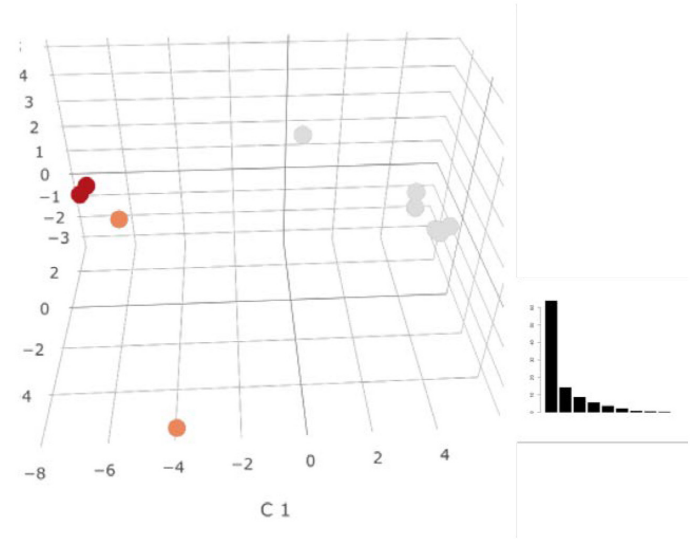

Figure 36. Three-dimensional classical MDS applied to Weishampel et al.'s (2004) data matrix for Oviraptorosauria. Members of Oviraptorosauria are shown in gray, *Velociraptor* and *Archaeopteryx* are in orange, and outgroup and *Herrerasaurus* are red. Scree plot indicates the first coordinate accounts for the vast majority of variance.

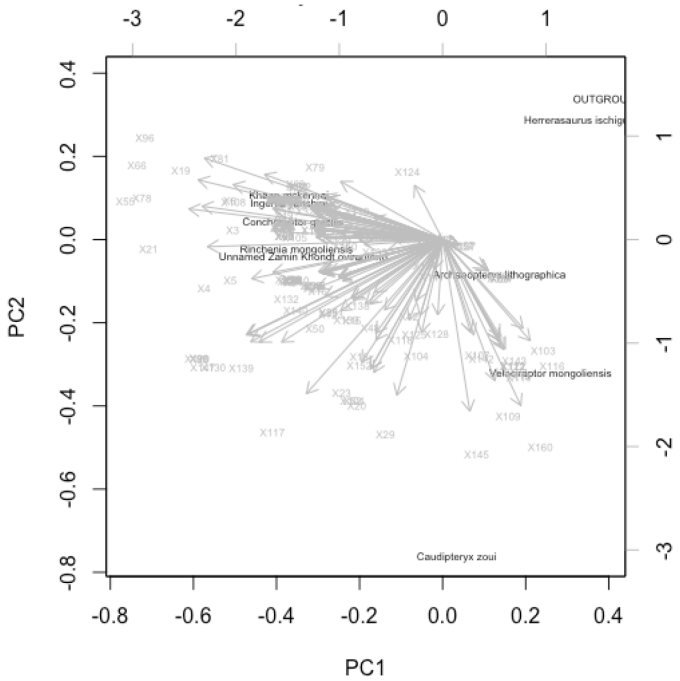

Figure 37. Biplot of PCA scores (black) and vectors (gray) for Weishampel et al.'s (2004) data matrix for Oviraptorosauria. PC 1 accounts for 59.2% of the variance and PC 2 accounts for 19.0% of the variance. Oviraptorosauria show clustering while *Caudipteryx* shows a distant ordination not visible to BDC or MDS results.

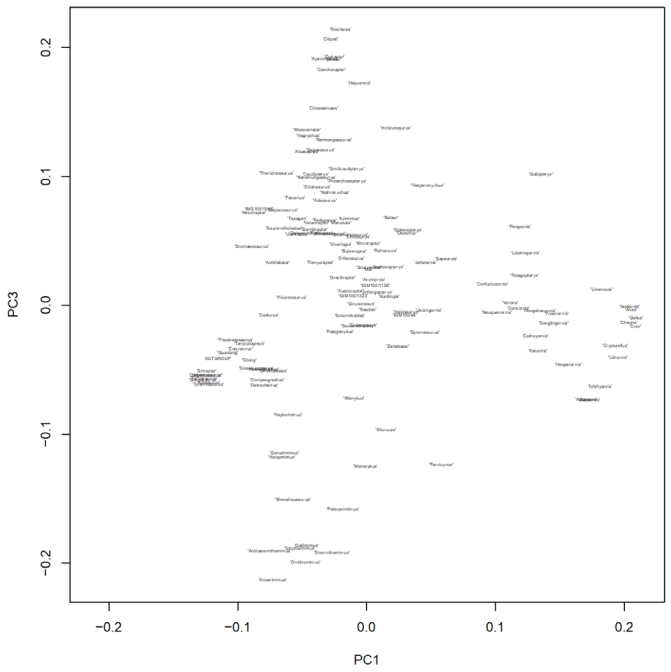

Figure 39. PCA scores for Foth and Rauhut's (2017) data matrix for maniraptorans with the most complete data. PC 1 accounts for 32.5% of the variance and PC 3 accounts for 16.5% of the variance.

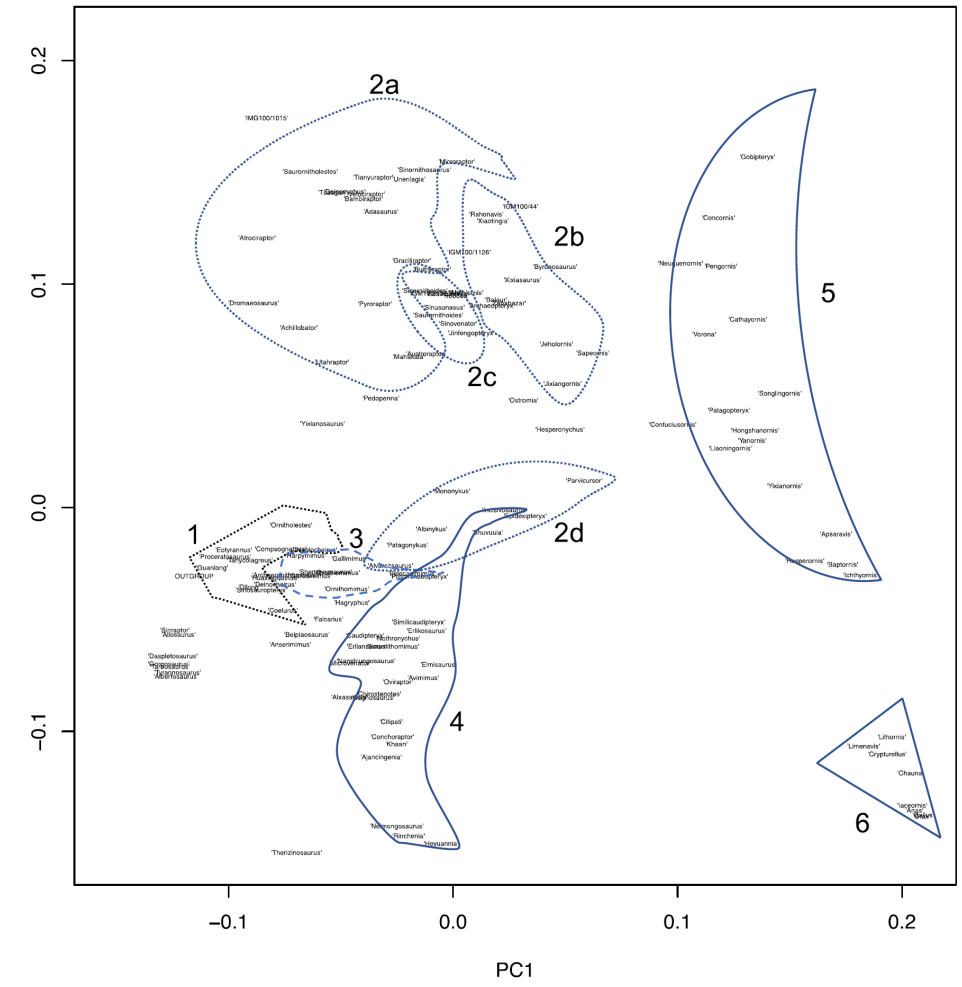

Figure 38 (right). PCA scores for Foth and Rauhut's (2017) complete data matrix for maniraptorans. PC 1 accounts for 32.5% of the variance and PC 2 accounts for 18.0% of the variance. Numbered groups: 1) "Basal" Coelurosauria; 2a) Dromaeosauridae; 2b) "basal" Avialae; 2c) Troodontidae; 2d) Alvarezsauroidea; 3) Ornithomimosauria; 4) Oviraptorosauria + Therizinosauria; 5) Non-avian Pygostylia; and 6) Aves + *Limenavis* + *Iaceornis*. Dromaeosaurids and "basal" avialans ordinate closely, with troodontids between. Numbers provide relative order of first appearance in fossil record. Initial members of groups labelled "2" appeared have nearly equal first appearances.

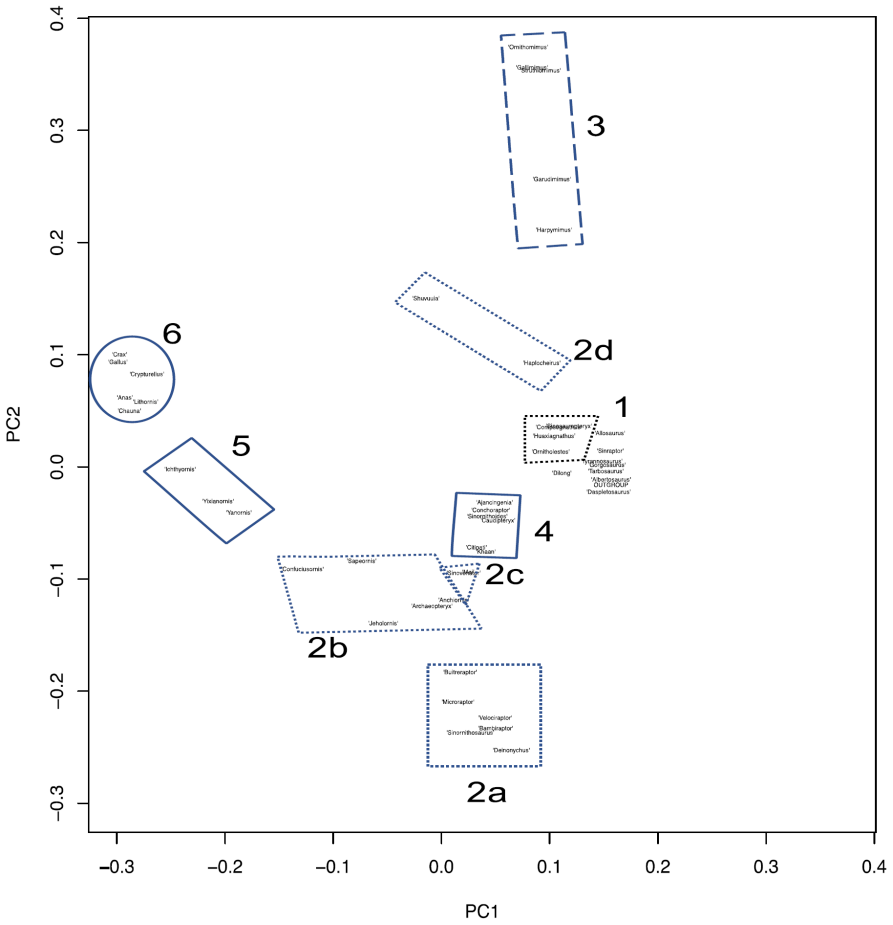

Figure 40. PCA scores for Foth and Rauhut's (2017) data matrix for maniraptorans with the most complete data. PC 1 accounts for 34.2% of the variance and PC 2 accounts for 17.6% of the variance. The more complete dataset reveals a bifurcation with two morphoseries. Dromaeosaurids, at the base of the bifurcation, ordinate separately from avialans for PC 2. Avialans connect two morphoseries. Numbered groups: 1) "basal" coelurosaurs; 2a) dromaeosaurids; 2b) "basal" avialans; 2c) troodontids; 2d) alvarezsaurids; 3) ornithomimids; 4) oviraptorosaurs; 5) ornithuromorphs; and 6) avians + *Lithornis*. Numbers provide relative order of first appearance in fossil record with initial members of the second group appearing nearly simultaneously.

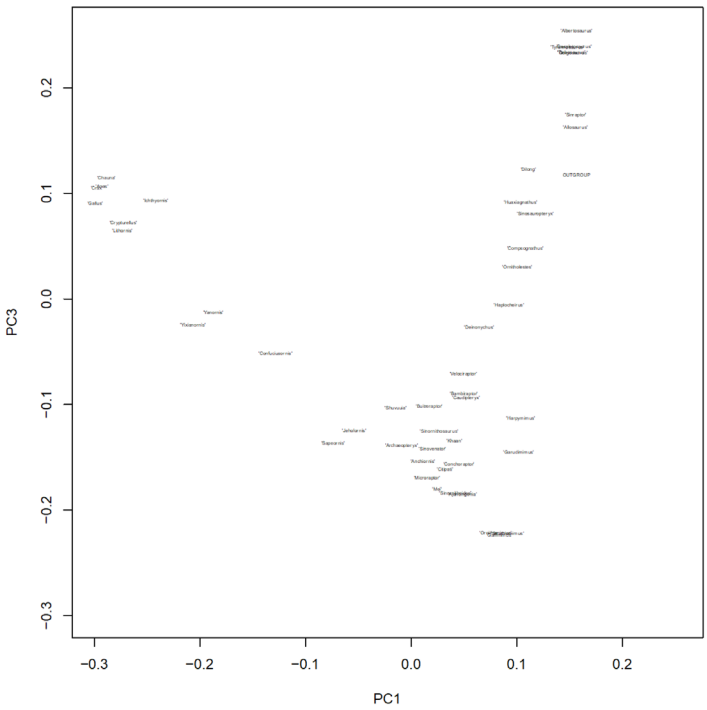

Figure 41. PCA scores for Foth and Rauhut's (2017) complete data matrix for maniraptorans with the most complete data. PC 1 accounts for 34.2% of the variance and PC 3 accounts for 14.5% of the variance. PC 1 and PC 3 reveals a similar morphospatial bifurcation though with overlap between dromaeosaurids, avialans, and oviraptorosaurs at the base of two morphoseries.

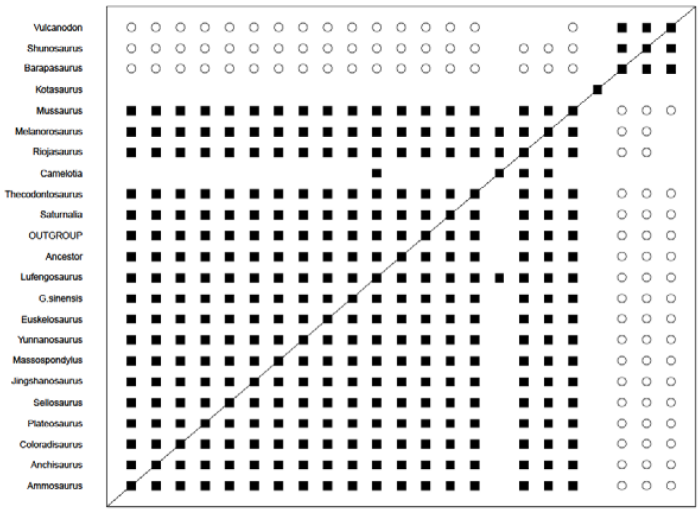

Figure 42. BDC results for Galton and Upchurch's (2004a) data matrix of "Prosauropoda", as calculated by BDISTMDS (relevance cutoff 0.8). Closed squares indicate significant, positive BDC; open circles indicate significant, negative BDC.

PC 3 likewise separates non-massopod sauropodomorphs (e.g., *Plateosaurus*, *Pantydraco*, etc.) from non-sauropod massopods (e.g., *Riojasaurus*, *Anchisaurus*, *Massospondylus*, etc.) (Fig. 46). *Thecodontosaurus* and *Pantydraco*, two "basal" "prosauropods", group together and are somewhat separated from the other taxa in Fig. 45, but in Fig. 46 they overlap with other "prosauropods". The guaiabasaurids (including *Panphagia*) and *Eoraptor*, which have all been controversially considered "basal" sauropodomorphs, also form a cluster distinct from other outgroup taxa except the herrerasaurid *Chindesaurus* in Fig. 45.

The BDC results for Otero et al.'s (2015) data matrix show two blocks of positive correlation separated from each other by negative correlation: a sauropod block and a block containing "basal" sauropods (*Antetonitrus* and *Gongxianosaurus*), "basal"sauropodomorphs, and some outgroup taxa (non-dinosaurian dinosauromorphs, herrerasaurids, etc.) (Fig. 47). There is one taxon pairing that links the two blocks with positive correlation: *Antetonitrus* and *Vulcanodon*. Removal of the sauropod and non-sauropodomorph taxa does not reveal obvious evidence for discontinuities within the larger block of positive correlation.

PCA results for Sauropodomorpha from Otero et al. (2015) paralleled BDC but again revealed complicated spatial relationships. PCA results agreed with BDC by clustering "basal" sauropodomorph taxa far from the sauropod taxa (Fig. 48). PC 1 and PC 2 reveal a trajectory of taxa stretching from the non-sauropodomorph outgroups up to the non-sauropod Plateosauria. Although the trajectory is a continuum, it is punctuated by gaps with no taxa. One gap occurs between non-dinosaurs and dinosaurs, the next (a small gap) between non-sauropodomorphs and the questionably "basalmost" sauropodomorphs (*Eoraptor* and *Saturnalia*), the next between *Saturnalia* and *Pantydraco* + *Thecodontosaurus*, and then the final between *Thecodontosaurus* and the non-sauropod plateosaurians. Though clustered, PC 1 and PC 2 groups most non-sauropod plateosaurian taxa near their closest taxonomic relatives (e.g., plateosaurids, non-sauropod sauropodiforms, etc.). PC 3 further separated non-massopodan sauropodomorphs from non-sauropod massopodans (Fig. 49). Among the non-sauropod massopodans, the family Massospondylidae is recognizable, although *Aardonyx* and *Anchisaurus* are clustered with the massospondylid taxa. Additionally, *Yunnanosaurus* and *Lufengosaurus* cluster with the non-sauropod sauropodiform taxa. Interestingly, *Eoraptor* and *Saturnalia* are not aligned with the non-sauropod sauropodomorph trajectory and are instead aligned in the subparallel outgroup trajectory, which forms a stratomorphic morphoseries (*Euparkeria* to *Marasuchus* to *Silesaurus* to the dinosaur taxa with Ornithischia first, then Sauropodomorpha and Herrerasauridae, and then Neotheropoda; Fig. 49).

I. Sauropoda

The BDC results for Upchurch et al.'s (2004) data matrix, in Weishampel et al. (2004), demonstrate separation between the Sauropoda and all other groups (Fig. 50). Sauropoda show positive BDC while having negative BDC against outgroups. Classical MDS reflects separation between sauropods and all outgroups, with *Shunosaurus* and *Omeisaurus* ordinating separately (Fig. 51). PCA results likewise suggest some discontinuity between sauropods and other groups yet suggests a separation within sauropods between Diplodocoidea (*Dicraeosaurus*, *Apatosaurus*, and *Diplodocus*) and other Sauropoda; this separation is not visible to either BDIST or MDS (Fig. 52). As interesting as these results are, they contain very few sauropod taxa, and whole, large sauropod groups (e.g., Titanosauria) are completely unrepresented.

2. Ornithischia

A. Basal Thyreophora

The BDC results for Norman, Witmer et al.'s (2004) data matrix, in Weishampel et al. (2004), are shown in Fig. 53. Positive BDC is present between Cerapoda, *Lesothosaurus*, *Scutellosaurus*, and the hypothetical outgroup. These four taxa all share negative correlation with Eurypoda (Stegosauria + Ankylosauria). *Emausaurus* and *Scelidosaurus* do not correlate with any other taxa in the analysis. Classical MDS results show the three "basal" thyreophorans widely separate from each other and from every other taxon (Fig. 54). PCA results show no clustering between the few groups represented, though *Lesothosaurus* and Cerapoda group the most closely (Fig. 55).

PCA for Breeden's (2016) matrix shows Pachycephalosauria far away from the other taxa and Ankylosauria and Stegosauria also relatively far removed (Fig. 56). The remaining taxa (ornithopods, ceratopsians, and "basal" thyreophorans) all cluster near each other for PC 1. Similar to the clusters within Sauropodomorpha (Figs. 48 and 49), PC 1 did not clearly separate ornithopods from "basal" thyreophorans. Only PC 2 separated the Eurypoda and other thyreophorans. Pachycephalosauria share overlapping ranges with Eurypoda on PC 2, though both are distantly divided by PC 1. Ornithopod groups connect to thyreophorans through *Heterodontosaurus* (a "basal" ornithischian), *Lesothosaurus* (either a "basal" ornithischian or a "basal" thyreophoran), and *Agilisaurus* (a "basal" neornithischian). PC 3 unites most groups, but it separates out *Heterodontosaurus* and the ceratopsians from the other taxa and from each other (Fig. 57). PC 3 also separates Psittacosauridae from the neoceratopsian taxa.

B. Stegosauria

The BDC results for Galton and Upchurch's (2004b) data matrix, in Weishampel et al. (2004), show a large block of positively correlated stegosaurid taxa that share negative correlation with the hypothetical ancestor (Fig. 58). *Huayangosaurus*, the most "basal" stegosaur, does not share positive or negative correlation with any other taxon in the analysis. Classical MDS results reflect the BDC results with the majority of Stegosauria spatially grouped. *Huayangosaurus* is the most distantly ordinated (Fig. 59). For PCA, only groups with at least 60% of character data were analyzed. PCA results likewise show Stegosauria separated from the outgroup with *Huayangosaurus* spaced halfway between *Kentrosaurus* (a stegosaur) and the hypothetical outgroup (Fig. 60). *Dacentrurus* is the farthest removed stegosaur on the plot.

All 22 taxa in Raven and Maidment's (2017) matrix were analyzed. Since removing taxa with less than 50% complete character data would remove more than half the taxa, all taxa were retained. PC 1 reveals separation between Eurypoda and all outgroups for PC 1 (Fig. 61). PC 2 separates stegosaurs from ankylosaurs except for *Tuojiangosaurus* (73% missing data) and *Paranthodon* (92% missing data), which group with the ankylosaur taxa. Interestingly,

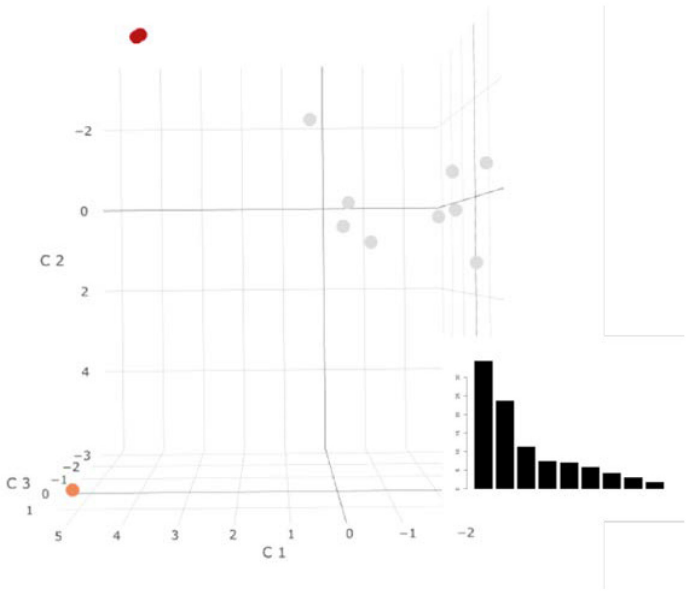

Figure 43. Three-dimensional classical MDS applied to Galton and Upchurch's (2004a) data matrix for "Prosauropoda". Members of "Prosauropoda" are shown in gray, *Shunosaurus* in orange, and two generic outgroups in red. Scree plot indicates the first two coordinates account for a majority of the variance.

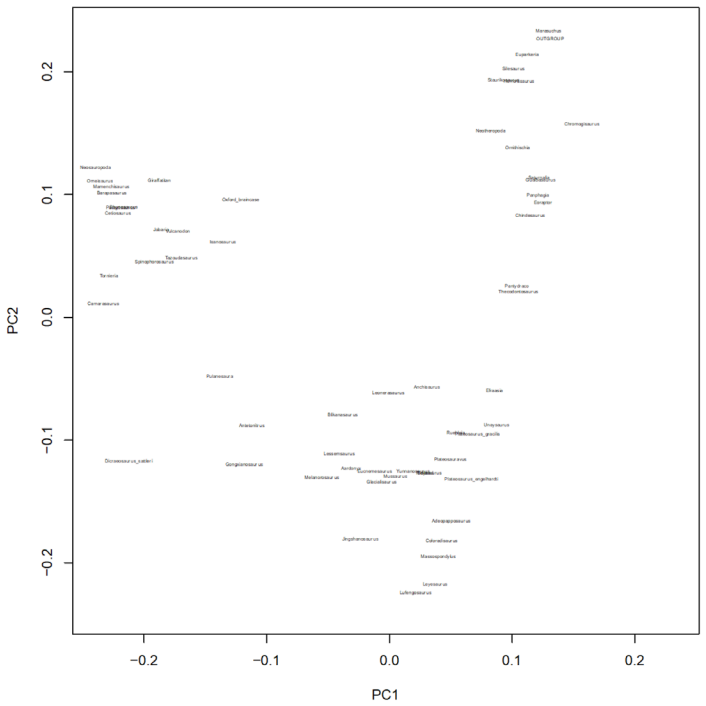

Figure 45. PCA scores for Bronzati's (2017) data matrix for "Prosauropoda". PC 1 accounts for 37.9% of the variance and PC 2 accounts for 22.9% of the variance. PC 1 separates sauropods (left) from other sauropodomorphs and the outgroup taxa. Outgroup taxa cluster in the upper right, Thecodontosauridae cluster between the outgroup taxa and the "prosauropods".

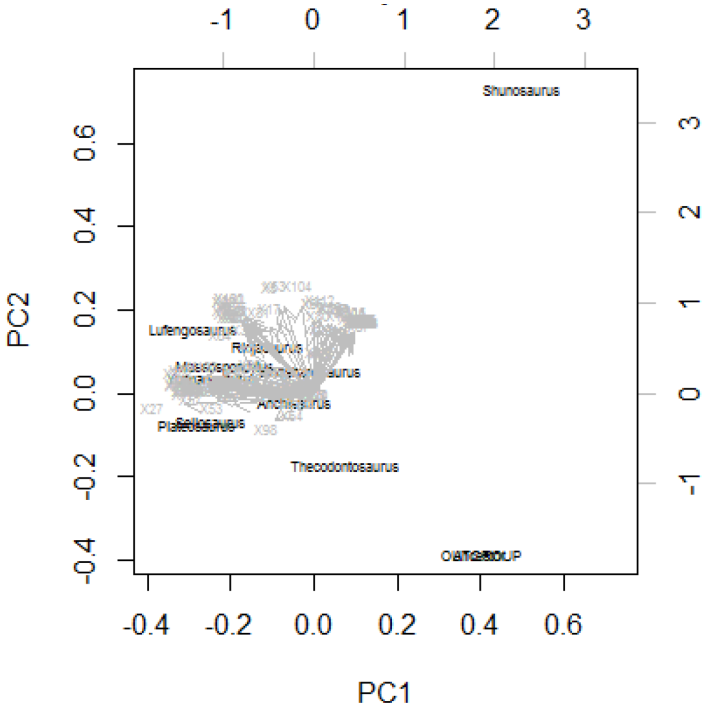

Figure 44. Biplot of PCA scores (black) and vectors (gray) for Galton and Upchurch's (2004a) data matrix for "Prosauropoda". PC 1 accounts for 35.8% of the variance and PC 2 accounts for 24.1% of the variance. Outgroups show similar separation as MDS results.

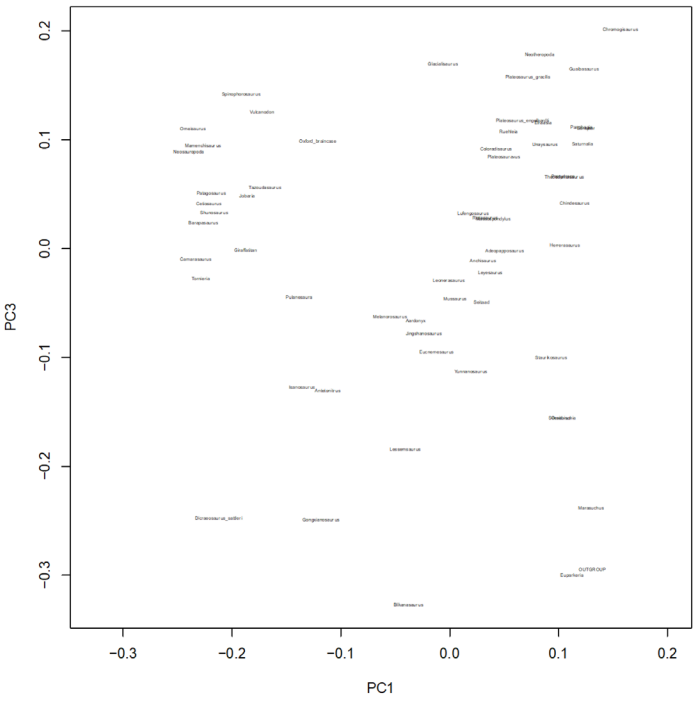

Figure 46. PCA scores for Bronzati's (2017) data matrix for Prosauropoda. PC 1 accounts for 37.9% of the variance and PC 3 accounts for 6.2% of the variance. PC 3 distinguishes non-massopod sauropodomorphs (above) from non-sauropod massopods (below).

Gigantspinosaurus groups closely with *Huayangosaurus*. The "basal" thyreophoran taxa, including *Lesothosaurus*, all cluster with each other in Fig. 61 and Fig. 62. PC 2 groups the "basal" thyreophorans with the outgroup, but PC 3 shows a large separation between the two. Once again, PC 3 was unable to separate *Tuojiangosaurus* and *Paranthodon* from an ankylosaur (*Euoplocephalus*). PC 3 also separated several stegosaurid genera from the rest: *Kentrosaurus*, *Huayangosaurus*, *Chungkingosaurus*, and *Gigantspinosaurus* (Fig. 62).

C. Ankylosauria

The BDC results for Vickaryous et al.'s (2004) data matrix, in Weishampel et al. (2004), show three major clusters of positive correlation: 1) Ankylosauridae, 2) Nodosauridae, and 3) outgroup taxa (Fig. 63). All of the nodosaurids share positive correlation except *Gastonia*, which is only positively correlated with *Gargoyleosaurus*, and *Gargoyleosaurus*, which is only correlated positively with *Gastonia* and *Pawpawsaurus*, which links it to the main block of nodosaurids. The ankylosaurid block appears to be made out of two blocks that share positive correlation between them. Almost all of the ankylosaurids share negative correlation with the main nodosaurid block and the outgroup taxa. Classical MDS results show separation between Ankylosauridae and Nodosauridae as two groups with *Gastonia* and *Gargoyleosaurus* positioned midway between them (Fig. 64). PCA results present a different image with groups distributed along an arc; the same two genera are positioned midway along the continuum (Fig. 65).

PCA results for Zheng et al.'s (2018) dataset provided a different topology for the Ankylosauria. Instead of an arc-shaped distribution of taxa, Zheng's larger dataset reveals a separation between the Ankylosauridae and Nodosauridae along PC 1 in two morphoseries (Fig. 66). PC 2 further shows a clustered series of ankylosaurids while the nodosaurid series displayed wider spatial separation. Nodosaurids *Gargoyleosaurus*, *Gastonia*, and *Hungarosaurus* alone overlap with ankylosaurs on PC 2. Comparing PC 3 with PC 1 separates ankylosaurids and nodosaurids in a similar fashion, clustering only the ankylosaurs (Fig. 67). One ankylosaurid (*Crichtonpelta*) and two nodosaurids (*Gargoyleosaurus* and *Gastonia*) are distinguished by PC 3.

D. Basal Ornithopoda

The BDC results for Norman, Sues et al.'s (2004) data matrix, in Weishampel et al. (2004), show two main clusters of positive correlation separated by negative correlation in some cases (Fig. 68). One cluster corresponds to *Heterodontosaurus* and the outgroup

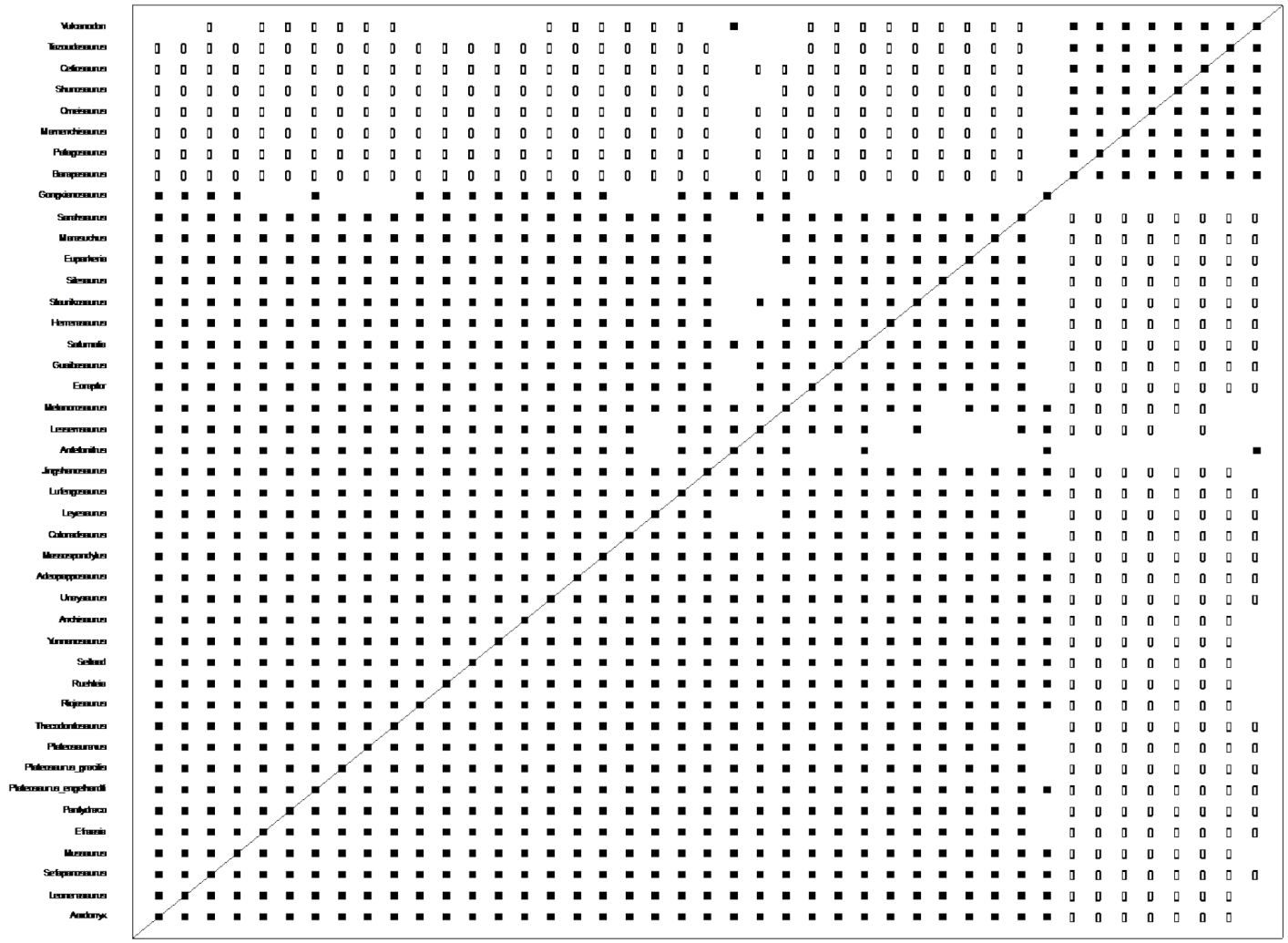

Figure 47. BDC results for Otero et al.'s (2015) data matrix for Sauropodomorpha, as calculated by BDISTMDS (relevance cutoff 0.75). Closed squares indicate significant, positive BDC; open circles indicate significant, negative BDC.

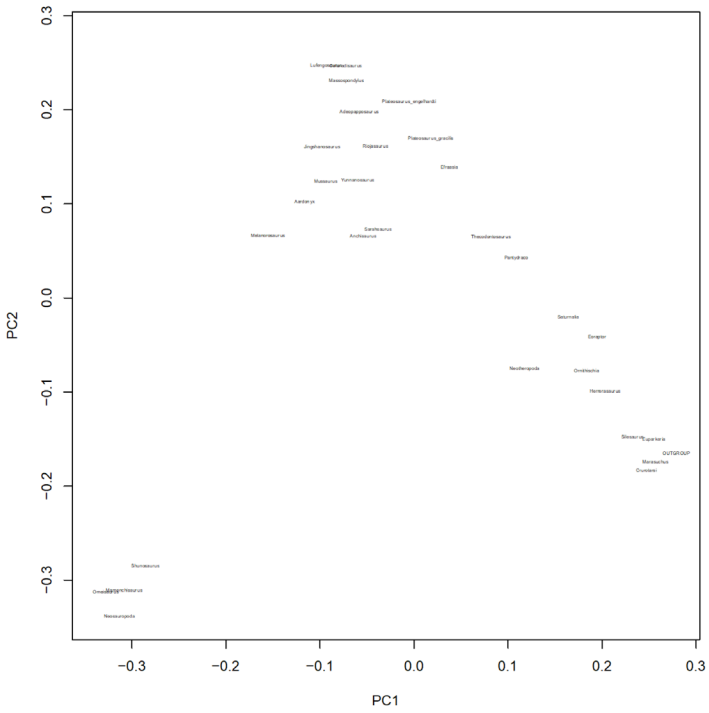

Figure 48. PCA scores for Otero et al.'s (2015) data matrix for Sauropodomorpha. PC 1 accounts for 33.9% of the variance and PC 2 accounts for 24.1% of the variance. The non-sauropodomorph outgroups (right) form a nearly complete stratomorphic morphoseries leading to the "prosauropods" (top). Sauropods form a discontinuous group (bottom left).

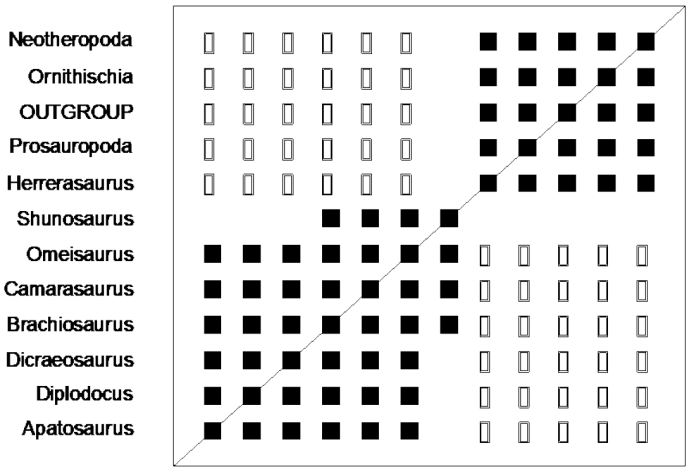

Figure 50. BDC results for Upchurch et al.'s (2004) data matrix of Sauropoda, as calculated by BDISTMDS (relevance cutoff 0.95). Closed squares indicate significant, positive BDC; open circles indicate significant, negative BDC.

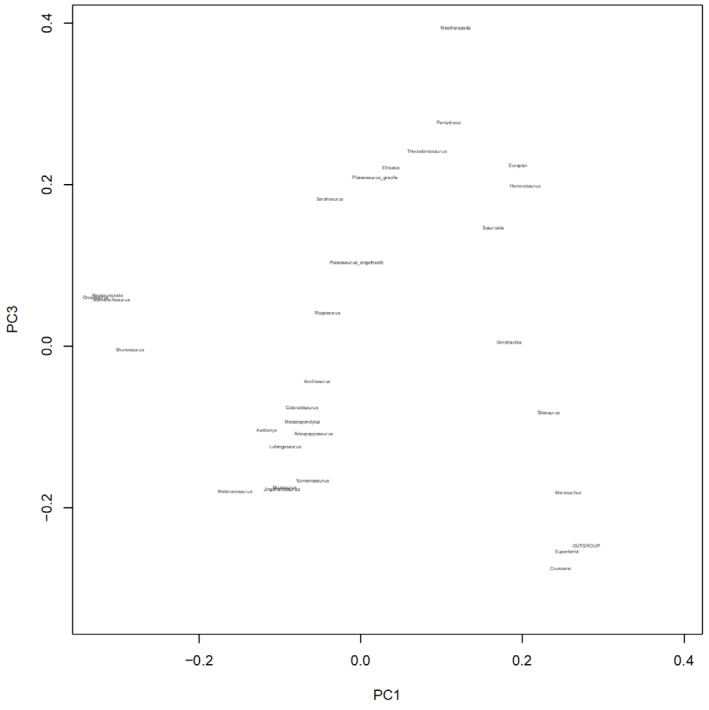

Figure 49. PCA scores for Otero et al.'s (2015) data matrix for Sauropodomorpha. PC 1 accounts for 33.9% of the variance and PC 3 accounts for 7.0% of the variance. PC 3 separates non-massopodan sauropodomorphs (top) from non-sauropod massopodans (bottom).

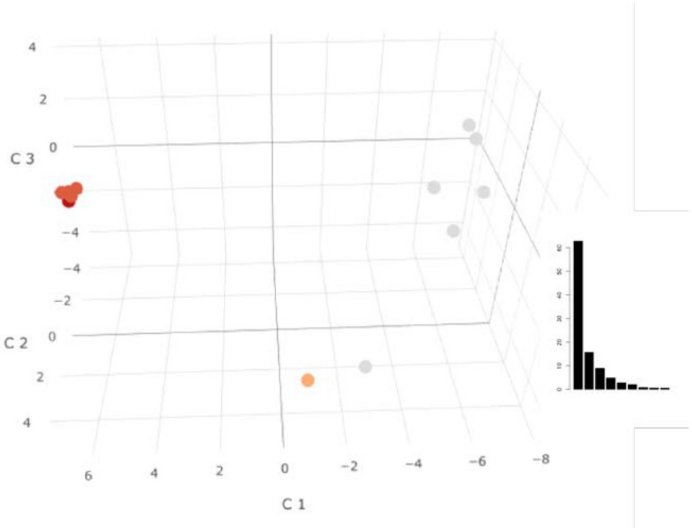

Figure 51. Three-dimensional classical MDS applied to Upchurch et al.'s (2004) data matrix for Sauropoda. Members of Neosauropoda (*Diplodocus*, *Apatosaurus*, *Brachiosaurus*, *Dicraeosaurus*, *Camarasaurus*) are in gray. *Shunosaurus* (orange) and *Omeisaurus* (gray) ordinate toward foreground with all other groups (light red) clustering with outgroup (dark red). Scree plot indicates the first coordinate accounts for a majority of the variance.

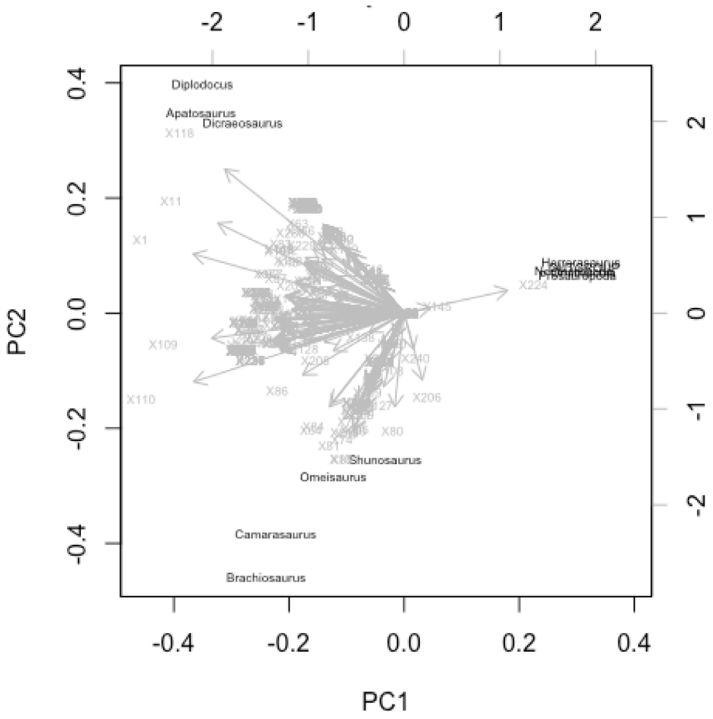

Figure 52. Biplot of PCA scores (black) and vectors (gray) for Upchurch et al.'s (2004) data matrix for Sauropoda. PC 1 accounts for 61.8% of the variance and PC 2 accounts for 16.6% of the variance. In contrast to the BDC or MDS results PCA ordinations suggest additional discontinuity between Diplodocoidea (specifically Flagellicaudata) members (top left) and other sauropods.

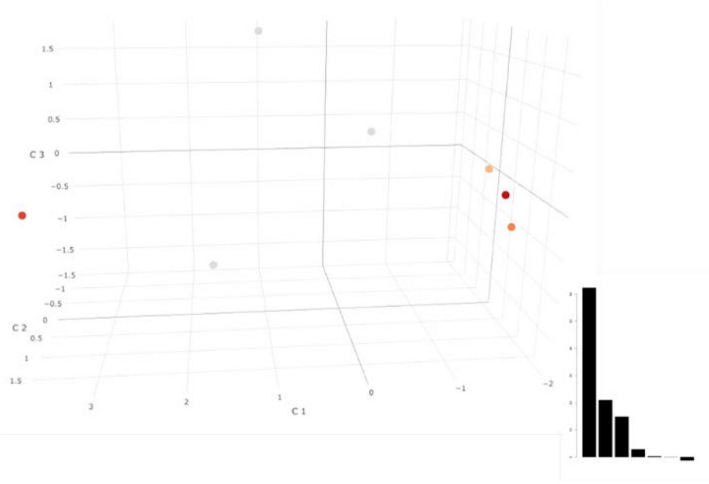

Figure 54. Three-dimensional classical MDS applied to Norman, Witmer et al.'s (2004) data matrix for "basal" Thyreophora. *Scelidosaurus*, *Scutellosaurus*, and *Emausaurus* are shown in gray (center), *Lesothosaurus* (orange) and Cerapoda (light orange) and the outgroup (red) are toward the right, while Eurypoda ordinates toward the far left (dark orange). The scree plot shows the first axis explains the majority of the variation.

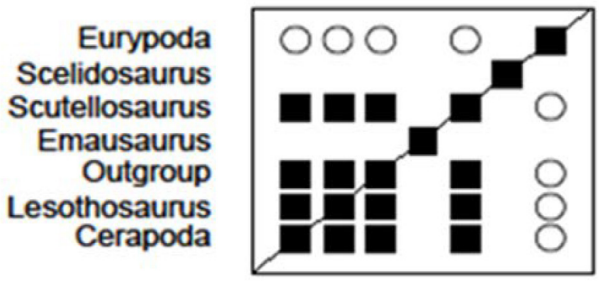

Figure 53. BDC results for Norman, Witmer et al.'s (2004) data matrix of "basal" Thyreophora, as calculated by BDISTMDS (relevance cutoff 0.85). Closed squares indicate significant, positive BDC; open circles indicate significant, negative BDC.

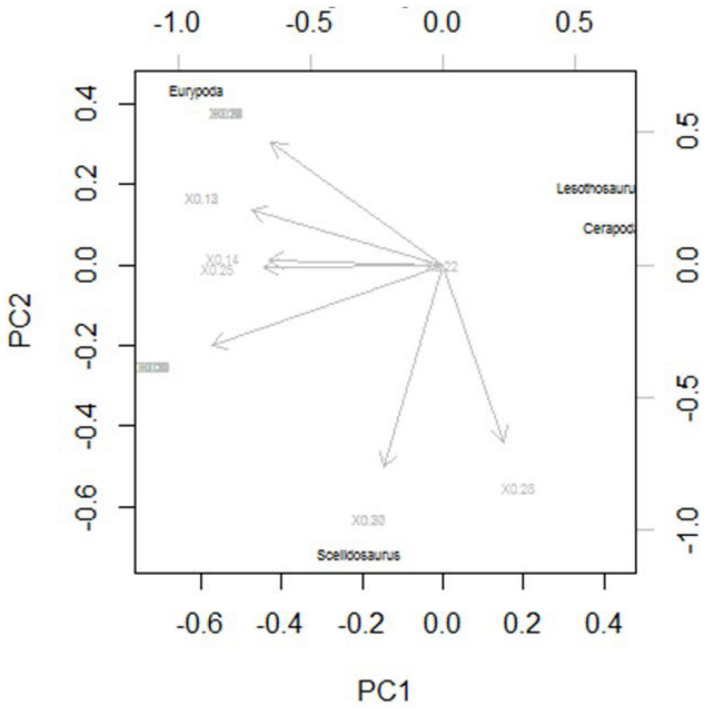

Figure 55. Biplot of PCA scores (black) and vectors (gray) for Norman, Witmer et al.'s (2004) data matrix for "basal" Thyreophora. PC 1 accounts for 76.9% of the variance and PC 2 accounts for 21.1% of the variance. Eurypoda is isolated the top left.

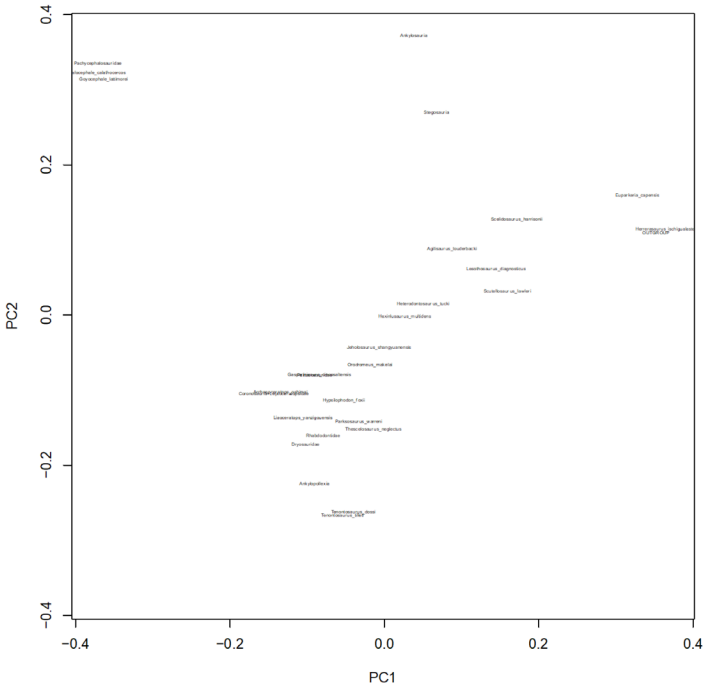

Figure 56. PCA scores for Breeden's (2016) data matrix for Thyreophora. PC 1 accounts for 23.4% of the variance and PC 2 accounts for 20.6% of the variance. A nearly stratomorphic morphoseries of ornithopods connects Thyreophora (middle right) to ornithopods and "basal" ornithischians from lower layers (center). PC 2 reveals a discontinuity between Stegosauria and Ankylosauria and other thyreophorans.

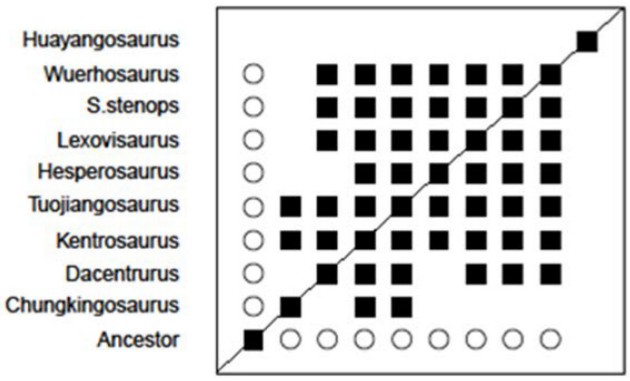

Figure 58. BDC results for Galton and Upchurch's (2004b) data matrix of Stegosauria, as calculated by BDISTMDS (relevance cutoff 0.80). Closed squares indicate significant, positive BDC; open circles indicate significant, negative BDC.

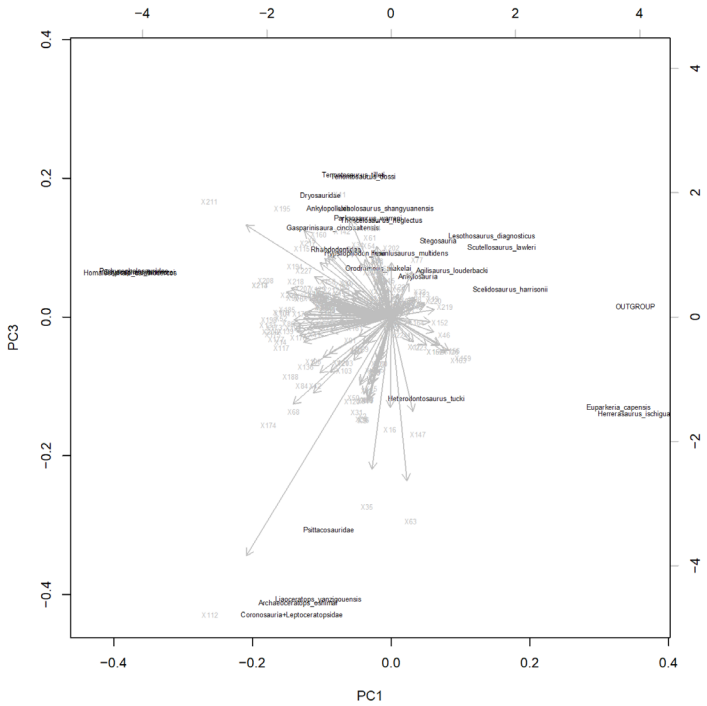

Figure 57. Biplot of PCA scores (black) and vectors (gray) Breeden's (2016) data matrix for Thyreophora. PC 1 accounts for 23.4% of the variance and PC 3 accounts for 16.6% of the variance. PC 3 groups ornithopods and thyreophorans while separating members of Ceratopsia (bottom).

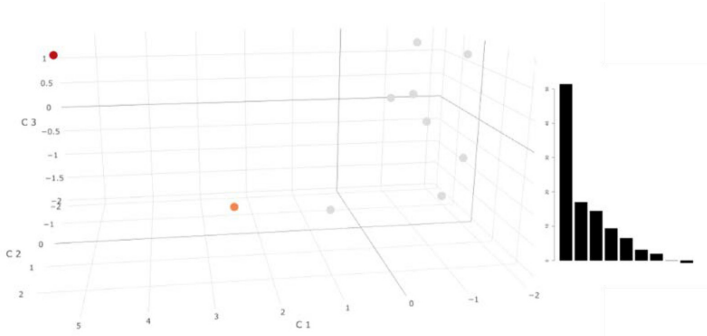

Figure 59. Three-dimensional classical MDS applied to Galton and Upchurch's (2004b) data matrix for Stegosauria. Members of Stegosauria are shown in gray with only *Huayangosaurus* in orange. The outgroup is located separately (red). The scree plot shows the first coordinate represents a majority of the variation.

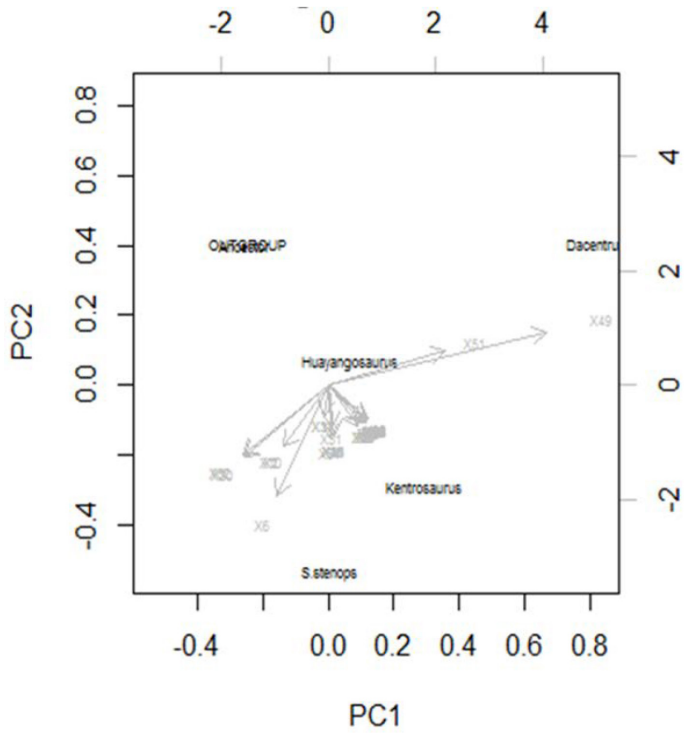

Figure 60. Biplot of PCA scores (black) and vectors (gray) for Galton and Upchurch's (2004b) data matrix for Stegosauria. PC 1 accounts for 67.7% of the variance and PC 2 accounts for 26.1% of the variance.

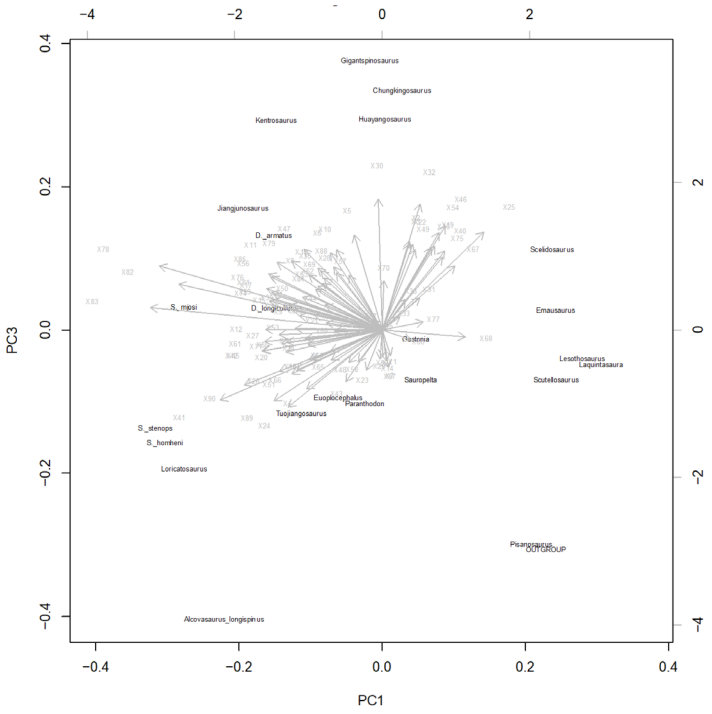

Figure 62. Biplot of PCA scores (black) and vectors (gray) Raven and Maidment's (2017) complete data matrix for Stegosauria. PC 1 accounts for 40.0% of the variance and PC 3 accounts for 16.4% of the variance. PC 3 distinguishes members of Huayangosauridae (top) from the remaining Stegosauria.

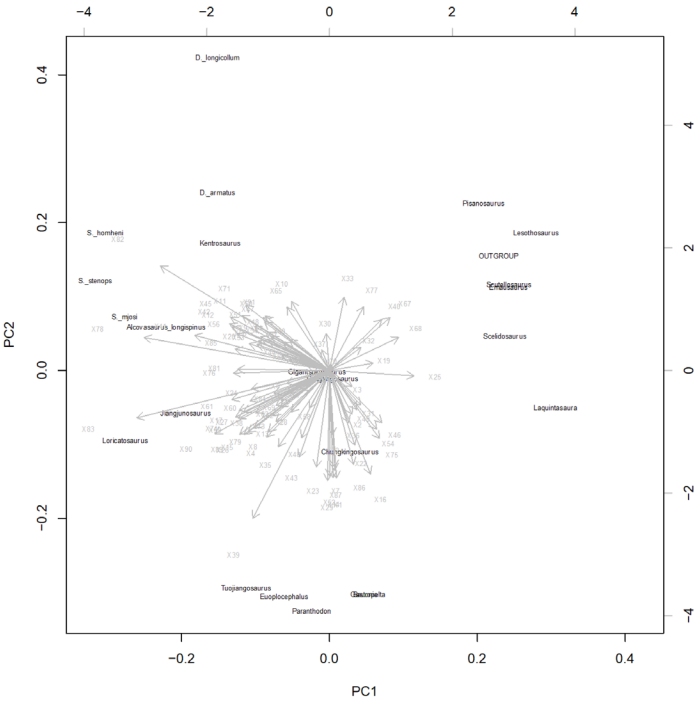

Figure 61. Biplot of PCA scores (black) and vectors (gray) Raven and Maidment's (2017) complete data matrix for Stegosauria. PC 1 accounts for 40.0% of the variance and PC 2 accounts for 26.6% of the variance. PC 1 separates Stegosauria from outgroups (except ankylosaurs). PC 2 suggests a division within the Stegosauria (taxa ordinating on left vs. center/bottom).

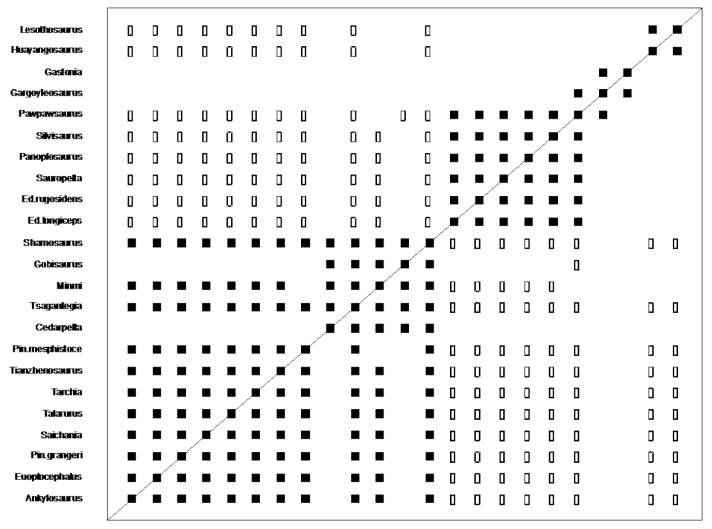

Figure 63. BDC results for Vickaryous et al.'s (2004) data matrix of Ankylosauria, as calculated by BDISTMDS (relevance cutoff 0.95). Closed squares indicate significant, positive BDC; open circles indicate significant, negative BDC.

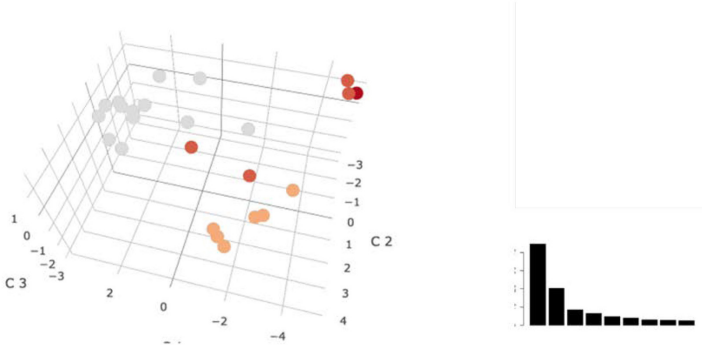

Figure 64. Three-dimensional classical MDS applied to Vickaryous et al.'s (2004) data matrix for Ankylosauria. Members of Ankylosauria are shown in gray, Nodosauridae in orange, and outgroups (in addition to *Gastonia* and *Gargoyleosaurus*) in red. Hypothetical outgroup in dark red. Scree plot suggests the first two axes represent most of the variation.

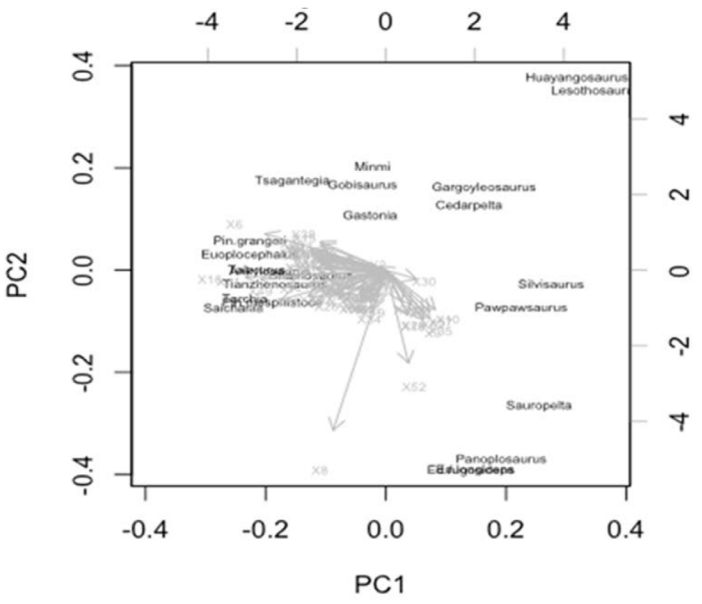

Figure 65. Biplot of PCA scores (black) and vectors (gray) for Vickaryous et al.'s (2004) data matrix for Ankylosauria. PC 1 accounts for 44.2% of the variance and PC 2 accounts for 20.8% of the variance. Members of Ankylosauria are tightly grouped to the left while Nodosauridae are more diffusely spaced on the right. *Gastonia* and *Gargoyleosaurus* again display central positions.

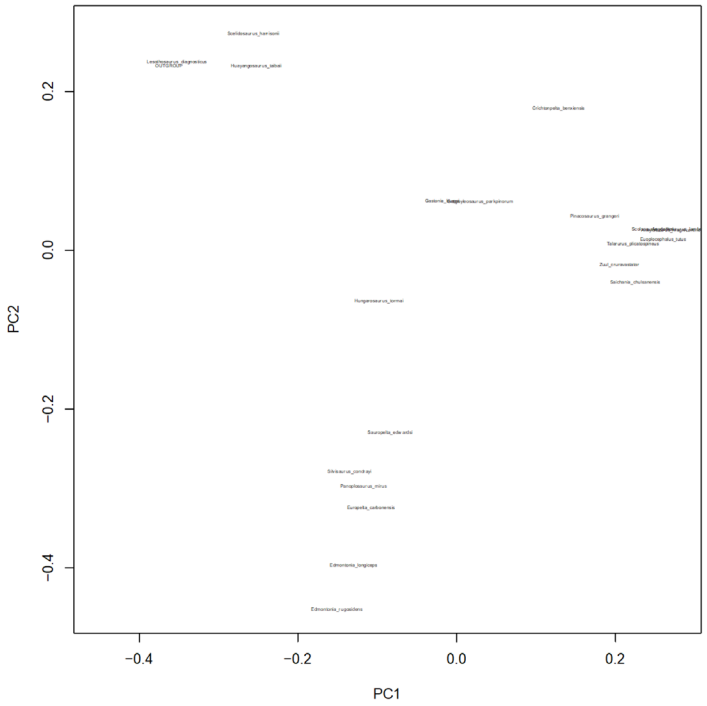

Figure 66. PCA scores for Zheng et al.'s (2018) data matrix for Ankylosauria. PC 1 accounts for 42.9% of the variance and PC 2 accounts for 24.3% of the variance. PC 1 distinguishes Ankylosauridae (left) from Nodosauridae (right). PC 2 distinguishes *Gargoyleosaurus*, *Gastonia*, and *Hungarosaurus* from other nodosaurids.

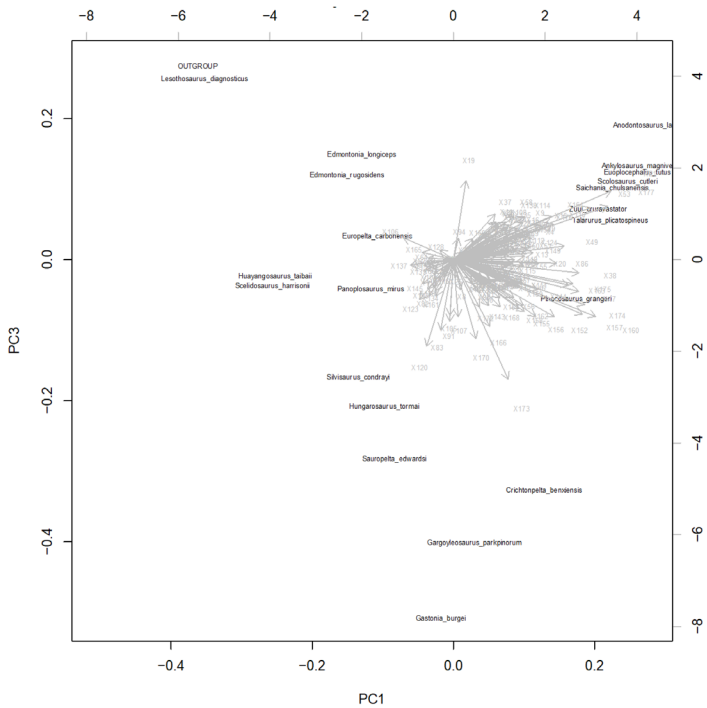

Figure 67. Biplot of PCA scores (black) and vectors (gray) for Zheng et al.'s (2018) data matrix for Ankylosauria. PC 1 accounts for 42.9% of the variance and PC 3 accounts for 12.4% of the variance. PC 3 groups the Ankylosauridae morphoseries (right) distinguishing *Pinacosaurus* and *Crichtonpelta*. *Gargoyleosaurus* and *Gastonia* are likewise distinguished within nodosaurids.

taxa (Marginocephalia and the hypothetical outgroup), whereas the other contains all of the "hypsolophodont"-grade ornithopods, including parksosaurids (thescelosaurids), which have recently been suggested to actually be outside Ornithopoda (Boyd 2015). Classical MDS results show separation between Ornithopoda and Marginocephalia, as well as between Ornithopoda and *Heterodontosaurus tucki* (Fig. 69). PCA results likewise suggest a general grouping of Ornithopoda separate from Marginocephalia and *Heterodontosaurus* (Fig. 70).

E. Basal Iguanodontia

The BDC results for Norman's (2004) data matrix, in Weishampel et al. (2004), show two blocks of positive correlation separated by negative correlation in most instances: 1) Hadrosauriformes and 2) non-hadrosauriform ornithopods + outgroup taxa (Fig. 71). Classical MDS results (Fig. 72) show two main clusters separated from each other by morphological space, which correspond to the blocks of positive correlation in the BDC results. PCA results show rhabdodontids and *Tenontosaurus* clustered with the outgroup taxa, but *Dryosaurus* and *Camptosaurus* are clustered together at a distance away (Fig. 73). There is a trajectory beginning with non-hadrosauroid iguanodonts and moving up to non-hadrosaurid hadrosauroids, and finally a hadrosaurid at the very top left corner.

The PCA results of the Madiza (2017) dataset reveal separation between Hadrosauriformes and non-hadrosauriform iguanodonts for PC 1 (Fig. 74). For PC 2, non-hadrosauromorph hadrosauriforms (e.g., *Iguanodon*, *Ouranosaurus*, etc.) are separated from non-hadrosaurid hadrosauromorphs, which are also separated from hadrosaurids. Although the outgroup overlaps with *Tenontosaurus* in Fig. 74, PC 3 separates the outgroup from these "basal" iguanodonts (Fig. 75). Additionally, PC 3 separates rhabdodontids (*Zalmoxes*) from other "basal" iguanodonts.

PCA separated Hadrosauriformes and non-hadrosauriform Iguanodontia along PC 1 for McDonald's (2012) data matrix (Fig. 76). PC 2 divided a series of Hadrosauroidea from non-hadrosauroid Hadrosauriformes and the "basal" hadrosauroid *Altirhinus*. Additionally, PC 2 separates non-hadrosauriform dryomorphs from non-dryomorphs (including *Tenontosaurus* and *Zalmoxes*). PC 3 separated several Hadrosauromorpha from the rest of the Iguanodontia and outgroups (Fig. 77).

F. Hadrosauridae

The BDC results for Horner et al.'s (2004) data matrix, in Weishampel et al. (2004), show two main blocks of positive correlation separated by negative correlation: 1) Hadrosauridae (the larger block) and 2) non-hadrosaurid taxa (Fig. 78). Within the hadrosaurid block, there are two separate blocks of positive correlation, which correspond to the two traditional hadrosaurid subfamilies: the crested lambeosaurines and the crestless hadrosaurines (now called saurolophines, to the exclusion of *Hadrosaurus*). Loose connections of positive correlation exist between the two subfamily blocks (mainly involving *Nipponosaurus* and *Parasaurolophus*). Classical MDS show separation of Hadrosauridae and outgroups and possibly suggests a small separation between the two hadrosaurid subfamilies (Fig. 79). PCA results likewise suggest separation of Hadrosauridae from outgroups by PC 1 and separation between the subfamilies by PC 2 (Fig. 80).

PCA for the Cruzado-Caballero and Powell (2017) matrix reveals three clear clusters for PC 1 and PC 2: Saurolophinae, Lambeosaurinae, and non-hadrosaurid Hadrosauriformes + the hypothetical outgroup (Fig. 81). Lambeosaurinae taxa form a tightly-spaced series (except for *Jaxartosaurus* and *Tsintaosaurus*, which are at a distance away) while the Saurolophinae taxa are more widely spaced. Additionally, the saurolophine morphoseries includes a gap. The morphoseries above ("Saurolophinae 1") is stratomorphic while the second is not. Saurolophinae 1 and Saurolophinae 2 are separated again by PC 3 (Fig. 82). Saurolophinae 1 corresponds to Kritosaurini + Brachylophosaurini + *Aralosaurus*, and Saurolophinae 2 corresponds to Edmontosaurini + Saurolophini + *Lophorhothon*. *Hadrosaurus* does not cluster with the hadrosaurids. PC 3 also separates the non-hadrosaurid hadrosauriforms into two groups: non-hadrosaurosauromorph hadrosauriforms (below) and non-hadrosaurid hadrosauromorphs (above).

G. Pachycephalosauria

The BDC results for Maryańska et al.'s (2004) data matrix, in Weishampel et al. (2004), show three blocks of positive correlation: traditional Pachycephalosauridae (domed), traditional Homalocephalidae (flat-headed), and the outgroup taxa (Fig. 83). None of the blocks share positive correlation between them, but the traditional pachycephalosaurids all share negative correlation with the outgroup taxa. Classical MDS results show separation between Pachycephalosauridae, the outgroups, and the two "homalocephalids". (Fig. 84). For PCA analysis, only groups with at least 75% of character data were analyzed. PCA results likewise suggest separation of Pachycephalosauridae from *Homalocephale*, *Goyocephale*, and Ceratopsia (Fig. 85).

Pachycephalosauridae for Schott (2011) demonstrated separation from outgroups along PC 1. PC 1 shows separation between Pachycephalosauridae, the "basal" pachycephalosaur *Wannanosaurus*, and the outgroup taxa (Fig. 86). The widely-space members of the morphoseries along PC 2 may indicate additional divisions exist among pachycephalosaurs. For example, PC 3 separates all of the flat-headed pachycephalosaurs (*Dracorex*, *Goyocephale*, *Homalocephale*, and *Wannanosaurus*) from the dome-headed pachycephalosaurs (Fig. 87). Additionally, the closest dome-headed pachycephalosaur to the flat-headed forms is *Stygimoloch*, which has a small, narrow dome, which is unlike the condition in most pachycephalosaurs. It has been suggested that *Dracorex* and *Stygimoloch* are not separate species, but a part of a single growth series that ends in *Pachycephalosaurus* (Horner and Goodwin 2009).

H. "Basal" Ceratopsia

The BDC results for Hailu and Dodson's (2004) data matrix, in Weishampel et al. (2004), show three blocks of positive correlation: 1) the non-neoceratopsian ceratopsians (*Psittacosaurus* and *Chaoyangsaurus*) and outgroup taxa, 2) the non-ceratopsid neoceratopsians, and 3) the two ceratopsid taxa (*Triceratops* and *Centrosaurus*) (Fig. 88). All of the neoceratopsians share negative correlation with the non-neoceratopsian + outgroup block except for *Archaeoceratops*. There is no correlation of any kind between

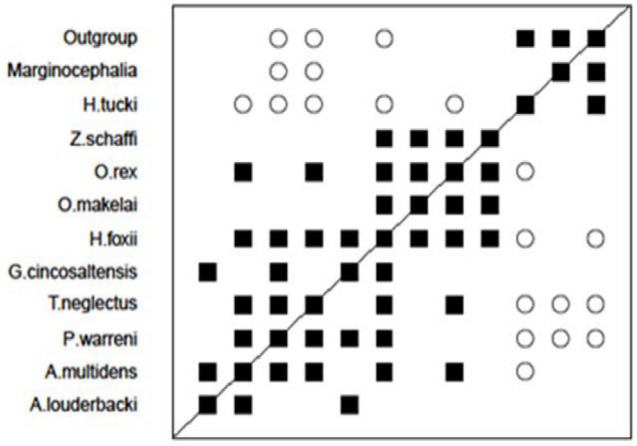

Figure 68. BDC results for Norman, Witmer et al.'s (2004) data matrix of "basal" Ornithopoda, as calculated by BDISTMDS (relevance cutoff 0.80). Closed squares indicate significant, positive BDC; open circles indicate significant, negative BDC.

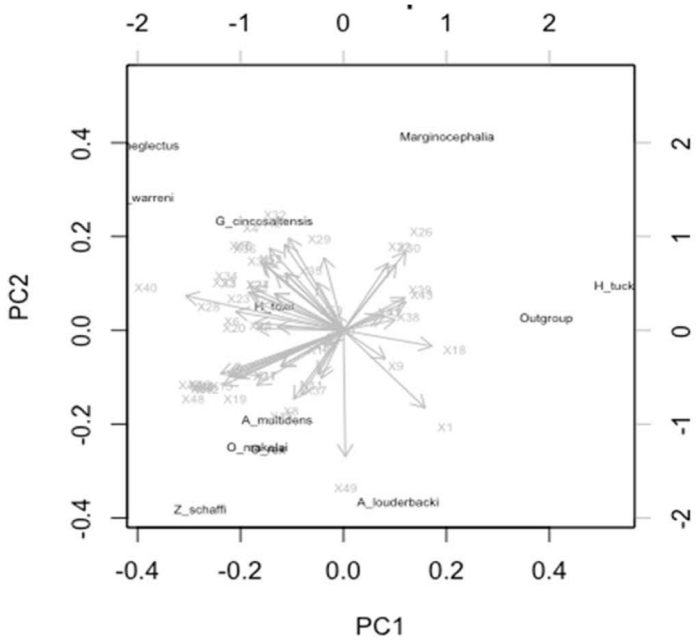

Figure 70. Biplot of PCA scores (black) and vectors (gray) for Norman, Witmer et al.'s (2004) data matrix for Ornithopoda. PC 1 accounts for 38.6% of the variance and PC 2 accounts for 20.8% of the variance. All are members of Ornithopoda, except for Marginocephalia (top right).

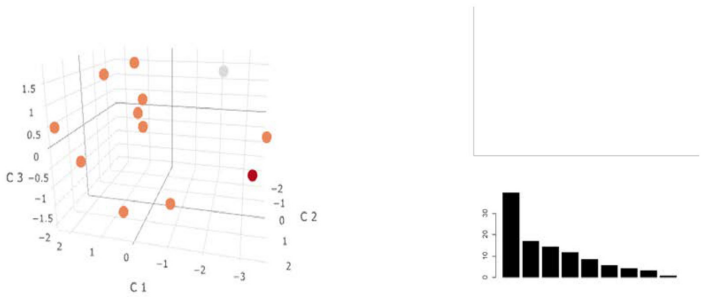

Figure 69. Three-dimensional classical MDS applied to Norman, Witmer et al.'s (2004) data matrix for "basal" Ornithopoda. Marginocephalia is shown in gray, members of Ornithopoda are shown in light red, and the outgroup is in dark red. *H. tucki* is closest to the outgroup. Scree plot suggests the first axis represents most of the variation.

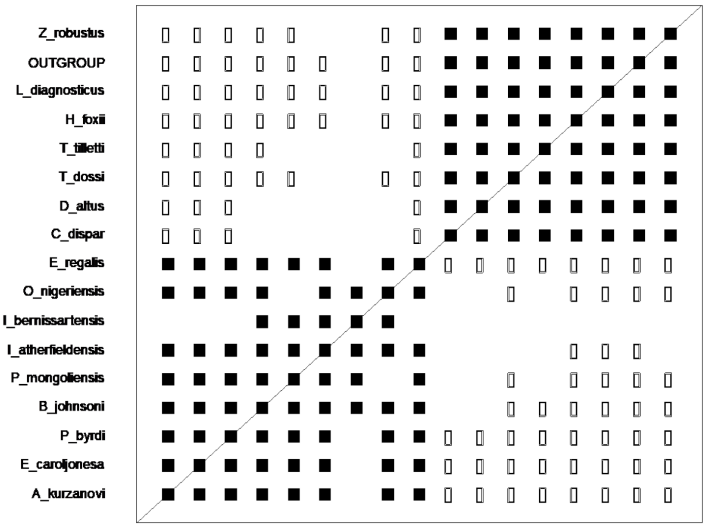

Figure 71. BDC results for Norman's (2004) data matrix of "basal" Iguanodontia, as calculated by BDISTMDS (relevance cutoff 0.95). Closed squares indicate significant, positive BDC; open circles indicate significant, negative BDC.

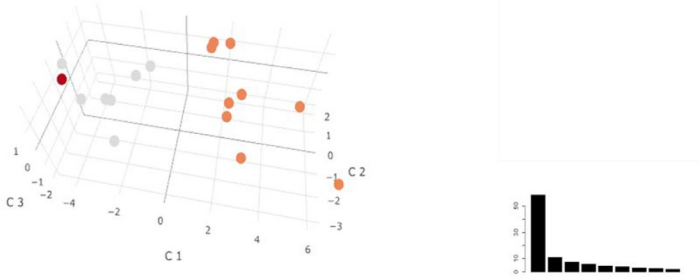

Figure 72. Three-dimensional classical MDS applied to Norman's (2004) data matrix for "basal" Iguanodontia. Non-hadrosauriform ornithischians are shown in gray. Hadrosauriformes is in orange. The imaginary outgroup is dark red, clustered near *L. diagnosticus* and *H. foxii*. Scree plot suggests the first axis represents most of the variation.

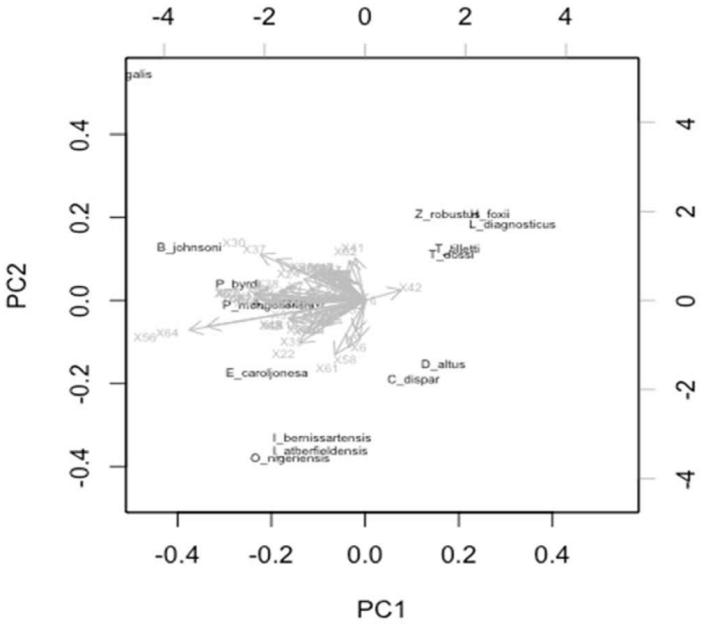

Figure 73. Biplot of PCA scores (black) and vectors (gray) for Norman's (2004) data matrix for Igunodontia. PC 1 accounts for 60.4% of the variance and PC 2 accounts for 10.6% of the variance. Hadrosauriform taxa are toward the left, whereas the non-hadrosauriform iguanodonts and outgroup are toward the middle.

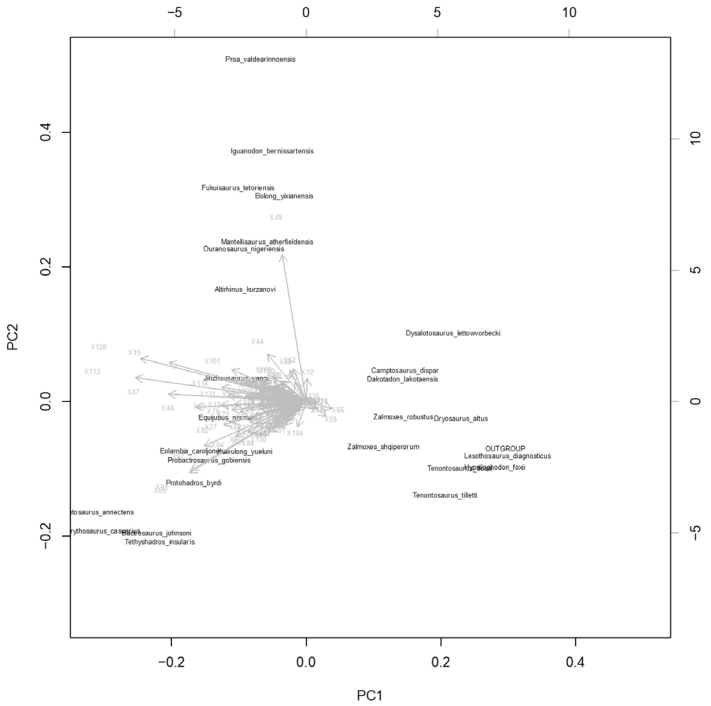

Figure 74. Biplot of PCA scores (black) and vectors (gray) for Madzia et al.'s (2017) data matrix for Ornithopoda. PC 1 accounts for 57.7% of the variance and PC 2 accounts for 11.8% of the variance. PC 1 separates non-hadrosauriform iguanodonts and outgroup taxa from Hadrosauriformes. PC 2 distinguishes non-hadrosauromorph hadrosauriforms (top) from hadrosauromorphs (bottom). The lower morphoseries is stratomorphic.

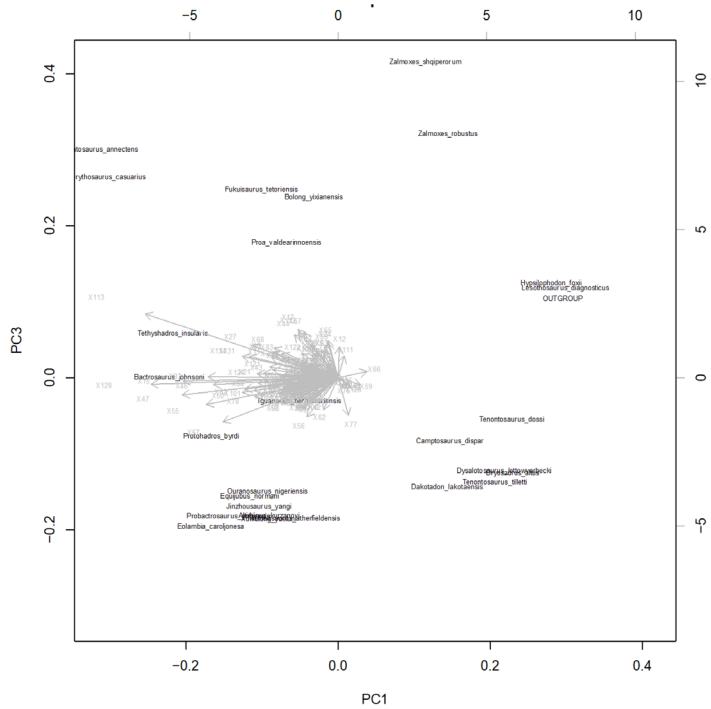

Figure 75. Biplot of PCA scores (black) and vectors (gray) for Madzia et al.'s (2017) data matrix for Ornithopoda. PC 1 accounts for 57.7% of the variance and PC 3 accounts for 7.3% of the variance. PC 3 separates rhabdodontids (top) from other iguanodont taxa.

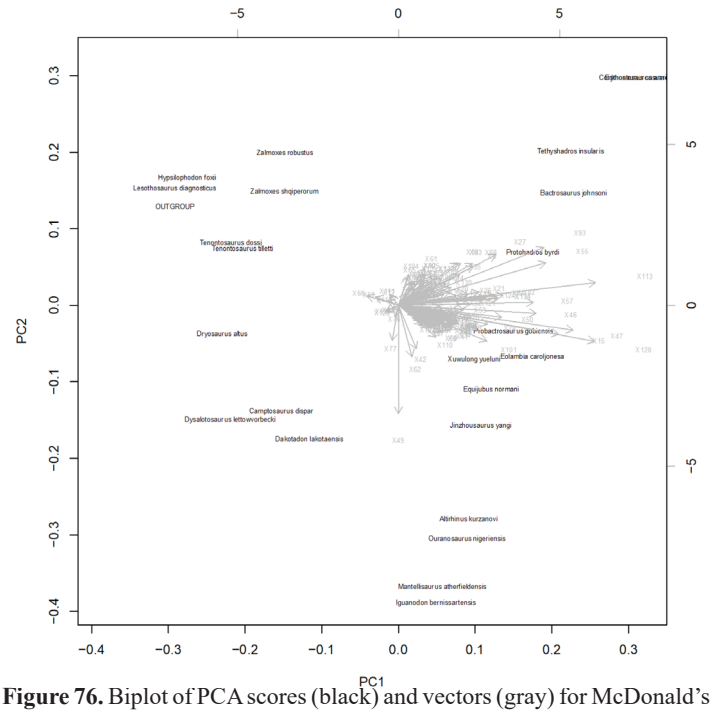

Figure 76. Biplot of PCA scores (black) and vectors (gray) for McDonald's (2012) data matrix for Iguanodontia. PC 1 accounts for 62.8% of the variance and PC 2 accounts for 9.2% of the variance. PC 1 separates non-hadrosauriform Iguanodontia (left) from Hadrosauriformes (right). PC 2 separates the non-dryomorph iguanodonts (top) from the dryomorphs (bottom) among the series on the left, and it separates three groups on the right: 1) non-hadrosauroid Hadrosauriformes + *Altirhinus* (bottom), 2) non-hadrosaurid Hadrosauroidea (middle), and 3) Hadrosauridae (top).

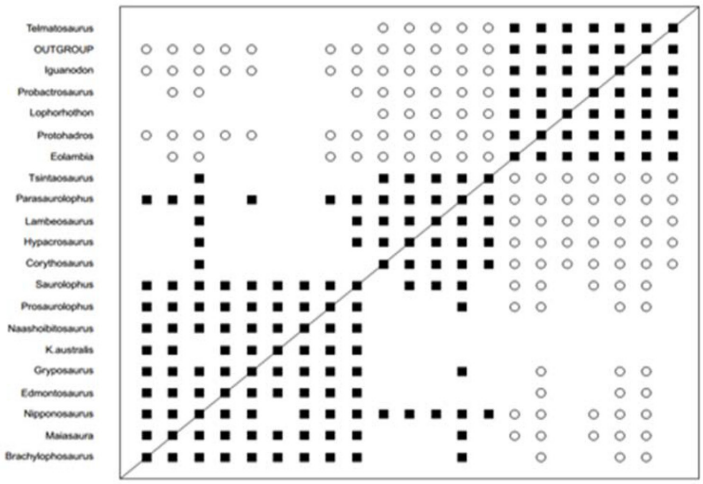

Figure 78. BDC results for Horner et al.'s (2004) data matrix of Hadrosauridae, as calculated by BDISTMDS (relevance cutoff 0.75). Closed squares indicate significant, positive BDC; open circles indicate significant, negative BDC.

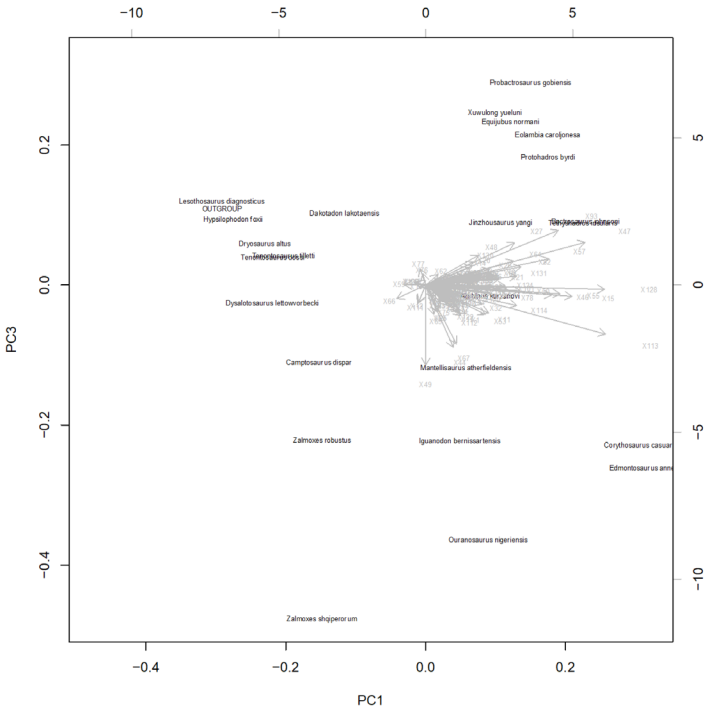

Figure 77. Biplot of PCA scores (black) and vectors (gray) for McDonald's (2012) data matrix for Iguanodontia. PC 1 accounts for 62.8% of the variance and PC 3 accounts for 6.8% of the variance. PC 3 separated "basal" Hadrosauriformes (traditional Iguanodontidae) from the other taxa.

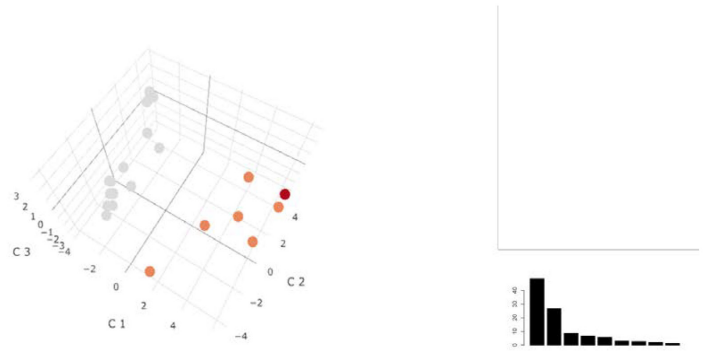

Figure 79. Three-dimensional classical MDS applied to Horner et al.'s (2004) data matrix for Hadrosauridae. Members of Hadrosauridae are shown in gray, with outgroups *Iguanodon*, *Probactrosaurus*, *Protohadros*, *Eolambia*, *Telmatosaurus*, and *Lophorhothon* (bottom center) shown in orange. Composite outgroup is dark red. Deeper separation within Hadrosauridae (gray) is suggested, though not conclusive. Scree plot suggests the first two axes represent most of the variation.

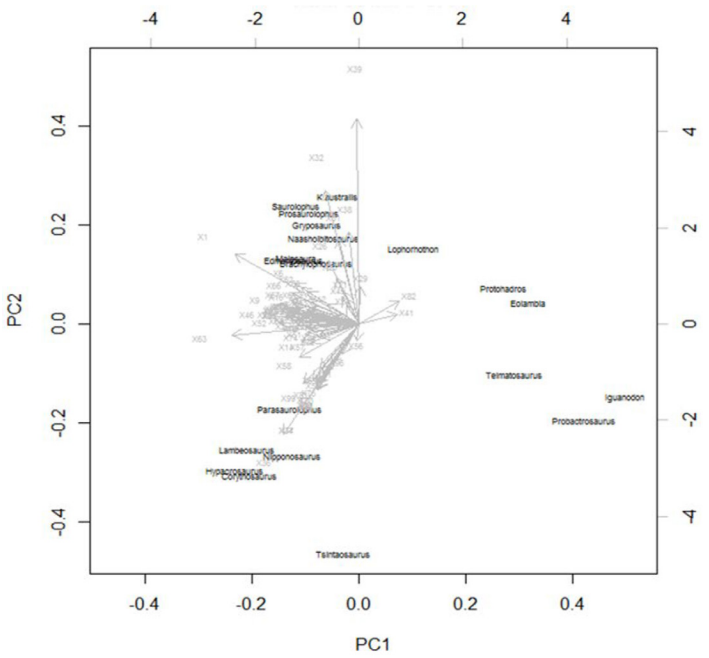

Figure 80. Biplot of PCA scores (black) and vectors (gray) for Horner et al.'s (2004) data matrix for Hadrosauridae. PC 1 accounts for 49.4% of the variance and PC 2 accounts for 31.5% of the variance. Members of Hadrosauridae are grouped in a series on the left. PC 2 separates lambeosaurine hadrosaurids (bottom) from saurolophine hadrosaurids (top).

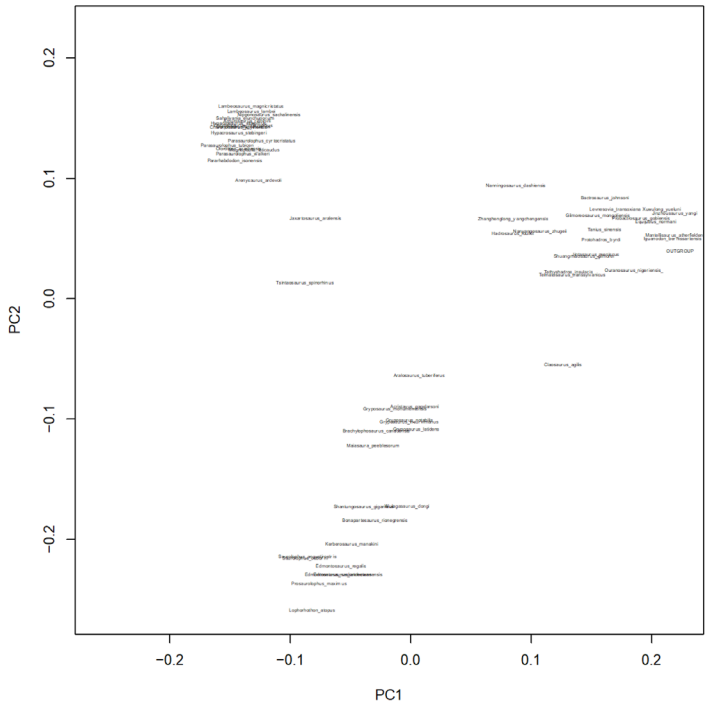

Figure 81. PCA scores for Cruzado-Caballero and Powell's (2017) data matrix for Hadrosauroidea. PC 1 accounts for 47.3% of the variance and PC 2 accounts for 20.2% of the variance. PC 1 and PC 2 reveal discontinuity between the Lambeosaurinae and Saurolophinae subfamilies. PC 2 further suggests additional division within the Saurolophinae morphoseries: 1) Kritosaurini + Brachylophosaurini (top) and 2) Edmontosaurini + Saurolophini. The lambeosaurine *Aralosaurus* clusters with Saurolophinae morphoseries 1.

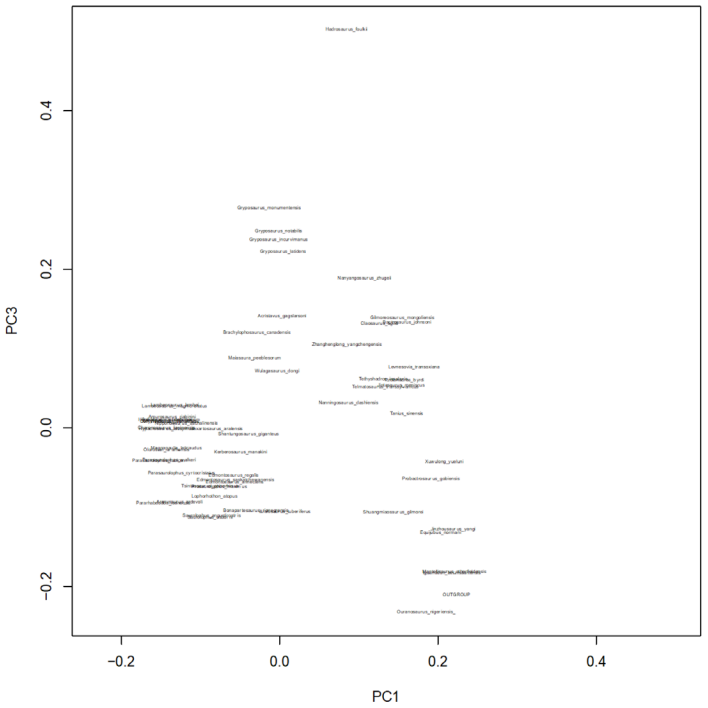

Figure 82. PCA scores for Cruzado-Caballero and Powell's (2017) data matrix for Hadrosauroidea. PC 1 accounts for 47.3% of the variance and PC 3 accounts for 15.6% of the variance. PC 3 separates the Lambeosaurinae from the Saurolophinae on the left, and it also separates the non-hadrosauromorph Hadrosauriformes from the non-hadrosaurid Hadrosauromorpha (right).

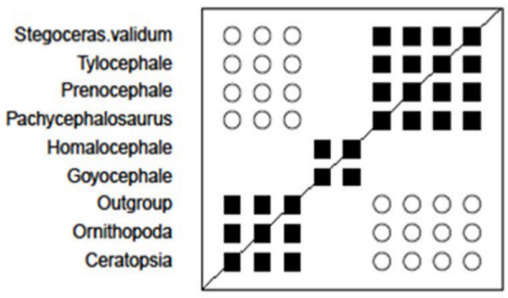

Figure 83. BDC results for Maryańska et al.'s (2004) data matrix of Pachycephalosauria, as calculated by BDISTMDS (relevance cutoff 0.80). Closed squares indicate significant, positive BDC; open circles indicate significant, negative BDC.

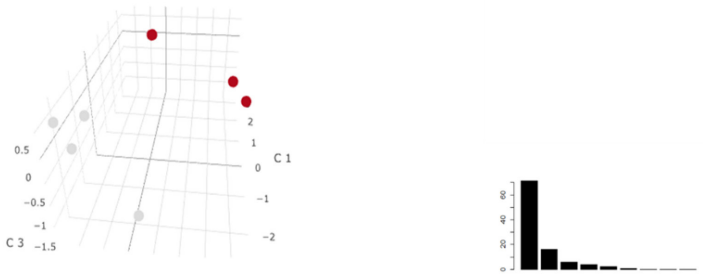

Figure 84. Three-dimensional classical MDS applied to Maryańska et al.'s (2004) data matrix for Pachycephalosauria. Members of Pachycephalosauridae are shown in gray, whereas all other members including *Homalocephale*, *Goyocephale*, and the outgroup are shown in dark red. The outgroup clusters near Ceratopsia, *Homalocephale*, and *Goyocephale*. Scree plot suggests the first axis represents most of the variation.

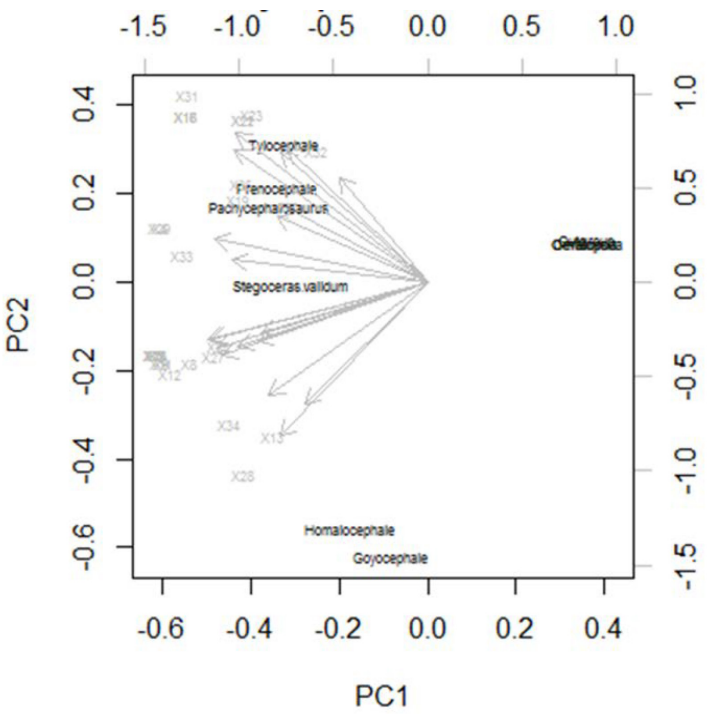

Figure 85. Biplot of PCA scores (black) and vectors (gray) for Maryańska et al.'s (2004) data matrix for Pachycephalosauria. PC 1 accounts for 70.2% of the variance and PC 2 accounts for 17.1% of the variance. Members of dome-headed Pachycephalosauridae are in the top-left.

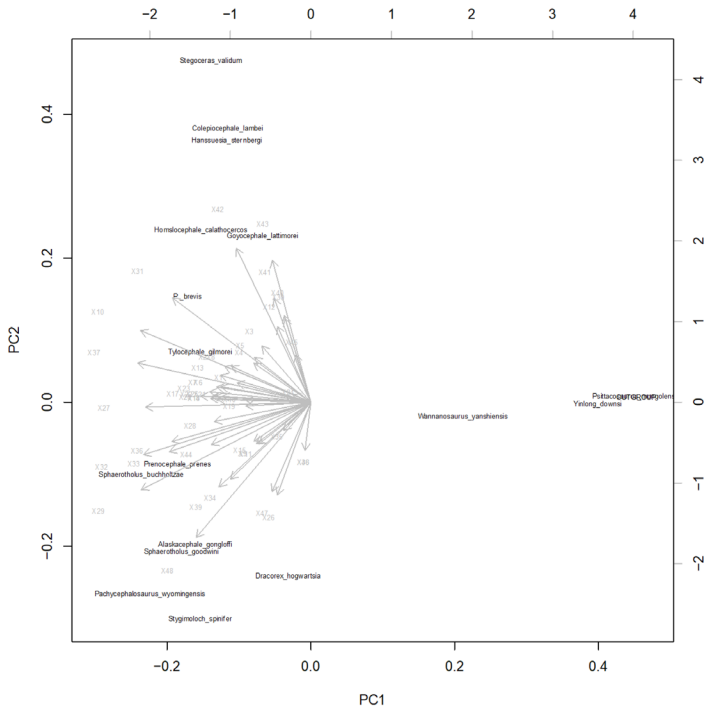

Figure 86. Biplot of PCA scores (black) and vectors (gray) for Schott's (2011) data matrix for Pachycephalosauria. PC 1 accounts for 50.0% of the variance and PC 2 accounts for 21.9% of the variance. PC 1 separates pachycephalosaurs (left) from the outgroup taxa (right), although *Wannanosarus* a "basal" pachycephalosaur, is closer to the outgroup taxa.

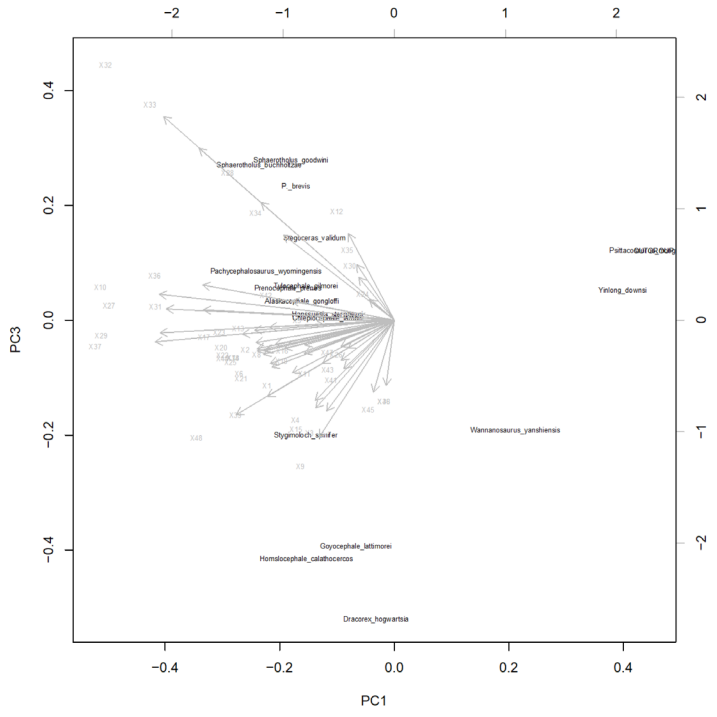

Figure 87. Biplot of PCA scores (black) and vectors (gray) for Schott's (2011) data matrix for Pachycephalosauria. PC 1 accounts for 50.0% of the variance and PC 3 accounts for 8.4% of the variance. PC 3 separates the flat-headed taxa *Goyocephale*, *Homalocephale*, and *Dracorex* from the majority of Pachycephalosauridae.

the ceratopsids and the non-ceratopsid neoceratopsians. Classical MDS results show a similar division, including placement of *Psittacosaurus* and *Chaoyangsaurus* with the outgroup taxa (Fig. 89). In agreement with the other methods, PCA suggests separation between Ceratopsidae and other ceratopsians and between neoceratopsians and the outgroup + *Psittacosaurus* (Fig. 90).

"Basal" Ceratopsia for Han et al.'s (2017) data matrix reveals separation between Ceratopsia and all outgroups, including pachycephalosaurs, for PC 1 (Fig. 91). Both PC 2 and PC 3 separate basal Ceratopsia (*e.g., Psittacosaurus* and *Yinlong*) and Neoceratopsia (Fig. 92). In PC 2, The ceratopsian taxa are also aligned stratigraphically with the Upper Jurassic "basalmost" ceratopsian, *Yinlong*, on the bottom and the more "derived" forms (*Protoceratops* and *Leptoceratops*) found in Upper Cretaceous rocks at the top. However, *Leptoceratops*, a Maastrichtian form, is found below *Protoceratops*, a Campanian form, in the series.

I. Ceratopsidae

The BDC results for Dodson et al.'s (2004) data matrix, in Weishampel et al. (2004), show three blocks of positive correlation: 1) non-ceratopsid outgroup, 2) Chasmosaurinae, and 3) Centrosaurinae (Fig. 93). Almost all of the ceratopsid taxa (Chasmosaurinae and Centrosaurinae together) share negative correlation with the non-ceratopsid outgroup taxa. There is only one instance of shared positive correlation between the two ceratopsid blocks (*Triceratops* and *Avaceratops*) and no instances of shared negative correlation. Classical MDS results show separation between Ceratopsidae and the outgroup taxa, as well as separation between the two ceratopsid subfamilies (Fig. 94). PCA results likewise show separation between the three groups, however it is also revealed that *Zuniceratops* is separated from *Protoceratops* and the hypothetical outgroup by PC 2 (Fig. 95).

PCA for Fry (2015) separates the Chasmosaurinae from the non-chasmosaurine taxa (centrosaurines and non-ceratopsids), with a suggestion of two parallel morphoseries. Triceratopsini forms a series within Chasmosaurinae with *Arrhinoceratops* and *Bravoceratops* clustering more closely with Triceratopsini members (Fig. 96). A parallel series is revealed in non-triceratopsin chasmosaurines. PC 3 groups taxa from all groups but reveals a separation for the three included centrosaurine species (Fig. 97).

DISCUSSION

These results answer a number of interesting questions regarding not only dinosaurs and the relationships of birds to dinosaurs, but also for methodologies aiding baraminology. Close analysis of the PCA results further suggest details for Flood-related burial of dinosaur assemblages.

We have inferred continuity between dinosaur taxa based on shared positive correlation (BDC) and close clustering/trajectories (MDS and PCA), whereas discontinuity was inferred for shared negative correlation (BDC) and distant spacing in MDS and PCA. Because of these patterns discussed in our Results section, we arrived at various conclusions on the baraminic status of various dinosaur taxa (Table 1, Appendix Table 2).

PCA analyses yielded unexpected insights. BDC analyses identified dinosaur holobaramins, often near the family level, as groups of taxa with significant similarity and dissimilarity. PCA revealed morphospatial relationships of dinosaurs across wider taxonomic ranges than BDC was designed for. Component plots provided additional details on the nature of holobaramins. For PCA, holobaramins are taxa confined to spatial clusters or, more often, linear series. Dinosaur holobaramins visualized in multivariate space could be defined as *discontinuity-bounded morphospatial series of related taxa*. That is, dinosaur holobaramins were frequently ordered in short series of taxa that were spatially-isolated from other series. The series of closely-spaced taxa in multivariate space represent trajectories through limited morphological space.

Morphospatial series yielded additional potential insights. Using conventional radiometric ages as relative chronometers, series can sometimes be identified as stratomorphic. Stratomorphic morphospatial series are defined as sequential morphospatial series whose morphological sequence appearance matches its fossil record first appearance order (Wise 1995). Of the 42 lineages, seven had strong suggestive stratomorphic overprints ("Yes" and "Nearly" in Table 1).

These results suggest that dinosaurs, like many other taxonomic groups examined through baraminology, frequently show discontinuity at or near the family level. Of 27 lineages examined in the most recent matrices which suggest holobaramins or near-holobaramins, six are at the family level, four are subfamilies, and fourteen are at suborder or between suborder or family (Table 1).

A further inference drawn from these observations raised questions about how dinosaur baramins were distributed within the Mesozoic. For example, all four of the proposed subfamily-level holobaramins were found in the Upper Cretaceous. Four of the seven stratomorphic holobaramins were entirely confined to the Cretaceous, and the remaining three included Cretaceous taxa.

The results also address a number of questions regarding dinosaur biosystematics and bird-dinosaur relationships.

1. Baraminology

A. Dinosaur Groups

The Dinosauria contain three large, morphologically-disparate groups. Baron's (2018) Dinosauria matrix provided the most diverse set of taxa for comparison. Analysis of the complete data with the ordination-based systematics employed here leads to a conclusion similar to Baron's phylogenetic analysis. That is, the complete data matrix suggests an association of ornithischians and theropods within an Ornithoscelida group (Figs. 1 and 2). From the standpoint of a creation model approach to systematics, the existence of an Ornithoscelida cluster is a neutral question; biological creation includes hierarchies of higher-order associations. However, after removing taxa with the highest proportions of missing data (*i.e.*, taxa with 50% or more missing data) a different ordination emerged: theropods, ornithischians, and sauropodomorphs formed three equally distant spatial associations (Figs. 3 and 4). This was consistent with ordinations of basal Saurischia (Fig. 8) that likewise divided sauropods and theropods. We propose that the ordination resulting in an Ornithoscelida cluster (*i.e.*, Fig. 1) was generated, in part, as a result of missing data. Taxa with large amounts of missing data likely function as "noise" that obscures underlying group spatial relationships; removal of problematic taxa results in different spatial geometries. Alternatively, another possibility is

Table 1. Dinosaur baramins and group characteristics estimated through PCA. Holobaramin (H), Apobaramin (A), and Monobaramin (M) are assigned approximate taxonomic levels. Taxa within baramins ordinate as clusters or series. Stratomorphic baraminic groups occur where morphological series (PC 1 and PC 2) reflect taxon order of first appearance in the fossil record. Series ranges are shown by conventional first appearance datum (FAD) and last appearance datum (LAD).

				Series Characteristics		Range	
Higher Taxonomy	**Baraminology**	**Taxonomic Equivalent**	**n**	**Ordination**	**Stratomorphic**	**FAD**	**LAD**
Saurichia	Herrerasauridae (H?)	Family	2	Cluster	No	233.23	225
Saurischia: Theropoda	Coelophysoidea (M)	Superfamily	5	Cluster	No	220	183
Saurischia: Theropoda	Noasauridae (H?)	Family	5	Cluster	No	161	70
Saurischia: Theropoda	Abelisauridae (minus *Eoabelisaurus*) (H)	Family	10	Series	No	110	66
Saurischia: Theropoda	"Basal" Tetanurae (??)	Unranked (above Family)	15?	Series	Nearly	201	91
Saurischia: Theropoda	Spinosauridae (M)	Family	2	Cluster	No	148	85
Saurischia: Theropoda	Tyrannosauroidea (minus some "basal" forms) (H)	Superfamily	13	Series	Nearly	130	66
Saurischia: Theropoda	Ornithomimosauria (H)	Unranked (below Suborder)	8	Series	Yes	140	66
Saurischia: Theropoda	Therizinosauridae (H)	Family	10	Cluster	Unclear	94	66
Saurischia: Theropoda	Oviraptorosauria (H)	Unranked (below Suborder)	8	Series	No	130	66
Saurischia: Theropoda	Deinonychosauria (H)	Superfamily	~30	Cluster	No	130	66
Saurischia: Sauropodomorpha	Thecodontosauridae (M)	Family	2	Cluster	No	203	199
Saurischia: Sauropodomorpha	Non-sauropod Massopoda (M)	Unranked (below Suborder)	~11	Cluster	No	228	189
Saurischia: Sauropodomorpha	Flagellicaudata (A?)	Superfamily	3	Cluster	No	170	122
Ornithischia: Thyreophora	Stegosauria (H)	Suborder	14	Series	No	169	125
Ornithischia: Thyreophora	Ankylosauria (H?)	Suborder	21	Series	No	168	66
Ornithischia: Ornithopoda	Non-hadrosauriform Iguanodontia (A?)	Unranked (below Suborder)	10+	Cluster	No	163	66
Ornithischia: Ornithopoda	Non-hadrosaurid Hadrosauriformes (H?)	Unranked (above Family)	~14	Series	Yes	~140	66
Ornithischia: Ornithopoda	Saurolophinae (H)	Subfamily	19	2 Series	1 No; 1 Yes	79	66
Ornithischia: Ornithopoda	Lambeosaurinae (H)	Subfamily	18	Cluster	No	85.8	66
Ornithischia: Marginocephalia	Pachycephalosauria (H)	Suborder	14	Series	No	86	66
Ornithischia: Marginocephalia	Non-neoceratopsian Ceratopsia (H?)	Unranked (above Family)	4	Cluster/ Series	No/Yes	158	101
Ornithischia: Marginocephalia	Non-ceratopsid Neoceratopsia (H?)	Unranked (above Family)	6	Series	Nearly	126	66
Ornithischia: Marginocephalia	Chasmosaurinae (H?)	Subfamily	25	Series	No	78	66
Ornithischia: Marginocephalia	Centrosaurinae (H?)	Subfamily	~6	Cluster	No	80.8	66

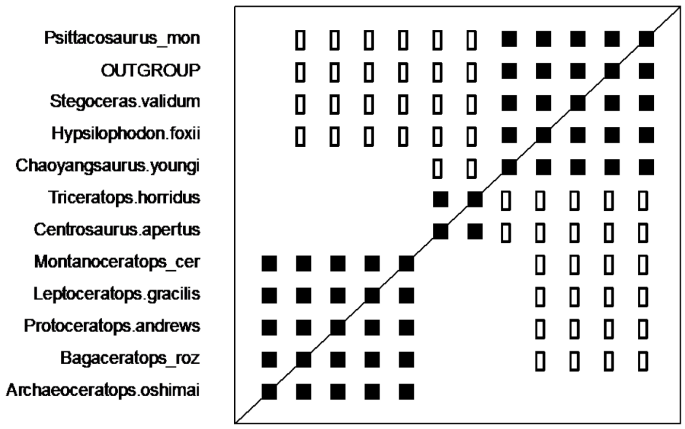

Figure 88. BDC results for Hailu and Dodson's (2004) data matrix of "basal" Ceratopsia, as calculated by BDISTMDS (relevance cutoff 0.95). Closed squares indicate significant, positive BDC; open circles indicate significant, negative BDC.

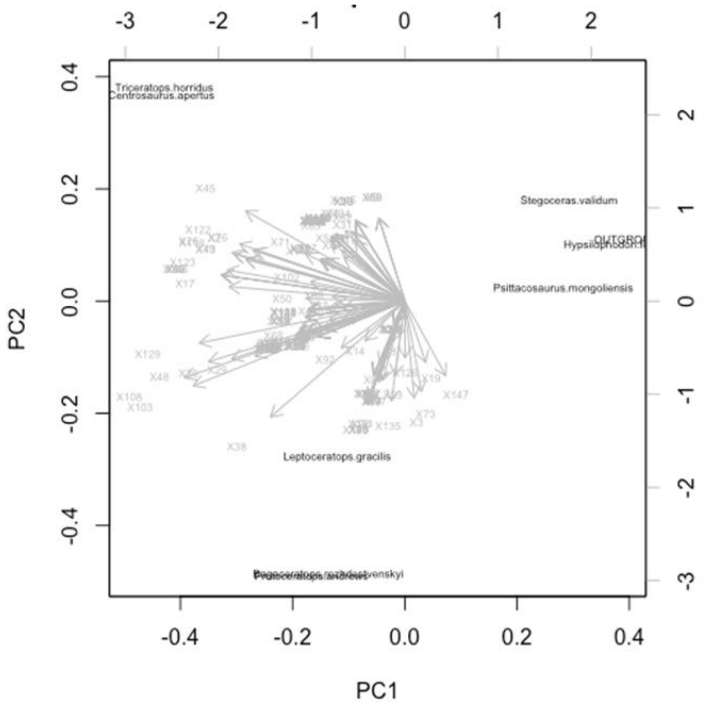

Figure 90. Biplot of PCA scores (black) and vectors (gray) for Hailu and Dodson's (2004) data matrix for Ceratopsia. PC 1 accounts for 58.6% of the variance and PC 2 accounts for 19.2% of the variance. Members of Psittacosauridae split into bottom and top-right. *Triceratops* and *Centrosaurus* show clear separation (top left).

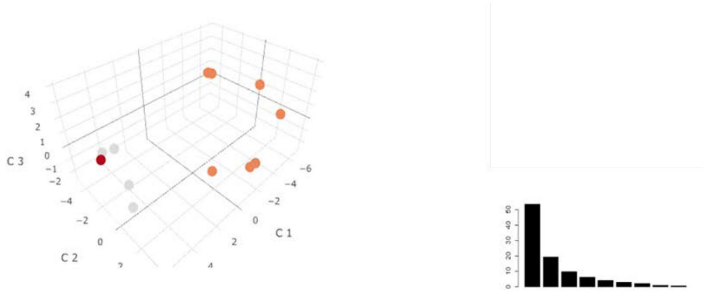

Figure 89. Three-dimensional classical MDS applied to Hailu and Dodson's (2004) data matrix for "basal" Ceratopsia. Outgroup members are light gray, Ceratopsia is light red, and the generic outgroup is dark red. The outgroup is clustered closest to *Psittacosaurus mongoliensis* and *Chaoyangsaurus youngi*. Scree plot suggests the first axis represents most of the variation.

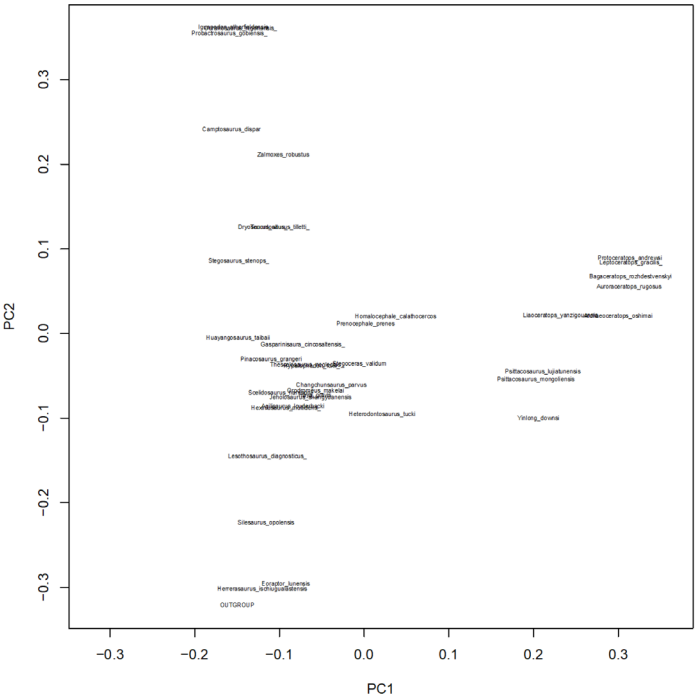

Figure 91. PCA scores for Han et al.'s (2017) data matrix for Ceratopsia. PC 1 accounts for 29.9% of the variance and PC 2 accounts for 19.5% of the variance. PC 1 separates ceratopsians (right) from the other taxa. PC 1 and PC 2 reveal a nearly stratomorphic morphoseries for Ceratopsia (right). Basal taxa also suggest a stratomorphic series (left).

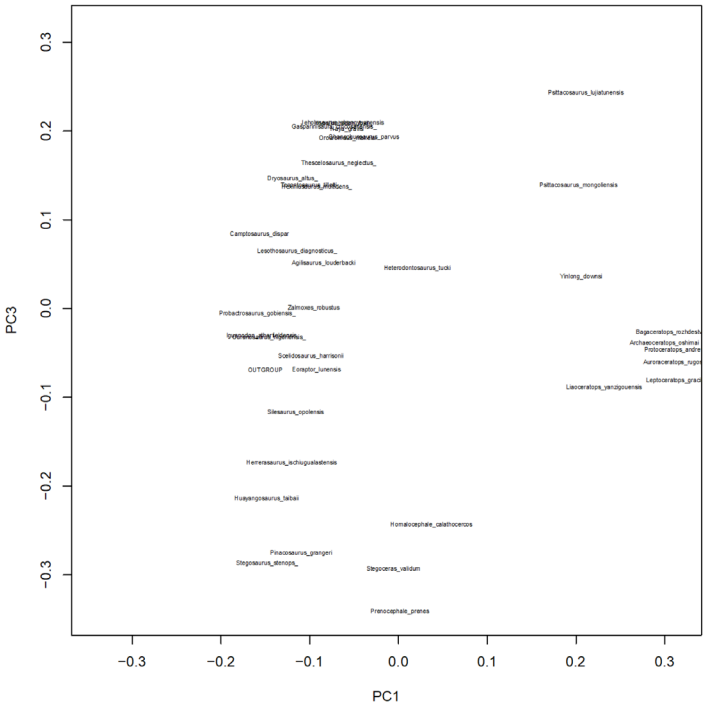

Figure 92. PCA scores for Han et al.'s (2017) data matrix for Ceratopsia. PC 1 accounts for 29.9% of the variance and PC 3 accounts for 17.0% of the variance. PC 3 separates Neoceratopsia from "basal" Ceratopsia (right).

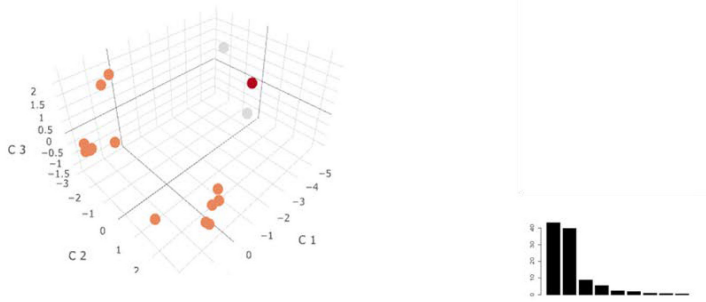

Figure 94. Three-dimensional classical MDS applied to Dodson et al.'s (2004) data matrix for Ceratopsidae. Members of Ceratopsidae are shown in light red, *Zuniceratops* and *Protoceratops* are shown in gray, the outgroup is dark red. The outgroup is clustered near *Protoceratops* and *Zuniceratops*. Scree plot suggests the first two axes represent most of the variation.

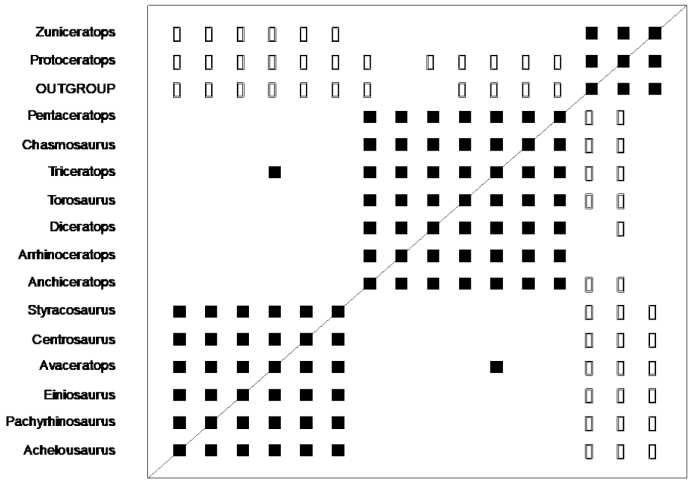

Figure 93. BDC results for Dodson et al.'s (2004) data matrix of Ceratopsidae, as calculated by BDISTMDS (relevance cutoff 0.75). Closed squares indicate significant, positive BDC; open circles indicate significant, negative BDC.

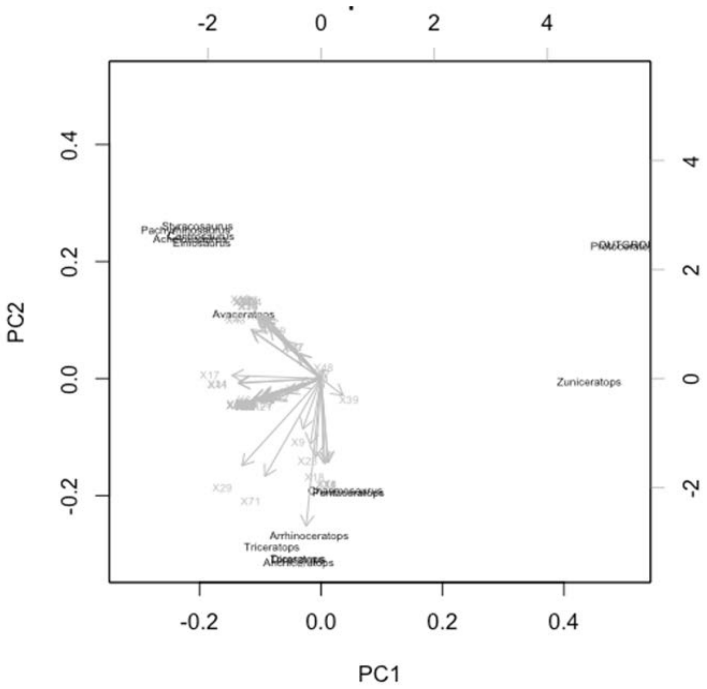

Figure 95. Biplot of PCA scores (black) and vectors (gray) for Dodson et al.'s (2004) data matrix. PC 1 accounts for 45.5% of the variance and PC 2 accounts for 38.1% of the variance. Members of Ceratopsidae are shown to the left. The outgroup, *Zuniceratops*, and *Protoceratops* show clear separation (far right).

that some of the taxa with less than 50% of available character data are transitional in morphology between the other groups so they fall in between them, creating a spatially-scattered ordination for the plot. This may be occurring in some situations, but removal of taxa with less than 50% of characters across the board should not preferentially remove taxa with transitional morphologies. As a result, we predict that future datasets with more complete data will continue to reveal these three major dinosaur divisions as discontinuity-bounded, morphospatially separate associations (apobaramins).

B. PCA-defined Holobaramins

Many dinosaur holobaramins could be clearly distinguished. Often, the additional material of newer datasets clarified uncertainty from earlier, less complete matrices (i.e., 2004 matrices). One example was "Prosauropoda." The 2004 BDC results (Fig. 42) showed positive BDC between all non-sauropod sauropodomorphs (except for *Camelotia*, which was only correlated with a few others). Both MDS and PCA suggested there may be discontinuities within this group, but it was not very clear. However, the Bronzati (2017) PCA results show various clusters and series of "prosauropods", which probably correspond to different holobaramins such as Thecodontosauridae and non-sauropod Massopoda (listed as monobaramins (but possibly holobaramins) in Table 1 and Appendix Table 2.

Another group that benefited from better data was the Ankylosauria. Ankylosauria BDC results for the 2004 matrix separated taxa into two groups. One group contained traditional nodosaurids and two polacanthines (a group of ankylosaurs that have been taxonomically difficult to place as either ankylsoaurids or nodosaurids). The non-polacanthine nodosaurid block was separated from the ankylosaurid block by negative correlation, but the polacanthines shared no correlation with the ankylosaurids at all. This pattern was explained well by the MDS plot and especially the PCA plot, which both show the polacanthines in a gap directly between the ankylosaurids and nodosaurids. These patterns suggest that all of Ankylosauria might be a holobaramin. Interestingly, the results from the Zheng et al. (2018) analysis show two different patterns. Comparing PC 1 and PC 2 results in a series of nodosaurids and a separate cluster of ankylosaurids. Polacanthine taxa fall in between. Comparing PC 1 and PC 3, however, shows the polacanthines at the base of a series of nodosaurids, far away from the ankylosaurids by PC 3, but still near them in PC 1. Surprisingly, the ankylosaurid *Crichtonpelta* clusters near the polacanthines and not the other ankylosaurids. These PCA results for Zheng et al. (2018) help to show why it is so difficult to classify polacanthines: some of their features are more ankylosaurid-like and some are more nodosaurid-like. It is likely, given these results, that ankylosaurs as a whole are a single holobaramin. Indeed, recent research into the evolution of the tail club in ankylosaurids (Arbour and Currie 2015) is consistent with the idea that nodosaurids and ankylosaurids share a single common ancestor. Some of the taxa that are considered transitional in tail morphology between the two groups have not been included in this analysis (*Liaoningosaurus* and *Gobisaurus*).

Hadrosauridae provided an example of group with potentially hidden morphological divisions. PCA supported the groupings of BDC and MDS (compare Figs. 78-80) yet PCA revealed a potentially deeper subfamily-level division. Hadrosauridae had positive BDC between group members, although two blocks of positive correlation within the hadrosaurid block were evident,

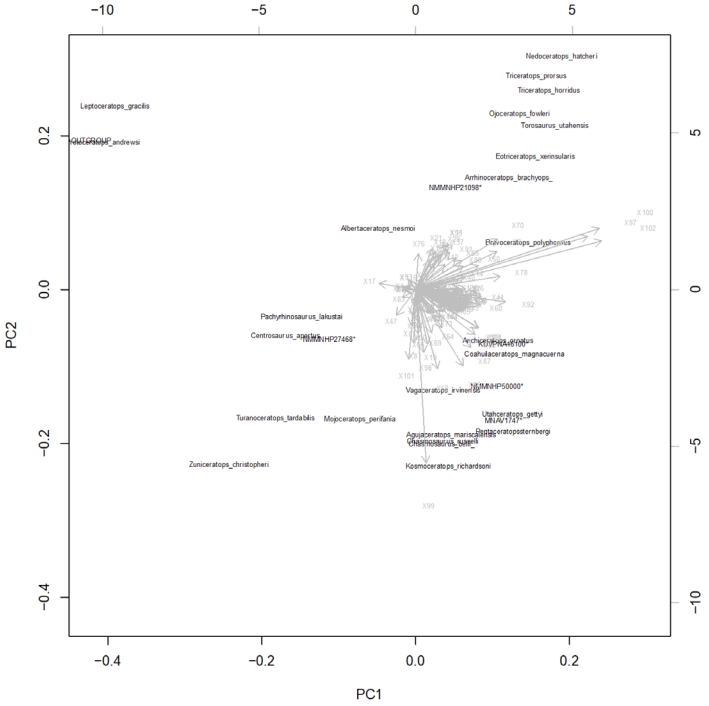

Figure 96. Biplot of PCA scores (black) and vectors (gray) for Fry's (2015) data matrix for Ceratopsidae. PC 1 accounts for 45.6% of the variance and PC 2 accounts for 19.2% of the variance. PC 1 separates Chasmosaurinae from non-chasmosaurine taxa. PC 2 reveals a separation between Triceratopsini (top) and non-triceratopsin chasmosaurines (below).

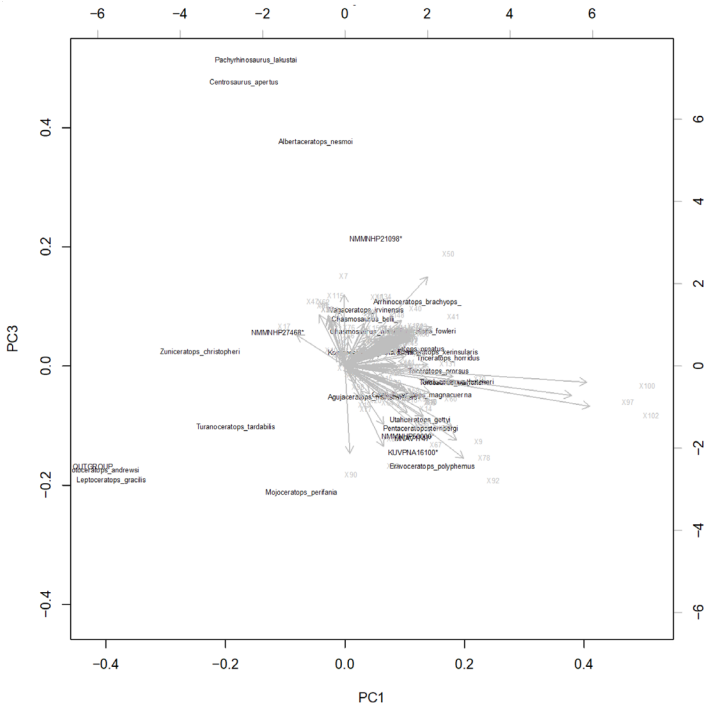

Figure 97. Biplot of PCA scores (black) and vectors (gray) for Fry's (2015) data matrix for Ceratopsidae. PC 1 accounts for 45.6% of the variance and PC 3 accounts for 14.0% of the variance. PC 3 divides centrosaurine taxa (top) from Chasmosaurinae (below).

with negative BDC against outgroups. MDS also separated all Hadrosauridae members from its outgroups, and the hadrosaurids did appear to be two clusters of taxa. The first two MDS axes explain nearly all the variance. PCA affirmed the separation of Hadrosauridae from its outgroups yet strongly suggested two morphological groups within Hadrosauridae: Saurolophinae and Lambeosaurinae. Analysis of Cruzado-Cabellero and Powell's (2017) more complete matrix made the subfamily division clear (Fig. 81). Additionally, a morphological gap in the Saurolophinae subfamily (Kritosaurini + Brachylophosaurini versus Edmontosaurini + Saurolophini) suggests deeper division may exist. The disjunct morphoseries appears to be series of taxa in two ends of a common spatial trajectory, as if linking taxa are missing. These groups may ultimately be connected or they could be two holobaramins whose similar ordinations reflect deeper biological similarities (*e.g.*, similar trophic or ecological functions).

C. Implications of morphospatial patterns

An even more interesting, and structurally deeper, disjunct morphoseries appears to be present between basal tetanurans and tyrannosauroids. The baraminic distance relationships were too complex to represent with BDC (Fig. 16). The BDC plot was poorly defined due to the inclusion of taxa from multiple taxonomic families. The same data plotted with PCA revealed several morphological clusters, with smaller groups nested within (Fig. 17). The divisions reflected distinct structural designs within Tetanurae: a Tyrannosauroidea series (top, numbered "1"); non-tyrannosauroid coelurosaurs (with numbered subgroups, left); and a non-coelurosaur tetanuran series (unnumbered, right). PCA was a better alternative for analyzing complex, multi-family matrices since morphological disparity is easily accommodated and clearly visible in multivariate space. Of interest here is the gap between the tyrannosauroids and tetanurans. The disjunct morphoseries within the Saurolophinae reflected smaller-scale differences within a subfamily. The tyrannosauroids and non-coelurosaur tetanurans have the appearance of a spatial connection across deeper morphological character space (*i.e.*, at least family-level discontinuity). This may suggest some intrabaraminic morphologies unfolded across common biological character-space trajectories. The closest biological analogy would be an ontogenetic-like unfolding of species. It is as if each successive species "step" was nearly identical but differed in key characteristics along a linear series with recognized end points (Wise 2014). If so, the aligned morphospatial ordination between tyrannosauroids and non-coelurosaur tetanurans may be due to similar ecological, functional, or biomechanical requirements shared by each group. This suggests tyrannosauroids and non-coelurosaur tetanurans possibly share deep common biological similarities (*e.g.*, developmental). Indeed, tyrannosaurids were originally classified as "carnosaurs" (essentially, the big meat-eating dinosaurs) alongside animals like *Allosaurus* and *Megalosaurus*. However, Matthew and Brown (1922) noted that "although paralleling megalosaurs in their huge size, massive proportions, short neck and large head, differ from them and resemble the coelurids and ornithomimids in the construction of the pelvis and elongate quadrate" (p. 375). Despite such observations tyrannosaurids were often classified as "carnosaurs" even into the late 20th century by some researchers (e.g., Molnar et al. 1990). It is very likely that tyrannosaurids are convergent with "carnosaur" tetanurans in acquiring their large size independently in the pre-Flood world (Aaron 2014b).

Tyrannosauroidea is also important since it was the first dinosaur assigned to a holobaramin (Aaron 2014*b*). Aaron applied BDC and MDS to four data matrices to make the determination (Brusatte et al. 2010; Carr and Williamson 2010; Xu et al. 2012; Lü et al. 2014). We report findings similar to Aaron: the Tyrannosauroidea (to the exclusion of *Yutyrannus*, *Dilong*, and the Proceratosauridae) show both positive BDC within their group and negative BDC outside. MDS results displayed linear arrangements of outgroup and Tyrannosauroidea taxa positioned at nearly right angles. The ordination of Tyrannosauroidea in PCA (not performed by Aaron but reported here) showed a complimentary but slightly different arrangement than MDS. PC 2 separated morphologies along an axis with coelurosaur morphologies on one end – ornithomimosaurs *Harpymimus* and *Pelecanimimus*, alongside *Archaeopteryx* – up through dromaeosaurids toward the middle of the axis, and Allosauroidea near the distant end. Tyrannosauroidea is clustered toward one end of PC 1 with member genera aligned nearly perpendicular to the theropod-maniraptoriform continuum on PC 1. Tyrannosauroid morphologies clustered in a smaller, separated portion of PCA morphospace. Close spatial clustering of Tyrannosauroidea is a function of nearly identical morphologies, suggestive of a holobaramin. The only outlier was *Eotyrannus*; Aaron (2014b) likewise pondered the relationship of *Eotyrannus*. A partial solution suggested by PCA is that incomplete *Eotyrannus* data hindered the analysis (only 30% of the 638 characters for *Eotyrannus* were present in the 2004 data matrix). The large proportion of missing data resulted in an *Eotyrannus* ordination near the middle of the PCA axes (or, near 0 values for both PCs 1 and 2 as seen in Fig. 22). The results here were consistent with Aaron's findings of the Tyrannosauroidea holobaramin.

Brusatte and Carr's (2016) matrix provided greater detail but with similar results. PCA confined the tyrannosauroid series to a narrow range of PC 1 while distributing them along PC 2 with the larger Tyrannosaurinae and smaller Albertosaurinae on opposite ends of the series. The ordinations of *Bistahieversor*, *Raptorex*, *Xiongguanlong*, and *Eotyrannus* were orthogonal, or outside of, the Tyrannosaurinae but closer to Albertosaurinae (Fig. 23). While PC 3 arranged most of the tyrannosaurs in the same series as PC 2, PC 3 grouped the other tyrannosaurid members separately (Fig. 24). The most recent data therefore suggests *Tarbosaurus*, *Tyrannosaurus*, *Daspletosaurus*, *Teratophoneus*, *Qianzhousaurus*, and *Alioramus* form a series. *Gorgosaurus* and *Albertosaurus* are part of the series but are distinct within it. The remaining tyrannosauroids ordinate outside the others and their relationship is uncertain. If holobaramins are always linear series, then these other members fall outside. At the same time, tyrannosauroids may be an example of a holobaramin with complex spatial relationships. Indeed, we might not expect series to always be linear, but for various branching patterns to be possible (e.g., equids in Cavanaugh et al. 2003).

An unexpected finding was the identification of stratomorphic outgroup series. Sauropod, thyreophoran, and ceratopsian ordinations included series of taxa connecting the outgroups to the ingroups. BDC results for Otero et al. (2015) revealed little

distinction among sauropodomorphs and outgroups – including outgroup taxa as diverse as *Herrerasaurus*, *Silesaurus*, or *Marasuchus* (Fig. 50). The reason was a close morphological gradation for all members along PC 1 (Fig. 51); only PC 2 and PC 3 suggested a separation between sauropodomorphs and outgroups. The combined PC 1 and PC 2 ordination revealed the outgroup taxa ordination was stratomorphic: the morphological series leading from the outgroup strongly aligned with the fossil record first-appearance order of its members.

Thyreophorans and neornithischians also followed a general, though not perfect, stratomorphic morphoseries from the Jurassic through Cretaceous. Lower Jurassic thyreophorans *Scelidosaurus* and *Scutellosaurus* merged with ornithischians and neornithischians (*e.g.*, *Agilisaurus, Heterodontosaurus*, *Hexinlusaurus*) and followed a series leading to *Thescelosaurus* and *Parksosaurus* in the Upper Cretaceous. However, the very end of the series was *Tenontosaurus*, a "basal" iguanodont from the Lower Cretaceous. The series aligned along both PC 1 and PC 2 (Fig. 56).

The stratomorphic outgroups used for ceratopsians began with Triassic "basal" dinosaurs and silesaurids, moved into Lower Jurassic ornithischians, and then branched along PC 1 into marginocephalians on the right and thyreophorans + ornithopods on the left (Fig. 91). PC 1 also revealed a discontinuity between the outgroups and ceratopsians. Interestingly, the ceratopsian series was also stratomorphic; the ceratopsian series ranges from the Middle Jurassic to Upper Cretaceous. *Yinlong* and two *Psittacosaurus* species formed the base of the series and were separated from neoceratopsians by a gap. The ceratopsian stratomorphic series had an additional element: phylogeography. The conventional scenario is that an Asian *Protoceratops*-like ancestor crossed the Bering Straits and gave rise to later North American neoceratopsians in the Cretaceous. All the non-ceratopsid ceratopsians in the studied series, including neoceratopsians, were found in Asia; only *Leptoceratops* was from North America. However, the scenario has become more complicated with the discovery of Asian ceratopsoids *Turanoceratops* and *Sinoceratops* (a centrosaurine ceratopsid), both of which may suggest migration back to Asia in the conventional model (e.g., Sues and Averianov 2009), and with the discovery of a North American "basal" neoceratopsian (*Aquilops*), suggesting an earlier dispersion from Asia to North America. Indeed, Figs. 96 and 97 do not show a biogeographic pattern for non-ceratopsid neoceratopsians, but they do show a phylogenetic pattern. In other words, the Asian forms (*Turanoceratops* and *Protoceratops*) do not cluster together apart from the North American forms (*Leptoceratops* and *Zuniceratops*). Rather, *Protoceratops* and *Leptoceratops*, non-ceratopsoids, cluster together and *Zuniceratops* is farther from the ceratopsids than *Turanoceratops*, which is the case in multiple recent ceratopsian phylogenies (Farke et al. 2014; Fry 2015). The increasing complexity of dinosaur biogeography presents an interesting opportunity for future creationist work.

For the datasets here all stratomorphic outgroup series began in the Lower to Middle Mesozoic. It is suggested here that morphological series reflected the functional considerations of the skeletal anatomy of the species. Functional similarity was likely a reflection of ecological requirements. These results imply that some early Mesozoic communities included ecological gradient overprints. It is possible some gradients at the beginning of the Mesozoic are traceable into the mid-Mesozoic. Other researchers have noted convergence between Triassic communities and later Mesozoic communities, especially between pseudosuchians/"basal" archosauromorphs and dinosaurs (Stocker et al. 2016).

2. Bird-dinosaur relationships

Among all the morphospatial patterns examined for the Dinosauria, the bird-dinosaur relationships were both the most unique and interesting. There are at least two different lessons derived from comparing the 2004 with the later 2017 datasets. One clear conclusion is that bird-dinosaur interpretations change substantially based on the quality of the data – all analyses warrant caution.

Bird-dinosaur data through 2004 was sparse. The most relevant data matrix for bird-like theropods (e.g., Maniraptoriformes) was limited due to the amount of missing data. Standard baraminological techniques yielded two groups. One group included dromaeosaurids, a troodontid, and an avialan representative (*Archaeopteryx*). The positive BDC between members, and negative BDC with some outlying groups, implied a holobaramin. Yet caution is warranted since BDC with disparate baramins can produce spurious correlation (e.g., tetanurans plus tyrannosauroids, Fig. 16) and few taxa were included. Additionally, this broad dromaeosaurid-affiliated group showed no negative correlation to outgroup taxa (*Tyrannosaurus*, *Allosaurus*, and a generic composite outgroup). The second group was an ornithomimid-association that also lacked negative BDC against the outgroups. MDS results separated both groups but was tentative since the first coordinate axis explained only 35% of the variance, leaving 65% to be explained across the remaining axes.

PCA was more instructive, though incomplete data hindered the analysis. In order to have a sufficient number of taxa in the analysis, all genera – including those missing up to 80% of their character data – were included (Fig. 27). In spite of the high proportion of missing data, group distinctions still emerged with several relationships evident. Oviraptorosaurs, dromaeosaurids, troodontids and ornithomimosaurs showed distinct clusters. We interpret the complex spatial relationships as an indication that bird-like theropod assemblages were distinct while simultaneously exhibiting complex mosaic relationships. In spite of the limited data, enough of a pattern may be evident to apply Hartwig-Scherer's description of hominids as, "schmetztiegal unterschiedlicher morphologiemosaic" – or, "melting pot of morphological mosaics" – to bird-like theropod groups (Hartwig-Scherer 2002). Only two avialan taxa were included in the analysis (*Archaeopteryx* and *Confuciusornis*). As a result, very little can be said about bird-dinosaur relationships from the 2004 data.

Matrices with bird-dinosaur data have improved since 2004 and have offered a consistent picture. Garner et al. (2013) employed six matrices, ranging from 2001 to 2011, with a general improvement in BDC distinctions over time. It is clear that modern birds and dinosaurs group separately, but also that some Jurassic and Cretaceous avians grouped with dinosaurs. In particular, *Archaeopteryx* and *Wellnhoferia* grouped with Deinonychosauria suggesting an affinity between some avialans and dromaeosaurs.

PCA applied to Foth and Rauhut's (2017) larger maniraptoran dataset revealed several helpful insights to the dromaeosaurid-

avialan question. As with other dinosaur groups, missing data was still an issue. To account for this, two ordinations were performed – one employing the entire dataset (regardless of the amount of missing data) and a second ordination that retained only taxa with a minimum of 50% of their character data. Both ordinations yielded instructive observations.

PCA divided the complete maniraptoran dataset into four groups (Fig. 38). PC 1 divided non-avian Pygostylia and Aves + *Limenavis* + *Iaceornis* from all non-pygostylian maniraptorans, supporting Garner et al.'s (2013) conclusion that modern birds and dinosaurs were distinct. Although many avialans do not cluster with non-avialan maniraptorans, some do. Group 2b contains "basal" avialans, but they are mixed with troodontids (*Zanabazar* and *Byronosaurus*) and a dromaeosaurid (*Hesperonychus*). Instead of the break being between avialans and non-avialans, the obvious break along PC 1 occurs between pygostylians and non-pygostylians.

Additional division was revealed along PC 2. PC 2 grouped dromaeosaurs, "basal" avialans, and troodontids while separating them from "basal" coelurosaurs, alvarezsauroids, ornithomimosaurs, oviraptorosaurs, therizinosaurians, tyrannosauroids, a scansoriopterygid, and the non-coelurosaur outgroup. Most groups retained internal morphospatial distinctions among their members, although therizinosaurians and oviraptorosaurs overlap significantly. One possibility was that each group retains ecological affinities among members yet differences between groups. In addition to these divisions, the timing of the appearances of member subgroups was notable. The fossil record first-appearance order of each subgroup reflects the approximate Flood burial order. "Basal" coelurosaurs (Fig. 38, "1") appeared first stratigraphically while the dromaeosaurid, avialan, troodontid, and alvarezsaurid morphologies appeared at essentially the same time (groups 2a, 2b, 2c, and 2d, respectively). This was followed by ornithomimosaurs (3), oviraptorosaurs (4), non-avian Pygostylia (5) and Aves (6). Though some dinosaur baramins occur within stratomorphic morphoseries, the morphology and appearance order of maniraptoran groups appear to reflect no relationship between morphology and stratigraphic position.

One potential problem of these ordinations is the possibility that missing data could have created spurious patterns. To account for this a second ordination using more complete data was generated (Fig. 40). This more selective ordination resulted in a notable Y-shaped ordination. The ordination included two morphoseries that corresponded to the groups in the more inclusive ordination (Fig. 40). Dromaeosaurids, "basal" avialans, and troodontids formed the connecting point for both morphoseries. One morphoseries included oviraptorosaurs, the outgroup taxa, tyrannosauroids, "basal" coelurosaurs, alvarezsaurids, and ornithomimosaurs. The other included the "derived" avialans and avians. The somewhat random stratigraphic appearance of group members shows that the morphoseries are functional, ecological, or morphological series – not stratomorphic series. Both ordinations agree in displaying a close, but distinct, relationship between "basal" avialans and dromaeosaurids. Neither ordination shows a discernible first-appearance pattern among the subgroups beyond the observation that all feather-bearing groups appear at essentially the same time and that modern bird species ordinate distinctly and appear stratigraphically higher.

3. Does baraminology work for dinosaurs?

The findings here are consistent with over a decade of research in baraminology on extant groups: dinosaurs show discontinuity at or near the family level. This study provides an instructive comparison to previous studies on extant groups since the dinosaur fossil record is both incomplete and wholly reliant on hard-part anatomy. For those skeptical of the methods of statistical baraminology the findings here reinforce the case that holistic analysis of biological character traits, for both plant and animal groups, tend to identify discontinuity near the family level – whether for neontological or paleontological subjects.

One skeptical critique was Senter's (2011) report that taxon correlation analysis found a "continuous morphological spectrum" within the Dinosauria that united groups as diverse as basal Saurischia, Sauropodomorpha, Ornithischia, and other members. While acknowledging that sauropodomorphs and thyreophorans had some evidence for stratomorphic morphoseries, we did not find a continuous morphological spectrum. Senter's conclusion was that the "creationist camp will have to acknowledge the genetic relatedness of a very broad morphological spectrum of dinosaurian species" (Senter, 2011). Here Senter (understandably) equated morphological similarity with genetic relatedness. A creationist approach, however, acknowledges both genetic and structural realties. Creationist structuralism should recognize the nuances of Aristotelian distinctions (Thompson 1942). That is, genetics may be the *instrumental* cause of dinosaurian relationships but all analyses – whether BDC or phylogenetic – are founded upon only the *material* causes (*i.e.,* the skeletal elements themselves). Skeletal anatomies, in turn, reflect the mechanical, architectural, or functional requirements of their possessors. In other words, whether or not *Apatosaurus* neck and tail architecture functioned as a cantilever bridge, there is no question the functional requirements of a sauropod skeleton necessarily differ, at almost every point, from the requirements imposed by a bird-like theropod existence. This may be why nearly every dinosaur cited within Senter's morphological continuum were (1) relatively large, (2) bipedal dinosaurs with (3) short forearms, and (4) long counterbalancing tails. Given the functional requirements of this architecture it would likely be difficult to distinguish ancestry from structure, particularly when datasets are often incomplete. Re-stating Senter in structuralist terms, it appears that creationists should acknowledge the *functional* and/or *ecological* relatedness of a very broad spectrum of dinosaurian species.

Wilson (2010) tried to address a similar problem of the holobaramin grouping members at too broad a level. One solution was to encourage emphasis on genetics and the genetic programs underlying regulatory changes. In order to do this, baraminologists were advised to pursue things such as hybridization, synapomorphies, and other measures of genomic equivalence. Wilson's proposal is sound (particularly for neonatologists). Unfortunately, these criteria rule out the fossil record. Yet the question is still valid; it is possible statistical baraminology misses some discontinuities. The analyses here may have captured some distinctions that would otherwise have been missed with other methods and deserve consideration

for future fossil record studies.

One reason we introduced PCA alongside other statistical baraminology approaches was to examine its utility in elucidating the structure of dinosaurian morphospace and discerning holobaramins. In fact, while agreeing with other methods, PCA additionally revealed complex morphospatial patterns in a number of groups. For example, PCA revealed a division within Ceratopsidae at the subfamily level (Fig. 95-96). The lack of negative BDC, and spatial gap in MDS, suggested – though did not require – the same division. Sauropods provided an even clearer example. Both BDC and MDS united two sauropod groups (Diplodocoidea and Macronaria) without revealing much distinction (Fig. 47 and 48). In contrast, PCA identified a clear separation between Diplodocoidea and Macronaria (Fig. 49). Other divisions visible within the 2004 data were found for Ornithomimosauria, Therizinosauroidea, Oviraptorosauria, Stegosauria, Hadrosauridae, as well as deep separation between members of various basal groups (*e.g.,* Saurischia, Tetanurae, etc.). Though the fossil record cannot yield the biological information Wilson called for, the results here suggest that new statistical tools may aid our ability to capture discontinuities between natural groups (holobaramins) in the context of multivariate space.

Senter (2010) posed an interesting challenge concerning MDS, namely that time will fill in all morphological gaps. After comparing the 2004 data to later matrices it is entirely possible that the reverse is true: improved Dinosauria datasets may provide better definition of discontinuities and groupings in the morphospace of these intriguing organisms. Our analyses here may only be scratching the surface.

ACKNOWLEDGMENTS

We would like to thank two anonymous reviewers for helpful comments and corrections. Neal Doran would also like to thank his family for patient assistance during this project: Nicole, Andrea, Priscilla, and Danielle. Matt McLain would like to thank his family for their patience, Todd Wood for helpful baraminology discussions, and John Whitmore for his encouragement in finishing this paper.

REFERENCES

Aaron, M. 2014a. Baraminological analysis of the Caseidae (Synapsida: Pelycosauria). *Journal of Creation Theology and Science Series B*: *Life Sciences* 4:19–22.

Aaron, M. 2014b. Discerning tyrants from usurpers: A statistical baraminological analysis of Tyrannosauroidea yielding the first dinosaur holobaramin. *Answers Research Journal* 7:459–477.

Arbour, V.M., and P.J. Currie. 2015. Ankylosaurid dinosaur tail clubs evolved through stepwise acquisition of key features. *Journal of Anatomy* 227:514-523.

Baron, M.G. 2018. *The Origin and Early Evolution of the Dinosauria* [PhD thesis]. Cambridge University, Cambridge.

Baron, M.G., D.B. Norman, and P.M. Barrett. 2017. A new hypothesis of dinosaur relationships and early dinosaur evolution. *Nature* 543:501-506.

Boyd, C.A. 2015. The systematic relationships and biogeographic history of ornithischian dinosaurs. *PeerJ* 3:495-520.

Breeden, B.T. 2016. *Observations on the osteology of Scutellosaurus lawleri Colbert, 1981 (Ornithischia: Thyreophora) on the basis on new specimens from the Lower Jurassic Kayenta Formation of Arizona* [Master's Thesis]. University of Texas, Austin.

Brissón Egli, F., F.L. Agnolín, and F. Novas. 2016. A new specimen of *Velocisaurus unicus* (Theropoda, Abelisauroidea) from the Paso Córdoba locality (Santonian), Río Negro, Argentina. *Journal of Vertebrate Paleontology* 36:4. doi: 10.1080/02724634.2016.1119156

Bronzati, M. 2017. *Braincase Anatomy in Non-Neosauropodan Sauropodomorphs: Evolutionary and Functional Aspects* [PhD thesis]. Ludwig-Maximilians-Universität München, München.

Brusatte, S. L., M. A. Norell, T. D. Carr, G. M. Erickson, J. R. Hutchinson, A.M. Balanoff, G.S. Bever, J.N. Choiniere, P.J. Makovicky, and X. Xu. 2010. Tyrannosaur paleobiology: New research on ancient exemplar organisms. *Science* 329:1481.

Brusatte, S.L., and T.D. Carr. 2016. The phylogeny and evolutionary history of tyrannosauroid dinosaurs. *Scientific Reports*, 6:20252.

Carr, T.D., and T.E. Williamson. 2010. *Bistahieversor sealeyi* a new tyrannosauroid from New Mexico and the origin of deep snouts in Tyrannosauroidea. *Journal of Vertebrate Paleontology* 30:1–16.

Carrano, M.T., R.B.J. Benson, and S.D. Sampson. 2012. The phylogeny of Tetanurae (Dinosauria: Theropoda). *Journal of Systematic Palaeontology* 10:2, 211-300. doi: 10.1080/14772019.2011.630927

Cavanaugh, D., T. Wood, and K. Wise. 2003. Fossil equidae: a monobaraminic, stratomorphic series. In *Proceedings of the Fifth International Conference on Creationism*, ed. R.L. Ivey Jr., pp. 143–153. Pittsburgh, Pennsylvania: Creation Science Fellowship.

Cavanaugh, D. 2011. An ANOPA Study of coelurosaurian theropods. *Journal of Creation Theology and Science Series B: Life Sciences* 1:18.

Chinzorig, T., Y. Kobayashi, K. Tsogtbaatar, P.J. Currie, R. Takasaki, T. Tanaka, M. Iijima, and R. Barsbold. 2018. Ornithomimosaurs from the Nemegt Formation of Mongolia: Manus morphological variation and diversity. *Palaeogeography, Palaeoclimatology, Palaeoecology* 494: 91-100.

Clark, J.M., T. Maryańska, and R. Bardbold. 2004. Therizinosauroidea. In *The Dinosauria*, 2nd eds. D.B. Weishampel, P. Dodson, and H. Osmólska, pp. 151-164. Berkeley: University of California Press.

Cruzado-Caballero, P., and J. Powell. 2017. *Bonapartesaurus rionegrensis*, a new hadrosaurine dinosaur from South America: Implications for phylogenetic and biogeographic relations with North America. *Journal of Vertebrate Paleontology* 37(2). doi: 10.1080/02724634.2017.1289381

DeWitt, D.A. 2010. Baraminological analysis places *Homo habilis*, *Homo rudolfensis* and *Australopithecus sediba* in the human holobaramin: discussion. *Answers Research Journal* 3:156-158.

Dodson, P., C.A. Forster, and S.D. Sampson. 2004. Ceratopsidae. In *The Dinosauria*, 2nd eds. D.B. Weishampel, P. Dodson, and H. Osmólska, pp. 494-516. Berkeley: University of California Press.

Farke, A.A., W.D. Maxwell, R.L. Cifelli, and M.J. Wedel. 2014. A ceratopsian dinosaur from the Lower Cretaceous of western North America, and the biogeography of Neoceratopsia. *PLoS ONE* 9(12): e112055.

Foth C., and Rauhut O.W.M. 2017. Re-evaluation of the Haarlem *Archaeopteryx* and the radiation of maniraptoran theropod dinosaurs. *BMC Evolutionary Biology* 17:236

Fry, J. J. 2015. *Redescription of a specimen of Pentaceratops (Ornithischia: Ceratopsidae) and phylogenetic evaluation of five referred specimens from the upper Cretaceous of New Mexico* [Masters Theses]. 45. http://scholars.fhsu.edu/theses/45

Galton, P.M., and P. Upchurch. 2004. Prosauropoda. In *The Dinosauria*, 2nd eds. D.B. Weishampel, P. Dodson, and H. Osmólska, pp. 232-258. Berkeley: University of California Press.

Galton, P.M., and P. Upchurch. 2004b. Stegosauria. In *The Dinosauria*, 2nd eds. D.B. Weishampel, P. Dodson, and H. Osmólska, pp. 343-362. Berkeley: University of California Press.

Garner, G.A., T.C. Wood, and Ross, M. 2013. Baraminological analysis of Jurassic and Cretaceous Avialae. In *Proceedings of the Seventh International Conference on Creationism*. ed. M. Horstemeyer, pp. 143–153. Pittsburgh, Pennsylvania: Creation Science Fellowship.

Habermehl, A. 2010. Baraminological analysis places *Homo habilis*, *Homo rudolfensis* and *Australopithecus sediba* in the human holobaramin: discussion. *Answers Research Journal* 3:155-156

Hailu, Y., and P. Dodson. 2004. Basal Ceratopsia. In *The Dinosauria*, 2nd eds. D.B. Weishampel, P. Dodson, and H. Osmólska, pp. 478-493. Berkeley: University of California Press.

Han, F.L., C.A. Forster, X. Xu, and J.M. Clark. 2017. Postcranial anatomy of *Yinlong downsi* (Dinosauria: Ceratopsia) from the Upper Jurassic Shishugou Formation of China and the phylogeny of basal ornithischians. *Journal of Systematic Palaeontology*. doi.org/10.1080/14772019.2017.1369185

Hartwig-Scherer, S. 2002. Wurde Europa doch früher besiedelt? Überraschungen aus Ost und West. *Studium Integrale Journal* 9:67–73.

Holtz, T.R. Jr. 2004. Tyrannosauroidea. In *The Dinosauria*, 2nd eds. D.B. Weishampel, P. Dodson, and H. Osmólska, pp. 111-136. Berkeley: University of California Press.

Holtz, T.R., Jr., R.E. Molnar, and P.J. Currie. 2004. Basal tetanurae. In *The Dinosauria*, 2nd eds. D.B. Weishampel, P. Dodson, and H. Osmólska, pp. 71-110. Berkeley: University of California Press.

Horner, J. R., D.B. Weishampel, and C.A. Forster. 2004. Hadrosauridae. In *The Dinosauria*, 2nd eds. D.B. Weishampel, P. Dodson, and H. Osmólska, pp. 438-464. Berkeley: University of California Press.

Horner, J.R., and M.B. Goodwin. 2009. Extreme cranial ontogeny in the Upper Cretaceous dinosaur *Pachycephalosaurus*. *PLoS ONE* 4(10):e7626.

Langer, M.C. 2004. Basal Saurischia. In *The Dinosauria*, 2nd eds. D.B. Weishampel, P. Dodson, and H. Osmólska, pp. 25-46. Berkeley: University of California Press.

Lü, J., L. Yi, S. L. Brusatte, L. Yang, H. Li, and L. Chen. 2014. A new clade of Asian Late Cretaceous long-snouted tyrannosaurids. Vol. 5. *Nature Communications*, 5, no. 3788. doi:10.1038/ncomms4788

Mace, S., and T. Wood. 2005. Statistical evidence for five whale holobaramins (Mammalia: Cetacea). *Occasional Papers of the BSG* 5:15.

Madzia, D., C.A. Boyd, and M. Mazuch. 2017. A basal ornithopod dinosaur from the Cenomanian of the Czech Republic. *Journal of Systematic Paleontology*. doi: 10.1080/14772019.2017.1371258

McDonald, A.T. 2012. Phylogeny of basal iguanodonts (Dinosauria: Ornithischia): an update - *PLoS ONE* 7(5): e36745. doi:https://doi.org/10.1371/journal.pone.0036745.

Makovicky, P.J., and M.A. Norell. 2004. Troodontidae. In *The Dinosauria*, 2nd eds. D.B. Weishampel, P. Dodson, and H. Osmólska, pp. 184-195. Berkeley: University of California Press.

Makovicky, P.J., Y. Kobayashi, and P.J. Currie. 2004. Ornithomimosauria. In *The Dinosauria*, 2nd eds. D.B. Weishampel, P. Dodson, and H. Osmólska, pp. 137-150. Berkeley: University of California Press.

Maryańska, T., R.E. Chapman, and D.B. Weishampel. 2004. Pachycephalosauria. In *The Dinosauria*, 2nd eds. D.B. Weishampel, P. Dodson, and H. Osmólska, pp. 464-477. Berkeley: University of California Press.

Matthew, W.D., and B. Brown. 1922. The family Deinodontidae with notice of a new genus from the Cretaceous of Alberta. *Bulletin of the American Museum of Natural History* 46:367-385.

McLain, M.A., M. Petrone, and M. Speights. 2018. Feathered dinosaurs reconsidered: New insights from baraminology and ethnotaxonomy. In *Proceedings of the Eighth International Conference on Creationism*, ed. J.H. Whitmore, pp. 472-515. Pittsburgh, Pennsylvania: Creation Science Fellowship.

Menton, D.H. 2010. Baraminological analysis places *Homo habilis*, *Homo rudolfensis*, and *Australopithecus sediba* in the human holobaramin: discussion. *Answers Research Journal* 3:153–155.

Molnar, R.E., S.M. Kurzanov, and D. Zhiming.1990. Carnosauria. In *The Dinosauria*, 1st ed. D. B. Weishampel, P. Dodson, and H. Osmólska, pp. 169-209. Berkeley: University of California Press.

Nesbitt, S.J., N.D. Smith, R.B. Irmis, A.H. Turner, A. Downs, and M.A. Norell. 2009. A complete skeleton of a Late Triassic saurischian and the early evolution of dinosaurs. *Science* 326: 1530-1533.

Norell, M.A. and P.J. Makovicky. 2004. Dromaeosauridae. In *The Dinosauria*, 2nd eds. D.B. Weishampel, P. Dodson, and H. Osmólska, pp. 196-209. Berkeley: University of California Press.

Norman, D.B. 2004. Basal Iguanodontia. In *The Dinosauria*, 2nd eds. D.B. Weishampel, P. Dodson, and H. Osmólska, pp. 413-437. Berkeley: University of California Press.

Norman, D.B., L.M. Hans-Dieter Sues, L.M. Witmer, and R.A. Coria. 2004. Basal Ornithopoda. In *The Dinosauria*, 2nd eds. D.B. Weishampel, P. Dodson, and H. Osmólska, pp. 393-412. Berkeley: University of California Press.

Norman, D.B., L.M. Witmer, and D.B. Weishampel. 2004. Basal Thyreophora. In *The Dinosauria*, 2nd eds. D.B. Weishampel, P. Dodson, and H. Osmólska, pp. 335-342. Berkeley: University of California Press.

Otero, A., E. Krupandan, D. Pol, A. Chinsamy, and J. Choiniere. 2015. A new basal Sauropodiform from South Africa and the phylogenetic relationships of basal sauropodomorphs. *Zoological Journal of the Linnean Society* 174(3):589-634

Osmólska, H., P.J. Currie, and R. Barsbold. 2004. Oviraptorosauria. In *The Dinosauria*, 2nd eds. D.B. Weishampel, P. Dodson, and H. Osmólska, pp. 165-183. Berkeley: University of California Press.

Padian, K. 2004. Basal Avialae. In *The Dinosauria*, 2nd eds. D.B. Weishampel, P. Dodson, and H. Osmólska, pp. 210-231. Berkeley: University of California Press.

Polly, P. D., A.M. Lawing, A.-C. Fabre, and A. Goswami. 2013. Phylogenetic principal components analysis and geometric morphometrics. *Hystrix, the Italian Journal of Mammalogy* 24:33–41.

Raven, T.J., and S.C. Maidment. 2017. A new phylogeny of Stegosauria (Dinosauria, Ornithischia). *Palaeontology* 60: 401–408.

Robinson, D., and D. Cavanaugh. 1998. A quantative approach to baraminology with examples from Catarrhine primates. *Creation Research Society Quarterly* 34:196–208.

Schott, R.K. 2011. Ontogeny, diversity, and systematics of pachycephalosaur dinosaurs from the Belly River Group of Alberta. Master's Thesis, University of Toronto, Toronto.

Senter, P. 2010. Using creation science to demonstrate evolution:

application of a creationist method for visualizing gaps in the fossil record to a phylogenetic study of coelurosaurian dinosaurs. *Journal of Evolutionary Biology* 23:1732–1743.

Senter, P. 2011. Using creation science to demonstrate evolution 2: morphological continuity within Dinosauria. *Journal of Evolutionary Biology* 24:2197–2216.

Stacklies, W., H. Redestig, M. Scholz, D. Walther, J. Selbig. 2007. pcaMethods--a bioconductor package providing PCA methods for incomplete data. *Bioinformatics* 23, issue 9, 1164-1167.

Stacklies, W., H. Redestig, and K. Wright. 2017. A collection of PCA methods. Version 1.71.0. L https://github.com/hredestig/pcamethods.

Stocker, M.R., S.J. Nesbitt, K.E. Criswell, W.G. Parker, L.M. Witmer, T.B. Rowe, R. Ridgely, and M.A. Brown. 2016. A dome-headed stem archosaur exemplifies convergence among dinosaurs and their distant relatives. *Current Biology* 26:2674-2680.

Sues, H.-D., and A. Averianov. 2009. *Turanoceratops tardabilis* - the first ceratopsid dinosaur from Asia. *Naturwissenschaften* 96:645-652.

Thompson, D'A. W. 1942. *On growth and form*, 2nd ed. Cambridge University Press, Cambridge.

Tykoski, R.S. and T. Rowe. 2004. Ceratosauria. In *The Dinosauria*, 2nd eds. D.B. Weishampel, P. Dodson, and H. Osmólska, pp. 47-70. Berkeley: University of California Press.

Upchurch, P., P.M. Barrett, and P. Dodson. 2004. Sauropoda. In *The Dinosauria*, 2nd eds. D.B. Weishampel, P. Dodson, and H. Osmólska, pp. 259-322. Berkeley: University of California Press.

Vickaryous, M.K., T. Maryańska, and D.B. Weishampel. 2004. Ankylosauria. In *The Dinosauria*, 2nd eds. D.B. Weishampel, P. Dodson, and H. Osmólska, pp. 363-392. Berkeley: University of California Press.

Wang, S., J. Stiegler, R. Amiot, X. Wang, G.-h. Du, J.M. Clark, and X. Xu. 2017. Extreme ontogenetic changes in a ceratosaurian theropod. *Current Biology* 27:144-148.

Weishampel, D.B., P. Dodson, and H. Osmólska. 2004. *The Dinosauria*. Berkeley: University of California Press.

Wilson, G.L. 2010. Revisiting the "Clear Synapomorphy" Criterion. *Occasional Papers of the BSG -- Proceedings of the Ninth BSG Conference* 17:5-6.

Wise, K.P. 1995. Towards a creationist understanding of transitional forms. *CEN Tech. J.* 9(2): 216-222

Wise, K.P. 2005. The Flores skeleton and human baraminology. *Occasional Papers of the BSG* 6:1–13.

Wise, K.P. 2014. Ontogeny as a diversification analog. *Journal of Creation Theology and Science Series B: Life Sciences* 4:27.

Wood, T.C. 2001. BDIST software, v. 1.0. Center for Origins Research and Education, Bryan College. Distributed by the author.

Wood, T. 2005. Visualizing baraminic distances using classical multidimensional scaling. *Origins* 57:9–29.

Wood, T.C. 2008a. Animal and plant baramins. *CORE Issues in Creation* 3:1-258.

Wood, T.C. 2008b. BDISTMDS software, v. 2.0. Center for Origins Research and Education, Bryan College. Distributed by the author.

Wood, T.C. 2010. Baraminological analysis places *Homo habilis, Homo rudolfensis*, and *Australopithecus sediba* in the human holobaramin. *Answers Research Journal* 3:71–90.

Wood, T.C. 2011a. Baraminology, the image of God, and *Australopithecus sediba*. *Journal of Creation Theology and Science Series B: Life Sciences* 1:6–14.

Wood, T.C. 2011b. Using creation science to demonstrate evolution? Senter's strategy revisited: Using creation science to demonstrate evolution. *Journal of Evolutionary Biology* 24:914–918.

Wood, T.C., M. Ross, and P.A. Garner. 2011. Detecting discontinuity in the Dinosauria using baraminic distance correlation. *Journal of Creation Theology and Science Series B: Life Sciences* 1:26.

Wood, T.C. 2013. *Australopithecus sediba*, statistical baraminology, and challenges to identifying the human holobaramin. In *Proceedings of the Seventh International Conference on Creationism*. ed. M. Horstemeyer. Pittsburgh, Pennsylvania: Creation Science Fellowship, n.p.

Wood, T.C. 2016a. A list and bibliography of identified baramins. *Journal of Creation Theology and Science Series B: Life Sciences* 6:91–101.

Wood, T.C. 2016b. An evaluation of *Homo naledi* and "early" *Homo* from a young-age creationist perspective. *Journal of Creation Theology and Science Series B: Life Sciences* 6:14–30.

Xu, X., K. Wang, K. Zhang, Q. Ma, L. Xing, C. Sullivan, D. Hu, S. Cheng, and S. Wang. 2012: A gigantic feathered dinosaur from the Lower Cretaceous of China. *Nature* 484:92–95.

Zanno, L. E. 2010. A taxonomic and phylogenetic review of Therizinosauria. *Journal of Systematic Palaeontology* 8:503–543.

Zelditch, M.L., D.L. Swiderski, H.D. Sheets, and W.L. Fink. 2004. *Geometric Morphometrics for Biologists: A Primer*. Elsevier Academic Press, San Diego, California, p. 146.

Zheng, W., J. Xingsheng, Y. Azuma, Q. Wang, K. Miyata, and X. Xu. 2018. The most basal ankylosaurine dinosaur from the Albian-Cenomanian of China, with implications for the evolution of the tail club. *Scientific Reports* 8, no. 3711. doi:10.1038/s41598-018-21924-7

THE AUTHORS

Neal Doran is professor of biology and director of Bryan College's Center for Creation Research (CRC), in Dayton, Tennessee. Prior to coming to Bryan he taught at Patrick Henry College. He is a founding member of the Creation Biology Society and member of the Creation Geology Society. His graduate training is in paleontology (Ph.D., geology) and the History of Science (M.A.). At Bryan College he teaches courses on biology, geology and the philosophy of science.

Matthew McLain is assistant professor of biology and geology at The Master's University in Santa Clarita, CA, where he teaches courses on paleontology and geology. He has a BS in Geology (Cedarville University) and a PhD in Earth Sciences (Loma Linda University). He has published paleontology papers in both the conventional and creationist literature.

Natalie Young is a senior majoring in biology at Bryan College in Dayton, Tennessee.

Adam Sanderson is a junior majoring in biology at Bryan College in Dayton, Tennessee.

APPENDIX

Table 2. Baraminic status of the various taxa analyzed in this paper with a focus on the evidences for continuity, discontinuity, or both.

Group	Baraminic Status	Discontinuity Evidence	Continuity Evidence	Other Analyses	Notes
Dinosauria	Apobaramin	**Nesbitt et al. (2009)** No clustering with non-dinosaurs (PCA: PC 1/PC 2). Evidence of discontinuity among members in other analyses.	-		
Saurischia	Apobaramin?	**Langer (2004)** Negative correlation with other taxa (BDC). No clustering with other taxa (MDS/PCA). Not all members share continuity.	-		Very weakly supported: few taxa included.
Herrerasauridae	Holobaramin?	**Langer (2004)** Negative correlation with other taxa (BDC). No clustering with other taxa (MDS/PCA).	**Langer (2004)** Members are positively correlated (BDC). Members cluster together (MDS).		Weakly supported: 1) few taxa, 2) no non-dinosaur taxa represented.
Theropoda	Apobaramin	**Nesbitt et al. (2009)** No clustering with other taxa (PCA: PC 1/PC 2). Other analyses demonstrate discontinuity among members.	-		
Coelophysoidea	Monobaramin	-	**Carrano et al. (2012)** Members cluster together (PCA).		Coelophysoidea is here defined as Coelophysidae + *Dilophosaurus.*
Ceratosauridae	Monobaramin	-	**Brissón Egli et al. (2016)** Members cluster together (PCA).		Ceratosauridae is here defined as including *Ceratosaurus*, *Eoabelisaurus*, and *Genyodectes*.
Abelisauroidea	Apobaramin	**Tykoski and Rowe (2004)** Negative correlation or no correlation with non-abelisauroids (BDC). No clustering with non-abelisauroids (MDS/PCA). Other studies demonstrate discontinuity within Abelisauroidea.	-		Weakly supported: few taxa included.
Noasauridae	Holobaramin?	**Brissón Egli et al. (2016)** Distant from all other taxa in PC 3/PC 1 (PCA).	**Brissón Egli et al. (2016)** Positive correlation unites members (BDC). Members cluster together (PCA).		Weakly supported: most analyses did not show discontinuity.
Abelisauridae	Holobaramin	**Brissón Egli et al. (2016)** Negative correlation with non-abelisaurids (BDC). Clear separation from non-abelisaurid taxa (PCA).	**Brissón Egli et al. (2016)** Positive correlation unites members (BDC). Abelisaurids ordinate along a single trajectory (PCA).		
"Basal" Tetanurae	Inconclusive	-	**Caranno et al. (2012)** Members make a series along PC 2/PC 1 (PCA).		At first these taxa appear to be in a stratomorphic series, but *Monolophosaurus*should be lower than it is. Additionally, there are "basal" coelurosaurs (*Compsognathus* and *Ornitholestes*) mixed in with this non-coelurosaur group.
Spinosauridae	Monobaramin	-	**Carrano et al. (2012)** Members cluster together (PCA).		Very weakly supported: 1) few taxa included, 2) cluster near a non-spinosaur in PC 3/PC 1 (PCA)

Tyrannosauroidea	Holobaramin	**Holtz et al. (2004) [2 Analyses]; Brusatte and Carr (2016)** Negative correlation with other taxa (BDC). Clear separation from other taxa (MDS/PCA).	**Holtz et al. (2004) [2 Analyses]** Positive correlation unites members (BDC). Members ordinate along a single trajectory (MDS/PCA). **Brusatte and Carr (2016)** Members cluster together (PCA)	Aaron (2014) McLain et al. (2018)	Excludes proceratosaurids, *Yutyrannus*, and *Dilong*. Most "basal" tyrannosauroids were unknown in 2004. *Eotyrannus* doesn't cluster closely with the other tyrannosauroids in PCA of Weishampel et al. (2004). PC 3/PC 1 plot may show that *Dilong*, *Guanlong*, and *Yutyrannus* are continuous with other tyrannosauroids, although this is not shown in other analyses.
Ornithomimosauria	Holobaramin	**Makovicky et al. (2004)** No positive correlation or negative correlation with other taxa (BDC). Clear separation from other taxa (MDS/PCA). **Chinzorig et al. (2018)** Clear separation from other taxa (PCA). **Foth and Rauhut (2017)** Clear separation from other taxa in PC 3 (PCA).	**Makovicky et al. (2004)** Members share positive correlation (BDC). Members cluster together (MDS/PCA). **Chinzorig et al. (2018)** Members cluster together (PCA). **Foth and Rauhut (2017)** Members cluster together (PCA).	McLain et al. (2018)	
Non-therizinosaurid Therizinosauroidea	Inconclusive	**Clark (2004)** No positive correlation or negative correlation with other taxa (BDC). Clear separation from other taxa (MDS/PCA). **Zanno (2010)** Not separated from other taxa (PCA).	**Clark (2004)** Members share positive correlation (BDC). Members cluster together (MDS/PCA). **Zanno (2010)** Members don't clearly cluster together (PCA).	Part of therizinosauroidea holobaramin according to McLain et al. (2018).	
Therizinosauridae	Holobaramin	**Clark (2004)** No positive correlation or negative correlation with other taxa (BDC). Clear separation from other taxa (MDS/PCA). **Zanno (2010)** Clear separation from other taxa (PCA).	**Clark (2004)** Members share positive correlation (BDC). Members cluster together (MDS/PCA). **Zanno (2010)** Members cluster together (PCA).	Disagrees with McLain et al. (2018) where Therizinosauroidea is the holobaramin.	*Nothronychus* is excluded from holobaramin in Weishampel et al. (2004) analyses, but it is included in Zanno (2010).
Oviraptorosauria	Holobaramin	**Osmólska et al. (2004)** No positive correlation or negative correlation with other taxa (BDC). Clear separation from other taxa (MDS/PCA).	**Osmólska et al. (2004)** Members share positive correlation (BDC). Members cluster together (MDS/PCA). **Foth and Rauhut (2017)** Members cluster together (PCA)	McLain et al. (2018)	*Avimimus* does not correlate positively with other oviraptorosaurs in the oviraptorosaur Weishampel et al. (2004) BDC. *Caudipteryx* does not cluster with other oviraptorosaurs in the oviraptorosaur Weishampel et al. (2004) PCA.
Dromaeosauridae	Monobaramin	-	**Makovicky et al. (2004)** Members cluster together (PCA). **Foth and Rauhut (2017)** Members cluster together (PCA).	McLain et al. (2018)	May include *Archaeopteryx*. *Utahraptor* is not clustered with other dromaeosaurids in PC 2/PC 1, but this is probably an artifact of missing data. Deinonychosauria (Troodontidae + Dromaeosauridae) seems to be a holobaramin, although the placement of *Archaeopteryx* and anchiornithids in relation to this group is uncertain.
Troodontidae	Monobaramin	-	**Makovicky et al. (2004)** Members cluster together (PCA). **Foth and Rauhut (2017)** Members cluster together (PCA).	McLain et al. (2018)	EK troodontid is more distant in PC 2/PC 1. Probably an artifact of missing data. Deinonychosauria (Troodontidae + Dromaeosauridae) seems to be a holobaramin, although the placement of *Archaeopteryx* and anchiornithids in relation to this group is uncertain.

Non-avian Pygostylia	Apobaramin?	**Foth and Rauhut (2017)** Do not cluster with any other taxa (PCA).	**Foth and Rauhut (2017)** Although members are in the same region of space, the clustering pattern is not tight (PCA).	Garner et al. (2013)	No analyses specifically focused on avialans, so it's hard to say anything other than that pygostylians are distinct from non-avialan dinosaurs.
Aves + *Limenavis* + *Iaceornis*	Apobaramin	**Foth and Rauhut (2017)** Do not cluster with any other taxa (PCA).	-	Garner et al. (2013)	No analyses specifically focused on avians, so we can't say anything about relationships within Aves. However, there are several studies from other researchers looking at avians.
Sauropodomorpha	Apobaramin?	**Langer (2004)** Negative correlation with other taxa (BDC). No clustering with other taxa (MDS/PCA). Other analyses demonstrate discontinuity among members.	-		Very weakly supported: few taxa included.
Non-sauropod Sauropodomorpha	Inconclusive	All analyses including non-sauropod sauropodomorphs showed some kind of link to non-sauropodomorph outgroup.	Usually non-sauropod sauropodomorphs were on a similar trajectory in PCA and shared positive correlation in BDC, but not in every case.		*Eoraptor* and Guaibasauridae often seem to be discontinuous with other non-sauropod sauropodomorphs. Analyses probably biased by the fact that characters focus on more derived members of clades. If Otero et al. (2016) were broken up by family with outgroups, discontinuity might become obvious.
Thecodontosauridae	Monobaramin (or possibly Holobaramin)	**Otero et al. (2016)** One PCA plot shows discontinuity surrounding group but other does not. **Bronzati (2017)** One PCA plot shows discontinuity surrounding group but other does not.	**Otero et al. (2016)** Positive correlation among members (BDC). Members cluster together (PCA). **Bronzati (2017)** Members cluster together (PCA).		Thecodontosauridae is here defined as *Thecodontosaurus* + *Pantydraco*. Strong evidence for continuity, weak evidence for discontinuity.
Non-sauropod Massopoda	Monobaramin (or possibly Holobaramin)	**Otero et al. (2016)** One PCA plot shows discontinuity surrounding group but other does not. **Bronzati (2017)** One PCA plot shows discontinuity surrounding group but other does not.	**Otero et al. (2016)** Positive correlation among members (BDC). Members cluster together (PCA). **Bronzati (2017)** Members cluster together (PCA).		Strong evidence for continuity, weak evidence for discontinuity surrounding the group. *Sarahsaurus* does not cluster with the others in PC 1/PC 3 of Otero et al. (2015) PCA.
Sauropoda	Apobaramin?	**Upchurch et al. (2004) and Galton and Upchurch (2004a)** Negative correlation with other taxa (BDC). **Bronzati (2017)** No clustering with other taxa (PCA). Other analyses demonstrate discontinuity among members.	-		Very weakly supported: few taxa included. Otero et al. (2015) BDC results include several "basal" sauropods (e.g., *Gongxianosaurus* and *Antetonitrus*), which show positive correlation with "prosauropods". However, it is probably because of the large number of taxa from different baramins that these correlations appear.
Gravisauria	Apobaramin	**Otero et al (2015)** Negative correlation with other taxa (BDC). No clustering with other taxa (PCA). **Bronzati (2017)** Separated from other taxa along PC 1 (PCA).	-		

Flagellicaudata	Apobaramin?	**Upchurch et al. (2004)** No clustering with other taxa (PCA).	-		Very weakly supported: few taxa included. No rebbachisaurids or *Haplocanthosaurus* present so unable to say anything about Diplodocoidea or Diplodocimorpha
Ornithischia	Apobaramin	**Baron (2018)** No clustering with other taxa in PC 3/PC 1 (PCA). Other analyses show evidence for internal discontinuity.	-		
Non-eurypodan Thyreophora	Inconclusive	-	-		Analyses show them as discontinuous from Eurypodans, but nothing can be said about their relationships to each other or "basal" ornithischians.
Stegosauria	Holobaramin	**Raven and Maidment (2017)** No clustering with other taxa (PCA) except some probably flukes (see notes). Other analyses show stegosaurs as not clustering with "basal" thyreophorans or ankylosaurs.	**Galton and Upchurch (2004a)** Members positively correlate (BDC). Members cluster together (MDS). **Raven and Maidment (2017)** Members cluster along similar trajectory (PCA).		*Huayangosaurus* doesn't positively correlate with other stegosaurs in BDC of Weishampel et al. (2004), but all other analyses show it clustering with stegosaurs. Oddly, in Raven and Maidment (2017) PCA results, *Tuojiangosaurus* and *Paranthodon* both overlap with ankylosaur outgroup taxa. We believe this is a fluke due to missing data. BDC and MDS results (Appendix) do not show the same pattern.
Ankylosauria	Holobaramin?	**Vickaryous et al. (2004)** Negative correlation or no correlation with other taxa (BDC). No clustering with outgroup taxa (MDS/PCA). **Zheng et al. (2018)** No clustering with other taxa.	**Vickaryous et al. (2004)** Positive correlation within Ankylosauridae and within Nodosauridae (but not between them) (BDC). Continuous series of taxa (MDS/PCA). **Zheng et al. (2018)** Evidence for continuity is not strong between Ankylosauridae and Nodosauridae, however, Polacanthinae jumps from being closer to one and then closer to the other between the two PCA plots.		Alternatively, Ankylosauria may be split into two or three holobaramins. Some results showed evidence in favor of discontinuity between Nodosauridae and Ankylosauridae. However, polacanthines sometimes were closer to ankylosaurids, sometimes to nodosaurids, but were very often right in between them in MDS and PCA. This makes us suspect that Nodosauridae and Ankylosauridae are two monobaramins within a single holobaramin of Ankylosauria.
Ornithopoda	Apobaramin	**Norman, Sues et al. (2004)** Negative correlation or no correlation with outgroup taxa (BDC). No clustering with outgroup taxa (MDS/PCA).	-		*Heterodontosaurus*, as expected, does not cluster with ornithopods.
Non-hadrosauriform Iguanodontia	Inconclusive	Always separated from hadrosauriforms, but most analyses also included Lesothosaurus with evidence of positive correlation.	**Norman et al. (2004) and Norman (2004)** Members positively correlate (BDC). Members cluster together (MDS/PCA). **Madzia et al. (2017)** Members positively correlate (BDC). Members cluster together (MDS/PCA).		Almost certainly multiple holobaramins present. Datasets were focused on higher taxa, which means that all "basal" taxa appeared more similar to each other than they probably are.

Non-hadrosaurid Hadrosauriformes	Holobaramin?	**Horner et al. (2004)** Negative correlation or no correlation with other taxa (BDC). No clustering with other taxa (MDS/PCA). **Cruzado-Caballero and Powell (2017)** No clustering with other taxa (PCA). **McDonald (2012)** No clustering with non-hadrosauriform taxa (PCA). **Madzia et al. (2017)** No clustering with non-hadrosauriform taxa (PCA). **Norman (2004)** No clustering with other taxa (MDS/PCA).	**Horner et al. (2004)** Members share positive correlation (BDC). Members cluster together (MDS/PCA). **Cruzado-Caballero and Powell (2017)** Members cluster/make a series (PCA). **McDonald (2012)** Members cluster/make a series (PCA). **Madzia et al. (2017)** Members cluster/make a series (PCA). **Norman (2004)** Members cluster/make a series (MDS/PCA).		This group shows some evidence for internal discontinuity, but at the same time it also shows evidence for continuity with hadrosaurids. Most analyses that show evidence for continuity with hadrosaurids are analyses containing a larger iguanodont outgroup. As expected, such analyses would highlight differences between "derived" and "basal" iguanodonts more than the differences between various "derived" iguanodonts. On the other hand, several PCA plots show hadrosauriforms in a series with the "basal" members on one end and hadrosaurids on the other. This might mean that they are a single baramin, and that this trajectory indicates diversification within that group. Alternatively, they might just be different baramins along a similar morphological trajectory. More studies will be needed to determine how many holobaramins are represented.
Saurolophinae	Holobaramin	**Horner et al. (2004)** No clustering with other taxa (PCA). **Cruzado-Caballero and Powell (2017)** No clustering with other taxa (PCA).	**Horner et al. (2004)** Members share positive correlation (BDC). Members cluster together (MDS/PCA). **Cruzado-Caballero and Powell (2017)** Members cluster together (PCA).		Alternatively, Hadrosauridae may be a holobaramin containing Saurolophinae and Lambeosaurinae as monobaramins. PC 1/PC 2 of Cruzado-Caballero and Powell (2017) separate out two groups of saurolophines: 1) Kritosaurini + Brachysaurolophini and 2) Edmontosaurini + Saurolophini + Lophorhothon. The aralosaurinin lambeosaurine Aralosaurus clusters with saurolophine group 1. Hadrosaurus is not clustered with the saurolophines at all.
Lambeosaurinae	Holobaramin	**Horner et al. (2004)** No clustering with other taxa (PCA). **Cruzado-Caballero and Powell (2017)** No clustering with other taxa (PCA).	**Horner et al. (2004)** Members share positive correlation (BDC). Members cluster together (MDS/PCA). **Cruzado-Caballero and Powell (2017)** Members cluster together (PCA).		Alternatively, Hadrosauridae may be a holobaramin containing Saurolophinae and Lambeosaurinae as monobaramins. *Aralosaurus*, a lambeosaurine, clusters with saurolophines in the PCA of Cruzado-Caballero and Powell (2017).
Pachycephalosauria	Holobaramin	**Maryańska et al. (2004)** Negative correlation or no correlation with outgroup taxa (BDC). No clustering with outgroup taxa (MDS/PCA). **Schott (2011)** No clustering with other taxa (PCA).	**Schott (2011)** Members form a series (PCA).		Although the Maryańska et al. (2004) results seem to show separation between pachycephalosaurids and "homalocephalids", the Schott (2011) show that this separation is unfounded. Many paleontologists suspect that pachycephalosaurs with flat skulls are probably juveniles (as evidenced by the proposed *Dracorex-Stygimoloch-Pachycephalosaurus* ontogenetic series).

Non-neoceratopsian Ceratopsia	Holobaramin?	**Hailu and Dodson (2004)** Negative correlation with neoceratopsian taxa (BDC). No clustering with neoceratopsian taxa (MDS/PCA). **Madzia et al. (2017)** No clustering with other taxa (PCA). **Breeden (2016)** No clustering with other taxa in PC 3/PC 1 (PCA).	**Hailu and Dodson (2004)** Positive correlation among members (BDC). Members cluster together (MDS/PCA). **Madzia et al. (2017)** Members cluster together (PCA).		Very weakly supported: too few taxa are included. Nevertheless, *Psittacosaurus*, *Chaoyangsaurus*, and *Yinlong* consistently do not cluster or show positive correlation with neoceratopsians.
Non-ceratopsoidean Neoceratopsia	Holobaramin?	**Hailu and Dodson (2004)** Negative correlation or no correlation with other taxa (BDC). No clustering with other taxa (PCA). **Madzia et al. (2017)** No clustering with other taxa (PCA). **Breeden (2016)** No clustering with other taxa in PC 3/PC 1 (PCA).	**Hailu and Dodson (2004)** Members positively correlate (BDC). Members cluster together (MDS/PCA). **Madzia et al. (2017)** Members cluster together (PCA). **Breeden (2016)** Members cluster together (PCA).		These animals consistently cluster together and are separate from ceratopsoids and *Psittacosaurus*-like animals. This is relatively strong evidence for a holobaramin, but unfortunately there are few taxa included in most analyses, and "basal" ceratopsoid animals like *Turanoceratops* and *Zuniceratops* are not included.
Chasmosaurinae	Holobaramin?	**Dodson et al. (2004)** Negative correlation with outgroup taxa and almost no correlation of any kind with centrosaurines (BDC). No clustering with other taxa (MDS/PCA). **Fry (2015)** No clustering with other taxa (PCA).	**Dodson et al. (2004)** Chasmosaurines positively correlate and centrosaurines positively correlate, but only one positive correlation links them (BDC). Chasmosaurines and centrosaurines cluster separately, but members of the subfamilies cluster together (MDS/PCA). **Fry (2015)** Members cluster/make a series together (PCA).		It is unlikely that chasmosaurines and centrosaurines are in different baramins. At first glance, it might seem like Centrosaurinae and Chasmosaurinae should be treated as separate holobaramins. However, the Dodson et al. (2004) analysis is lacking many new taxa which seem to link centrosaurines and chasmosaurines (e.g., *Albertaceratops* and *Regaliceratops*). The Fry (2015) analysis does show clustering of all of the taxa or a series connecting the centrosaurine taxa to the chasmosaurines. However, the analysis is focused on chasmosaurines and is using centrosaurines as an outgroup. Firmer conclusions must await an analysis including many more centrosaurine taxa. Additional evidence for holobaraminic status for all of Ceratopsidae comes in the form of an incredibly restricted stratigraphic range (only Campanian-Maastrichtian) and geographic range (all North American except *Sinoceratops*, which is from China).
Centrosaurinae	Holobaramin?	**Dodson et al. (2004)** Negative correlation with outgroup taxa and almost no correlation of any kind with chasmosaurines (BDC).	**Dodson et al. (2004)** Chasmosaurines positively correlate and centrosaurines positively correlate, but only one positive correlation links them (BDC). Chasmosaurines and centrosaurines cluster separately, but members of the subfamilies cluster together (MDS/PCA).		See Chasmosaurinae for notes.

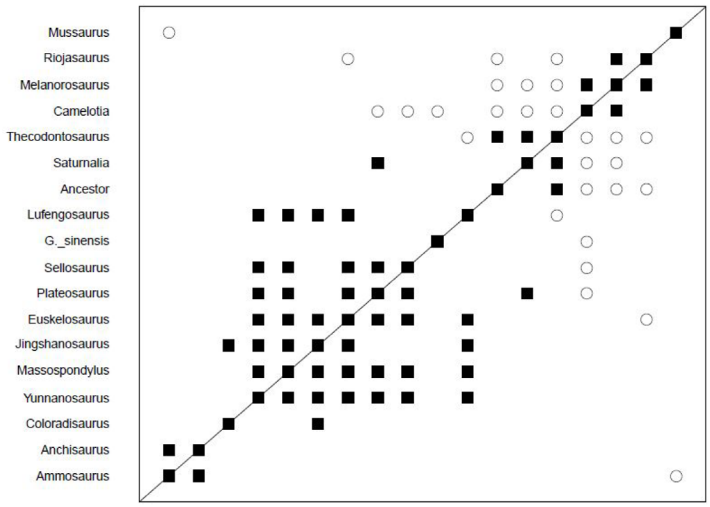

Figure 98: BDC results for Galton and Upchurch's (2004) data matrix of "Prosauropoda", as calculated by BDISTMDS (relevance cutoff 0.75). Sauropod taxa were excluded to show evidence for discontinuity within "Prosauropoda". Closed squares indicate significant, positive BDC; open circles indicate significant, negative BDC.